FIELDIANA
Geology

Published by Field Museum of Natural History

New Series, No. 6

THE MAMMALIAN FAUNA OF MADURA CAVE, WESTERN AUSTRALIA

PART IV

ERNEST L. LUNDELIUS, JR.

WILLIAM D. TURNBULL

February 27, 1981

Publication 1315

THE MAMMALIAN FAUNA OF MADURA CAVE, WESTERN AUSTRALIA

PART IV

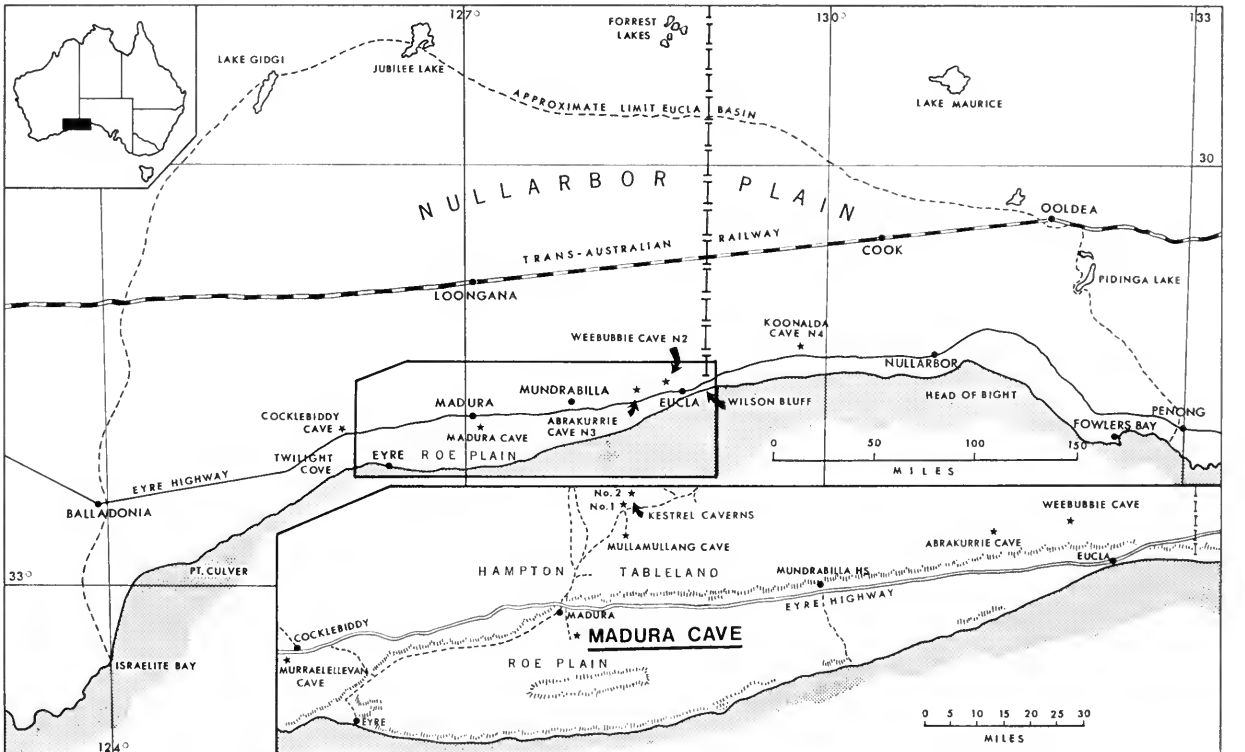

FRONTISPIECE. Maps of the Nullarbor Plain area showing Madura Cave on the Roe Plain to seaward of the Hampton Scarp. Also shown are some other nearby caves on the Hampton Tableland, above the scarp.

FIELDIANA
Geology

Published by Field Museum of Natural History

New Series, No. 6

THE MAMMALIAN FAUNA OF MADURA CAVE, WESTERN AUSTRALIA

PART IV

ERNEST L. LUNDELIUS, JR.
Professor of Geological Sciences
University of Texas at Austin
Research Associate
Field Museum of Natural History

WILLIAM D. TURNBULL
Curator, Fossil Mammals
Field Museum of Natural History
Committee on Evolutionary Biology
University of Chicago
Research Associate
Texas Memorial Museum

Accepted for publication January 3, 1979

February 27, 1981

Publication 1315

Library of Congress Catalog Card Number: 80-68335
US ISSN: 0096-2651
PRINTED IN THE UNITED STATES OF AMERICA

CONTENTS

LIST OF ILLUSTRATIONS

LIST OF TABLES

ABSTRACT

The peramelids represented in the Madura Cave deposits are *Perameles bougainvillei, Isoodon obesulus, Chaeropus ecaudatus,* and *Macrotis lagotis.*

Perameles bougainvillei is found in abundance in all stratigraphic units. Specimens from unit 1 (7420 B.P. and younger) show no qualitative differences from those in units 2 through 4–5 (15,000–22,000 B.P.). Post-Pleistocene reduction in size is indicated by significant differences in three of nine dental measures tested ($P < .05$, one sided "t" test).

Chaeropus ecaudatus and *Macrotis lagotis* are represented in all units and are known from the Nullarbor Plain in historic times. No morphological changes in these species are seen in the period of time represented by the Madura Cave deposits.

Isoodon obesulus is present in all units except unit 7. Its absence from unit 7 is possibly a sampling accident. The recovered specimens are intermediate in size between specimens of *I. obesulus* from southwestern Australia and Victoria and specimens of *I. auratus,* but they are closer to the former. No morphological differences are seen between the specimens from units 4–5 and unit 1. This taxon is not known to have been present on the Nullarbor Plain in historic time. Its presence in early Holocene deposits suggests a change to drier climatic conditions in this region during this time.

INTRODUCTION

This section of the Madura Cave work continues the systematic section begun in Part I (1973) and continued in Parts II (1975) and III (1978), in which 14 taxa of the Dasyuroidea and one of Thylacoleonidae were covered. Here we consider the Order Peramelina, which is represented in the Madura Cave deposits by at least four taxa: the very abundant *Peramelus bougainvillei* and smaller numbers of *Isoodon obesulus, Chaeropus ecaudatus,* and *Macrotis lagotis.*

Madura Cave is located on the Roe Plain 6 miles (9.6 km) south of the settlement of Madura, 110 miles (177 km) west of Eucla (see frontispiece). The cave system consists of a shallow oval doline whose long axis is oriented NW-SE, with two tunnels extending outward from its margins. One tunnel extends southwestward from the doline's southern end, the other northwestward from its northern end. No excavations were carried out in the southern tunnel.

The northern tunnel, which is much larger than the southern tunnel, has a floor 8–10 ft lower than the surface of the doline and a gentle gradient toward the back of the cave.

Five trenches were dug in the northern tunnel, two by Lundelius in 1955 and

three by us in 1964. The stratigraphic sequence in trenches 3 and 4, which produced the most faunal material, consists of the following: a top unit (unit 1 of both trenches) of loose, gray brown silt with many limestone fragments, abundant small bones, and organic material. This unit is separated from the underlying material by an irregular surface. A C-14 date (TX 1146) of 7,470±120 B.P. was obtained from the top foot of this unit in trench 4.

A sequence of red, clayey silts, sands, and limestone powder underlies unit 1. The following C-14 dates were obtained:

Trench 3

Unit 2, upper 1 ft, 15,600±250 years B.P. (TX 1145)
Unit 2, lower 1 ft, 22,400±580 years B.P. (TX 1142)

Trench 4

Unit 2, upper 6 inches, 18,990±220 years B.P. (TX 1140)
Unit 2, 6–12 inches, 20,000±430 years B.P. (TX 1141)
Units 4–5, 22,220±570 years B.P. (TX 1144)
Unit 7, lower 1 ft, exposed: 37,880±3,520 years B.P. (TX 1143)

Measurements and abbreviations used are either those in standard use or they have been outlined in one of the prior sections. The dental terminology has recently been summarized by Hershkovitz (1971), and the reader is referred to that work as containing the most complete compilation of terms and abbreviations available. Those we use are all listed there. The diagrams below indicate the manner used in taking the dental measures: L (=length), AW (=anterior width), PW (=posterior width). They also show some of the Hershkovitz symbols for certain of the stylar cusps and segments of the eocrista(id) that are convenient designations. Major cusp abbreviations follow the Cope-Osborne standard.

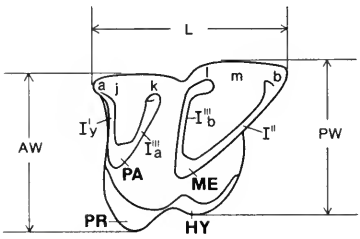

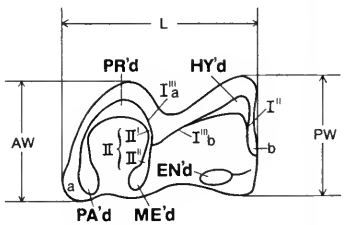

SYSTEMATICS (section continued)
Class Mammalia (continued)
Subclass Theria (continued)
Infraclass Eutheria (continued)
Cohort Marsupiata (*sensu* Turnbull, 1971: = Metatheria) (continued)
Order Peramelina (Gray, 1825; revised Ride, 1964)
Family Peramelidae (Waterhouse, 1838, 1841)
Perameles Geoffroy, 1803, 1804

Perameles bougainvillei Quoy and Gaimard, 1824

MATERIAL

Trench 1, top 1 ft

Lundelius (1963) listed *P. bougainvillei* as occurring in this level, but he gave no catalogue numbers, and we've not been able to locate specimens so assigned. Apparently they have been misplaced.

Trench 1, top 30 inches

PM 26183, right ramus with M_3 and alveoli of all other cheek teeth
PM 26184, left ramus with M_3 and alveoli of P_4–M_2 and M_4
PM 26185, edentulous left maxillary fragment with alveoli of premolars and M^{1-2}

Trench 2, 2½ ft below surface

PM 25223, edentulous left ramus fragment with alveoli of P_4–M_4
PM 25225, left ramus fragment with M_{2-3} and alveoli of M_1 and M_4
PM 25226, right ramus fragment with M_4 and alveoli of M_{2-3}

Trench 3, Unit 2, Level 1

TMM 41106-68, left mandible with P_4 and alveoli of rest of cheek teeth
TMM 41106-69, left ramus fragment with P_4 and alveoli of P_{1-3} and M_{1-3}
TMM 41106-70, right mandible with M_{3-4} and alveoli of I_3 and rest of teeth to M_3
TMM 41106-71, right ramus fragment with M_4 and alveoli of M_{1-3}
TMM 41106-72, right ramus fragment with C, P_{3-4} and alveoli of I_3, P_1, M_{2-3}
TMM 41106-73, right ramus fragment with broken M_4 and alveoli of M_{2-3}
TMM 41106-74, right ramus with M_{3-4} and alveoli of premolars and M_{1-2}
TMM 41106-75, right ramus with M_4 and alveoli of C-M_3
TMM 41106-76, left ramus fragment with M_{1-3} and alveoli of I_3 through P_4
TMM 41106-77, left mandible with C, $P_{1 \text{ or } 2}$, P_4, M_1, M_{3-4} and alveoli of incisors and intervening teeth (fig. 6A, B)
TMM 41106-78, left mandible with P_4 and M_4 and alveoli of C and rest of cheek teeth
TMM 41106-79, right mandible with M_{3-4} and alveoli of C–M_2
TMM 41106-80, right ramus fragment with M_3 and alveoli of I_2–M_2
TMM 41106-81, left ramus fragment with P_4 and alveoli of C–P_3, M_{1-2}
TMM 41106-82, left ramus fragment with M_4
TMM 41106-363, right maxillary with P^{3-4}, M^1, alveoli of rest of cheek teeth (fig. 4A, B)
TMM 41106-2753, left mandible with C–M_4, (P_3 broken), alveoli of I_{1-3} (fig. 7A, B, C)
PM 13339, edentulous right maxillary with alveoli for P^2, M^4
PM 13340, right maxillary with M^{2-3}, alveoli for P^3–M^1 and M^4 (fig. 4C, D)
PM 13341, left maxillary with P^3, alveoli for P^2, P^4, M^1
PM 13342, right maxillary with M^2, alveoli for M^{3-4}
PM 25584, right ramus fragment with C
PM 25585, left ramus fragment with parts of C and $P_{1 \text{ or } 2}$
PM 26990, left ramus fragment with M_4 and alveoli of M_3
PM 26991, right ramus fragment with P_4 and alveoli of C–P_3
PM 26992, right ramus fragment with broken P_4 and alveoli of P_{1-3}, M_{1-3}

Trench 3, Unit 2, Level 1 (continued)
PM 26993, left ramus fragment with M_3 and alveoli of M_2 and M_4
PM 26994, left ramus with M_4 in crypt, alveoli of P_3–M_3
PM 26995, right ramus fragment with P_4, alveoli of C–P_3 and M_{1-3}
PM 26996, left ramus fragment with P_{3-4}, alveoli of M_1
PM 26997-8, two right M_1s
PM 26999-7002, four left M_1s
PM 27003-23, 21 right M_2s or M_3s
PM 27024-40, 17 left M_2s or M_3s
PM 27041-3, three left M_4s
PM 27044-5, two right M_4s
PM 27046-9, four right M^1s
PM 27050-4, five left M^1s
PM 27055-75, 21 left M^2s or M^3s
PM 27076-90, 15 right M^2s or M^3s
PM 27091-2, two left M^4s
uncatalogued, ca. 100 edentulous ramus and maxillary fragments
uncatalogued, two specimens with label lost, probably this level
uncatalogued, one vial with hundreds of uncatalogued premolars

Trench 3, Unit 2, Level 2
TMM 41106-43, ?*Perameles* cranium
TMM 41106-322, left M^1
TMM 41106-2755, right M^4
TMM 41106-2756-9, four right M^1s
WAM 74.9.52-.53, two left M^2s or M^3s
WAM 74.9.54, right M_4
WAM 74.9.55, left M_1
PM 27093-112, 20 left M^2s or M^3s
PM 27113-5, three right M_4s
PM 27116-7, two left M_1s
PM 27118-20, three right M_1s
PM 27121-9, nine right M_2s or M_3s
PM 27130-2, three premolars
PM 27133-40, eight right M^2s or M^3s
PM 27141-52, 12 left M_2s or M_3s
PM 27219, left M_4

Trench 3, Unit 2, Level 4
TMM 41106-399, right ramus fragment with M_4, coronoid, and condyle
TMM 41106-400, right ramus fragment with M_{3-4}, coronoid, and condyle
TMM 41106-402, right ramus fragment with M_{3-4}, alveoli of M_{1-2}, coronoid, and condyle
TMM 41106-405, right ramus fragment with P_4, alveoli of C-P_3
TMM 41106-408, right ramus fragment with P_2 and P_3, alveoli of P_4-M_2
TMM 41106-414, right maxillary fragment with M^1, alveoli of P^{3-4}
PM 27162, left maxillary fragment with $M^{2 \text{ or } 3}$
PM 27163, left maxillary fragment with M^1, alveoli of M^2
PM 27164-5, two edentulous left maxillary fragments
PM 27166-71, five edentulous right maxillary fragments

Trench 3, Unit 3
- TMM 41106-38, left ramus with alveoli of C-M_3
- TMM 41106-39, left ramus with alveoli of P_2-M_4
- TMM 41106-40, left ramus with alveoli of M_1-M_4
- TMM 41106-41, right ramus with P_2, alveoli of P_3-M_3
- TMM 41106-42, right ramus with alveoli of M_3, M_4
- TMM 41106-2764, left ramus with M_4, alveoli of M_{2-3}
- TMM 41106-2765, right ramus with M_4, alveoli of M_3
- TMM 41106-2766, left ramus with M_2 or M_3, alveoli of P_4-M_1 or M_{1-2}
- TMM 41106-2754, left ramus alveoli of M_1-M_4
- TMM 41106-2760, edentulous left maxillary
- TMM 41106-2761, left maxillary fragment with M^3 and alveoli of M^2 and M^4
- TMM 41106-2762, right M^1
- uncatalogued, two edentulous ramus fragments

Trench 4, Unit 1, Level 1
- TMM 41106-475, right M^1
- TMM 41106-507, 10 edentulous mandibular fragments
- TMM 41106-508, left maxillary fragment with P^3, alveoli of P^2, P^4, and M^1
- TMM 41106-509, left P_3
- TMM 41106-512, right maxillary fragment with M^{1-4} (fig. 4E, F)
- TMM 41106-513, right maxillary fragment with M^{3-4}
- TMM 41106-514, left ramus fragment with P_4, alveoli of P_3, and M_1
- TMM 41106-515, premolar
- TMM 41106-518, edentulous left maxillary fragment with palatal bar and foramina, alveoli of P^1, P^3, and P^4, and M^1. P^4 is within crypt.
- TMM 41106-549, left M^3
- TMM 41106-550, left M^1
- TMM 41106-678, left M_2
- TMM 41106-5089, edentulous maxillary fragment
- TMM 41106-5090, four edentulous maxillary fragments
- TMM 41106-5091, two right M^2s
- TMM 41106-5092, right M^3
- TMM 41106-5093, three edentulous right ramus fragments
- TMM 41106-5094, two edentulous left ramus fragments
- TMM 41106-5095, three left M_2s
- TMM 41106-5096, left M^1
- TMM 41106-5097, right M^1
- PM 27153-4, two left M^2s
- PM 27155, left M^3
- PM 27156, left M^2
- PM 27157-8, right and left M^1s
- PM 27159-61, three right M^2s
- PM 27172-4, three left M_2s
- PM 27175, left M_3
- PM 27176, right M_4 talonid
- PM 27177-8, two right M_1s
- PM 27179-80, two left M_x fragments
- PM 27181-3, two left M_1s and one right M_1

Trench 4, Unit 1, Level 1 (continued)

PM 27184, broken right $M^{2 \text{ or } 3}$
PM 27185, right M^2
PM 27186, broken right $M^{2 \text{ or } 3}$
PM 27187-8, two right M^1s
PM 27189, right M^1
PM 27190, right $M^{1,2, \text{ or } 3}$, probably M^2
PM 27191-2, left and right M^1s
PM 27193, premolar
PM 27194-5, edentulous left and right maxillary fragments
PM 27196, edentulous ramus fragment
PM 27197, left M_3
PM 27198-9, right and left M_2s
PM 27200, premolar
PM 27201, left ramus fragment with M_4 in crypt, alveoli of M_3
PM 27202, edentulous right mandible
PM 27203-6, four edentulous left ramus fragments
PM 27207, one left, one right edentulous maxillary fragment
PM 27208, right I^3
PM 27209, left M_3
PM 27210, left M_1
PM 27211, left M_3
PM 27212-14, three left M_2s
PM 27215, left M_3
PM 27216, broken left $M_{2 \text{ or } 3}$
PM 27217, left M_3
PM 27220-21, two right M_1s
PM 27222, right M_2
PM 27223, right M_3
PM 27224, left M_2
PM 27225, left M_3
PM 27226-7, two left M_2s
PM 27228, left M_3
PM 27229-30, two right M_3s
PM 27231-6, six right M_2s

Trench 4, Unit 2, Level 1

PM 27237, right mandible with M_4, alveoli of other teeth
PM 27238, right mandible with P_4, M_{3-4}, alveoli of rest of teeth (fig. 5C, D)
PM 27239, left ramus fragment with M_3, alveoli of premolars, and other molars
PM 27240, left mandible edentulous except for parts of C and P_4
PM 27241, left ascending ramus fragment with coronoid, condyle, and angular process
PM 27242, right mandible with P_2, P_4, M_{3-4}, alveoli of other teeth (fig. 6C, D)
PM 27243, left ramus fragment with M_4 in crypt, alveoli of P_4-M_3
PM 27244, left maxillary fragment with M^2 or M^3
PM 27245, edentulous left ramus with alveoli of P_3-M_4
PM 27246, edentulous right ramus fragment with alveoli of M_{3-4}

Trench 4, Unit 2, Level 1 (continued)

PM 27247, edentulous right ramus fragment with alveoli of P_3-M_3
PM 27248, edentulous right ramus fragment with alveoli of M_4
PM 27249, edentulous left ramus fragment with alveoli of M_{2-3}?
PM 27250, edentulous right ramus fragment with alveoli of C-P_4
PM 27251, edentulous left ramus fragment with alveoli of C-P_2
PM 27252, edentulous right ramus fragment with alveoli of P_3-M_1
PM 27253, edentulous left ramus fragment with alveoli of P_{1-4}
PM 27254, edentulous ramus fragment with alveoli of premolars
PM 27255, left ramus fragment with P_2, alveoli of P_{3-4}
PM 27256, edentulous left maxillary fragment with alveoli of P^3-M^3
PM 27257, left ramus fragment with P_1, alveoli of I_3, C, P_3
PM 27258, edentulous left mandible with coronoid, condyle, and part of angular process
PM 27259, edentulous right maxillary fragment with alveoli of P^3, dP^4, M^1
PM 27260, edentulous left maxillary fragment with alveoli of cheek teeth
PM 27261-8, eight right M^1s
PM 27269-75, seven left M^2s or M^3s
PM 27276, edentulous left ramus fragment with alveoli of I_3-M_2
PM 27277, left ramus fragment with P_2 and P_3, alveoli of P_4-M_2
PM 27278, edentulous left ramus fragment with angle, coronoid, and condyle
PM 27279, edentulous right ramus fragment with alveoli of M_{1-4}
PM 27280, left ramus fragment with P_4, alveoli of I_3-P_3
PM 27281, edentulous left ramus fragment with alveoli of M_{3-4}
PM 27282, edentulous right ramus fragment with alveoli of C-M_2
PM 27283-5, three edentulous right ramus fragments with alveoli of M_{3-4}
PM 27286, edentulous right ramus fragment with alveoli of P_2-M_3
PM 27287, edentulous left ramus fragment with alveoli of C-P_3
PM 27288, edentulous right ramus fragment with alveoli of M_{3-4}, portion of angle
PM 27289, edentulous left ramus fragment with alveoli of P_{1-3}
PM 27290, edentulous right ramus fragment with alveoli of premolars
PM 27291, edentulous left ramus fragment with alveoli of M_4
PM 27292, edentulous left ramus fragment with alveoli of P_4-M_2
PM 27293, edentulous left ramus fragment with alveoli of premolars
PM 27294, right maxillary fragment with M^4, alveoli of P^4-M^3
PM 27295, left M_1
PM 27296-7, two premolars
PM 27298, edentulous right maxillary fragment with alveoli of P^4, M^1
PM 27299-300, two right M^2s or M^3s
PM 27301-7, seven left M^1s
PM 27308-12, five left M_1s
PM 27313-9, seven right M_1s
PM 27320-37, 18 left M_2s or M_3s
PM 27338-63, 26 M^2s or M^3s
PM 27364, left M^4
PM 27365-8, four left M^4s
PM 27369-99, 31 right M_2s or M_3s

Trench 4, Unit 2, Level 2

TMM 41106-713, right $M^{2 \text{ or } 3}$
TMM 41106-2767, premolar
TMM 41106-2768, left $M_{2 \text{ or } 3}$
TMM 41106-2769, partial left upper molar
TMM 41106-2770, left P^4
TMM 41106-2771, left mandible with M_{3-4}, alveoli of rest of teeth (fig. 5A, B)
TMM 41106-2772, edentulous left ramus with coronoid, condyle, angle, and alveoli of P_4-M_4
TMM 41106-2773, left ramus fragment with M_4 in crypt, alveoli of M_3
TMM 41106-2774, edentulous left ramus fragment with alveoli of M_{1-4}
TMM 41106-2775, edentulous left mandible with alveoli of all teeth
TMM 41106-2776, left maxillary with P^3, alveoli of rest of cheek teeth
TMM 41106-2777, left maxillary fragment with P^3
TMM 41106-2778, two right maxillary fragments, one with P^1, the other with P^4, probably same individual
TMM 41106-2779, left ramus fragment with M_3, alveoli of M_{1-2}
TMM 41106-2780, left ramus fragment with P_3, alveoli of I_3-P_1
TMM 41106-2781, right ramus fragment with M_4, alveoli of P_3-M_3
TMM 41106-2782, edentulous right ramus fragment with alveoli of all cheek teeth
TMM 41106-2783, edentulous right ramus fragment with coronoid, condyle, angle, and alveoli of M_4
TMM 41106-2784, edentulous right ramus fragment with broken P_1, P_4, M_1, alveoli of C-P_3
TMM 41106-2785, right ramus fragment with M_4, alveoli of P_3-M_3
TMM 41106-2786, right ramus fragment with P_3, alveoli of P_4-M_2
TMM 41106-2787, edentulous right ramus fragment with alveoli of M_{3-4}, coronoid, and condyle
TMM 41106-2788-95, eight left M_1s
TMM 41106-2796, right M_1 fragment
TMM 41106-2797-804, eight right M^1s
TMM 41106-2805, right M^1 fragment
TMM 41106-2806-10, five left M_4s
TMM 41106-2811-3, three right M^4s
TMM 41106-2814-6, three left M^4s
TMM 41106-2817-9, three left M^1s
TMM 41106-2820-7, eight left M^2s or M^3s
TMM 41106-5098, 20 edentulous ramus fragments
WAM 75.1.1-.5, five left M^1s
WAM 75.1.6-.11, six right M_1s
WAM 75.1.12-.16, five left M^2s or M^3s
PM 27400-425, 26 right M_2s or M_3s
PM 27426-7, two right M_2s or M_3s
PM 27428-452, 25 right M^2s or M^3s
PM 27453-460, eight right M_4s
PM 27461, right M^2 or M^3
PM 27462-9, eight left M^2s or M^3s

Trench 4, Unit 2, Level 2 (continued)
PM 27470-3, four left M^1s
Pm 27474-8, five right M_1s
PM 27479-517, 39 left M_2s or M_3s
PM 27518-96, 79 premolars
uncatalogued, 46 incisors or canines

Trench 4, Unit 2, Level 3
PM 27597-9, three left M^1s
PM 27600-1, two left M^2s or M^3s
PM 27602-4, three right M^2s or M^3s
PM 27605-8, four right M_1s
PM 27609-10, two left M_2s or M_3s
PM 27611, left lower molar fragment
PM 27612-3, two premolars
PM 27614-21, eight right M_2s or M_3s
uncatalogued, six edentulous maxillary fragments
uncatalogued, 21 edentulous ramus fragments

Trench 4, Units 4-5
TMM 41106-718, right $M^{2 \text{ or } 3}$
TMM 41106-728, trigonid of left M_x
TMM 41106-3001-85, 85 right M_1s
TMM 41106-3086-171, 86 left M_1s
TMM 41106-3172-221, 50 left M_4s
TMM 41106-3222-72, 51 right M_4s
TMM 41106-3273-312, 40 left M_2s or M_3s
TMM 41106-3313-41, 29 left M^1s
TMM 41106-3342-58, 17 left M^4s
TMM 41106-3359-90, 31 right M^4s
TMM 41106-3391-444, 54 right M^1s
TMM 41106-3445-65, 21 right M^2s
TMM 41106-3466-99, 34 right M^3s
WAM 75.1.17, left ramus with M_1
WAM 75.1.18, right ramus with $M_{3\text{-}4}$
WAM 75.1.19, left mandible, edentulous except for C
WAM 75.1.20, edentulous left mandible
WAM 75.1.21-.26, six left M_1s
WAM 75.1.27-.32, six left M_4s
WAM 75.1.33-.38, six right M_4s
WAM 75.1.39-.50, 12 left M_2s or M_3s (probably M_2)
WAM 75.1.51-.62, 12 left M_2s or M_3s (probably M_3)
WAM 75.1.63-.68, six left M^1s
WAM 75.1.69-.72, four left M^4s
WAM 75.1.73-.77, five right M^4s
WAM 75.1.78-.82, five right M^1s
WAM 75.1.83-.92, 10 right M^3s (measured)
WAM 75.1.93-.99, seven right M^2s
WAM 75.1.100-.103, four right M^2s or M^3s
WAM 75.1.104-.110, six right M^2s
WAM 75.1.111, right M_2 or M_3

Trench 4, Units 4-5 (continued)

WAM 75.1.112-.114, three right M^1s
WAM 75.1.115-.117, two right P^4s and a left P^4
PM 13401-20A, 40 right M_2s or M_3s
PM 26318-9, two left M_1s
PM 26330, left M^2
PM 27622, right ramus with P_3
PM 27623, left ramus with P_x
PM 27624, premolar
PM 27625, trigonid, left M_x
PM 27626, edentulous right ramus
PM 27627, edentulous left ramus fragment, alveoli of M_{3-4}
PM 27628-9, two edentulous right ramus fragments, alveoli of M_{3-4}
PM 27630, edentulous right ramus fragment, alveoli of P_2-M_1
PM 27631, edentulous left ramus fragment, alveoli of P_2-M_1
PM 27632, edentulous right ramus fragment, alveoli of P_2-M_1
PM 27633, edentulous left ramus, alveoli of cheek teeth
PM 27634, edentulous right maxillary, alveoli of M^{1-4}
PM 27635, left M_4
PM 27636, right M_4 in ramus fragment
PM 27637, left M_4 in crypt, ramus angle, alveoli of M_{2-3}
PM 27638, left P_3 in ramus fragment
PM 27639, edentulous right ramus
PM 27640, left edentulous ramus, alveoli of M_{1-4}
PM 27641 (A-G), seven edentulous right ramus fragments
PM 27642 (A-H), -43 (A-F), and -44 (A-F), 20 edentulous right ramus fragments
PM 27645 (A-E) and -46 (A-E), 10 edentulous left ramus fragments
PM 27647 (A-E) and -48 (A-F), 11 edentulous left ramus fragments
PM 27649-675, 27 right M_2s or M_3s
PM 27676-89, 14 left M_2s or M_3s
PM 27690, right $M_{2 \text{ or } 3}$
PM 27691-739 and PM 27741-52, 61 left M_2s or M_3s
PM 27753-7, five right M_2s or M_3s
PM 27758, left M_2 or M_3
PM 27759-85, 27 right M_2s or M_3s
PM 27786-801, 16 right M_4s
PM 27802-22, 21 right M_1s
PM 27825-30, six left M_4s
PM 27831-46, 16 left M^1s
PM 27847-66, 20 left M_1s
PM 27867, right M^4
PM 27868-92, 35 right M^1s
PM 27893-902, 10 premolars
PM 27903-8, six right M^2s or M^3s
PM 27909-15, seven left M_4s
PM 27916-28, 13 right M_4s
PM 27929-30, two left M_4s
PM 27946-68, 23 left M_2s (measured)

Trench 4, Units 4-5 (continued)

PM 27969-80, 12 left M_{2}s or M_{3}s (probably M_{2}s)
PM 33501-63, 63 left M_{2}s or M_{3}s (probably M_{2}s)
PM 33564-610, 47 left M_{2}s or M_{3}s (probably M_{3}s) (33564-89 measured)
PM 33611-24, 14 left P^{4}s
PM 33625-8, four left M_{1}s
PM 33629 (A-Z), PM 33630 (A-AA), and PM 33631 (A-M), 66 right M^{2}s or M^{3}s
PM 33632-58, 27 left M^{1}s
PM 33659 (A-C), three broken left M^{1}s
PM 33663-92, 30 left M^{2}s or M^{3}s
PM 33693-732, 40 left M^{2}s
PM 33733-6, four right P^{4}s
PM 33737-69, 33 left M^{2}s
PM 33770 (A-EE), 31 broken left M^{2}s or M^{3}s
PM 33771-2, two left M^{1}s
PM 33773-872, 100 left M^{3}s
PM 33873 (A-Y), PM 33874 (A-XX), and PM 33875 (A-N), 89 indet. premolars (no P^{4}s)
PM 33876 (A-L), PM 33877 (A-N), and PM 33878 (A-VV), 74 indet. premolars
PM 33879 (A-FFFFF), 110 indet. premolars
uncatalogued, ~400 isolated premolars
PM 33880 (A-AA), -81 (A-Z), and -82 (A-M), 56 broken right M_{2}s or M_{3}s
PM 33883-7, five right M_{1}s
PM 33888-91, four right M_{1}s or M_{2}s, (probably M_{1}s)
PM 33892-4054, 163 right M_{2}s or M_{3}s
PM 34055-6, two left M_{4}s
PM 34057-64, eight right P^{4}s
PM 34065-84, 20 right M^{2}s or M^{3}s
PM 34085-107, 23 right M^{2}s (measured)
PM 34108 (A-Z), 26 broken left M_{x}s
PM 34109 (A-U) and PM 34110 (A-U), 42 broken M_{x}s
PM 34111-26 (A-P), 16 right M^{3}s (measured)
PM 34127-37, 11 right M^{1}s
PM 34138-59, 22 right M^{2}s or M^{3}s
PM 34160 (A-ZZZ), 78 edentulous left ramus fragments
PM 34161 (A-DDDD), 82 edentulous right ramus fragments
PM 34162, five broken right M_{x}s
PM 34163, broken M^{x}
PM 34165, right mandible with M_{4} in crypt
PM 34166, right mandible with M_{4}
PM 34167, right mandible with P_{3}, M_{2-3}
PM 34168 (A-B), two broken left M_{x}s
PM 34169, left maxillary with M^{4}, alveoli of P^{4}-M^{3}
PM 34170, premolar
PM 34171 (A-B), fragments of two premolars
PM 34173 (A-H), eight upper incisors

Trench 4, Units 4-5 (continued)
PM 34174 (A-C), three I_1s or I_2s
PM 34175 (A-F), six left I_3s
PM 34176 (A-M), 13 right I_3s

Trench 4, Unit 7, Level 1
TMM 41106-707, right $M^{2 \text{ or } 3}$
WAM 75.1.119, right M_4
WAM 75.1.120-1, two left M_2s or M_3s
WAM 75.1.122, right M_2 or M_3
PM 34177, right M_4
PM 34179, left M_1
PM 34180, edentulous right maxillary fragment with alveoli of P^3
PM 34181, edentulous right ramus fragment with alveoli of M_4
PM 34182 (A-B), two edentulous left ramus fragments
PM 34183-94, 12 left M_2s or M_3s
PM 34195, right M_1
PM 34196-9, four left M^1s
PM 34200-3, four right M^3s
PM 34204-8, five right M^2s
PM 34209, right M^2 or M^3
PM 34210, right M_4
PM 34211-2, two left M^2s
PM 34213-4, two right M^1s
PM 34215-8, four left M^3s
PM 34219-31, 13 right M_2s or M_3s

Trench 4, Unit 7, Level ?
PM 34232, right ramus fragment with M_4 in crypt
PM 34233, left P^4
PM 34234, right ramus fragment with M_{3-4}
PM 34235, edentulous right ramus
PM 34236 (A-B), C-G, two left and five right edentulous ramus fragments

Trench 4, Unit 7, Level 2
TMM 41106-730, broken left M_4
WAM 75.1.123, left M_1
PM 34237-9, three right M_1s
PM 34240-8, nine left M_1s
PM 34249, left ramus fragment with P_4 in crypt
PM 34250, (A-B, C-H), two right and six left edentulous ramus fragments
PM 34253-4, two left M_4s
PM 34256-9, four left M^1s
PM 34260-4, five right M^1s
PM 34265-7, three right M^3s
PM 34268-9, two right M^2s
PM 34270-5, six left M^2s
PM 34276-8, three left M^3s
PM 34279-80, two left M^2s or M^3s
PM 34281, left M^4
PM 34282-5, four right M_4s

Trench 4, Unit 7, Level 2 (continued)
PM 34286-94, nine left M_2s or M_3s
PM 34295, left M_1
PM 34296 (A-C), three broken left M_2s or M_3s
PM 34297-314, 18 right M_2s or M_3s
PM 34315, broken right M_2 or M_3
PM 34316, right M_1

Trench 5, Unit 4
PM 34317, right P^4
PM 34318, right M^1
PM 34319, right M^2
PM 34320, right M^3
PM 34321-2, two left M^1s
PM 34323-5, three left M^2s
PM 34326, left M^3
PM 34327 (A-B), two edentulous right ramus fragments
PM 34328 (A-E), five edentulous left ramus fragments
PM 34329 (A-D), four edentulous left maxillary fragments
PM 34330 (A-D), four edentulous right maxillary fragments
PM 34331, left M_4

Trench 5, Unit 5
TMM 41106-692-3, edentulous right and left rami, respectively
PM 26332, broken right M^1 or M^2
PM 34332 (A-B), right and left maxillary fragments, each with P^3
PM 34333, edentulous left maxillary fragment
PM 34334 (A-C), three edentulous left ramus fragments
PM 34335, edentulous right ramus fragment
PM 34336, right cranial fragment
PM 34337-9, three left M_1s
PM 34340-1, two right M_1s
PM 34342-8, seven right M_2s or M_3s
PM 34349-54, six right M_3s
PM 34355, left M_4
PM 34356, broken left $M^{1, 2, \text{ or } 3}$
PM 34357, broken right M_2 or M_3
PM 34358-64, seven left M_2s or M_3s
PM 34365, left M_3 or M_2
PM 34366, left P_1?
PM 34367-75, nine left P^3s
PM 34376-9, four left P_4s or P_3s
PM 34380, left P^4
PM 34381-3, three right P_4s or P_3s
PM 34384-7, four left M_2s or M_3s
PM 34388-9, two left M^1s
PM 34390-95, six left M^3s or M^2s
PM 34396-7, three left M^3s
PM 34398, left M^4
PM 34399-402, four right M^1s
PM 34403-6, four right M^2s

Trench 5, Unit 5 (continued)
PM 34407-8, two right M^2s or M^3s
PM 34409-11, three right M^3s
PM 34412, right M^4
PM 34413-4, two right P^4s

Trench 5, Unit 6
PM 34415-6, two left M_2s or M_3s

The following Recent material was used for comparison: *Perameles myosura notina* Thomas, 1922 (= *P. bougainvillei notina*), A. 377-823, A. 377-822, A. 377-821 (9.2.181; fig. 2), A. 377-82 (9.2.182; fig. 3), from the Odontological Museum of the Royal College of Surgeons, London; TMM 40235-2 from Murraelellevan Cave (fig. 1).

Descriptions

Cranium.—One specimen (TMM 41106-143), a partial cranium consisting of sutured frontal bones with no unusual features, and a number of maxillaries have been recovered. The maxillaries show the infraorbital foramen opening into a broad depression above the anterior part of M^1. Within the depression, there is a foramen for a canal that extends anteriorly into the maxillary. The lateral side of the maxillary immediately ahead of the junction of the jugal is excavated. The palatal part of the maxillary of TMM 41106-363 (fig. 4A) shows part of both anterior and posterior palatal vacuities. The bridge between the vacuities is located opposite P^3 and is a thin strut of bone. None of our specimens preserves the complete perimeter of either vacuity, and so we cannot comment on the anterior limit of the anterior or the posterior limit of the posterior, or the widths of either. It is clear that the posterior palatal vacuities are large as in specimens from the surface of Murraelellevan Cave. Large posterior palatal vacuities are a characteristic of the *Perameles bougainvillei* group, according to Freedman (1967, p. 163).

Upper dentitions.—None of the recognized cranial fragments includes premaxillaries, and we have not attempted to characterize the isolated premaxillary fragments or upper incisors because of uncertainties of identification. The same applies to P^1. Several specimens of maxillaries do preserve part of the premolar tooth series, and a number have alveoli for all cheek teeth, but no P^1s are in position. Therefore, we begin our description with P^3.

The P^3 is a double-rooted tooth with a variable shape. One specimen (TMM 41106-363; fig. 4A) has a P^3 that is compressed laterally. There is a prominent principal cusp located at midlength. Low but distinct cingular cuspules are present, one at each end of the tooth. The posterior end is slightly wider than the anterior and has an indistinct cingulum associated with the posterior root. It is separated from the P^1 by a short diastema. Another specimen (TMM 41106-508) has a wider P^3, particularly posteriorly where a posterior cingulum encircles the posterior end of the tooth. A cingular tubercle is present at the posterolingual corner of the tooth, removed from the posterior cuspule. The diastema separating P^1 and P^3 is shorter than in TMM 41106-363.

The P^4 is two rooted with a triangular outline in crown view. There is a large centrally located principal cusp that is oval in cross section and slightly recurved

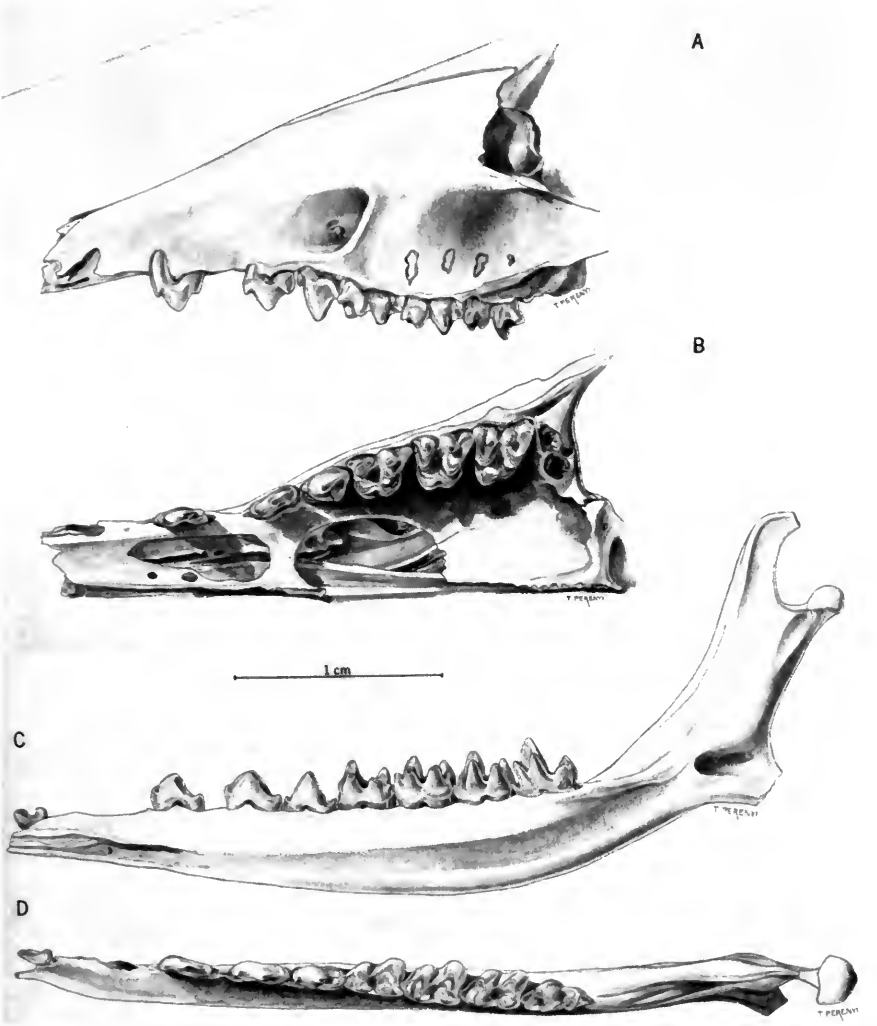

FIG. 1. *Perameles bougainvillei*, TMM-40235-2, a subfossil specimen from the surface of Murraelellevan Cave, Nullarbor Plain, Western Australia. **A & B,** Left lateral and ventral views of the facial portion of the skull and its dentition. **C & D,** Lingual and crown views of the right ramus and its dentition.

posteriorly. Cingular cusps are present on the anterior and posterior ends of the tooth. A prominent lingual cingular shelf with a cuspule is present. It varies considerably in size and position. In specimen TMM 41106-363, it is located lingual to the main cusp, whereas in TMM 41106-2778, it is smaller and located posterolingual to the main cusp. The anterior cingular cuspule is barely discernible on the latter specimen.

The upper molars have the basic tribosphenic form modified by the addition of a prominent hypocone (except for M^4) and by crown hypsodonty on the lingual side related to the protocone and hypocone. Also, they have a prom-

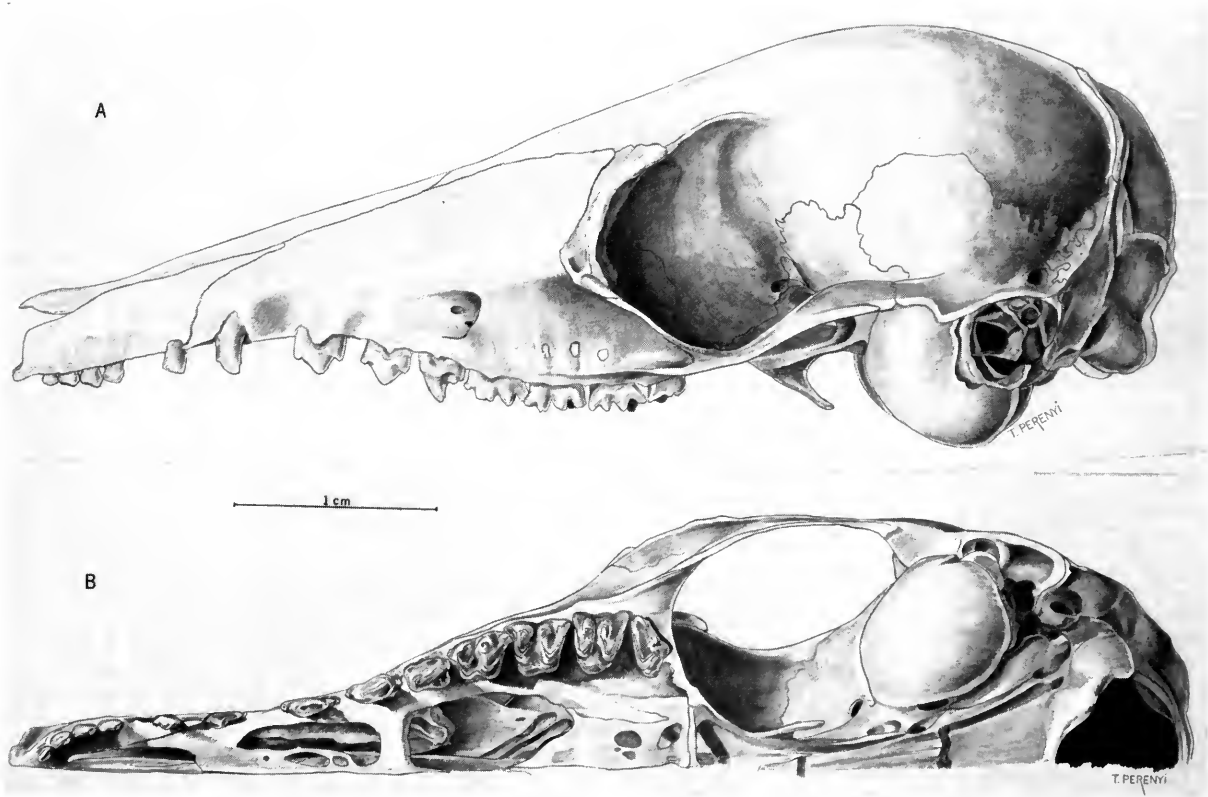

FIG. 2. *Perameles myosura notina* Thomas = *P. bougainvillei*. Specimen 9.2.181, Odontological Museum, Royal College of Surgeons, London. **A & B,** Left lateral and ventral views of the skull and its dentition.

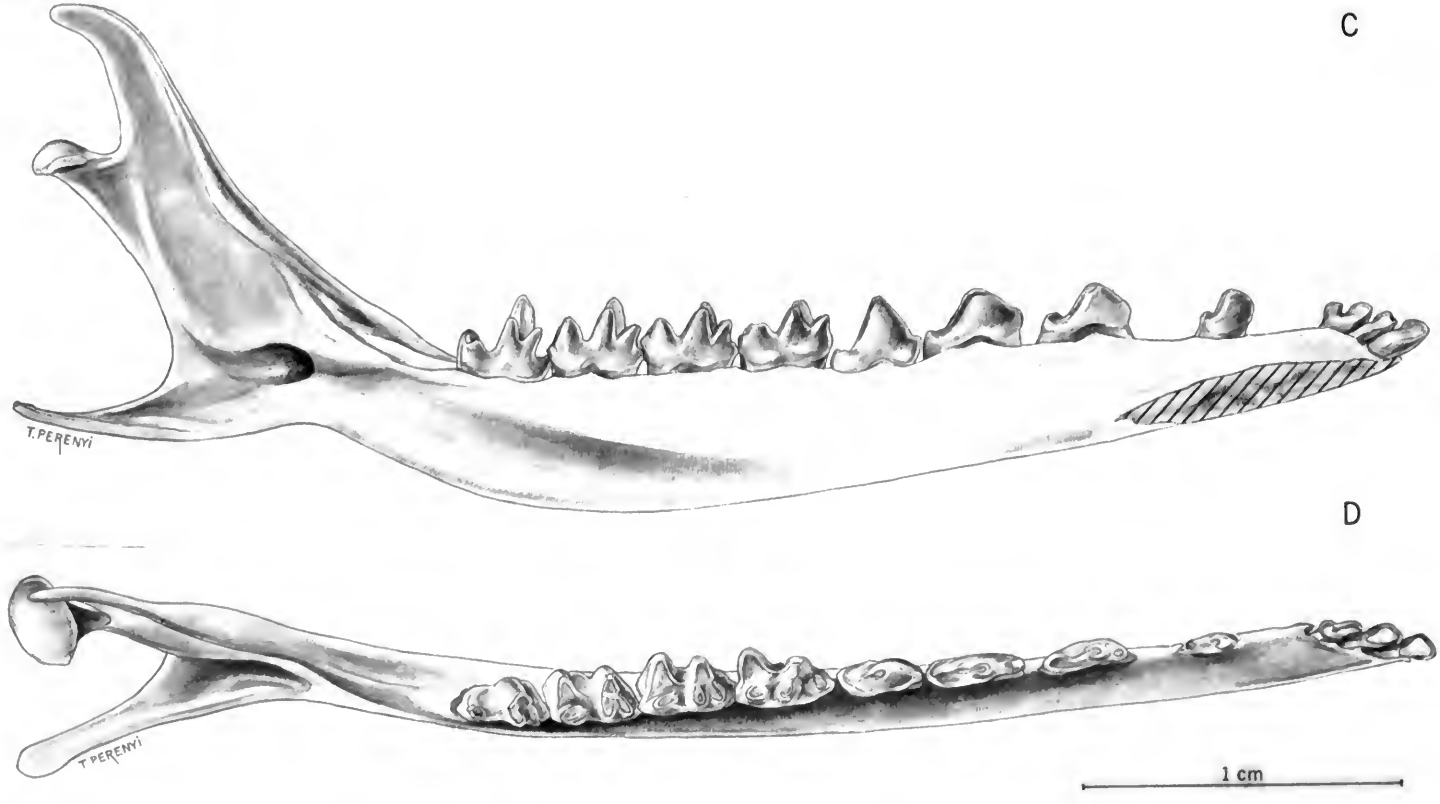

FIG. 2. **C & D,** Lingual and crown views of the left ramus and its dentition.

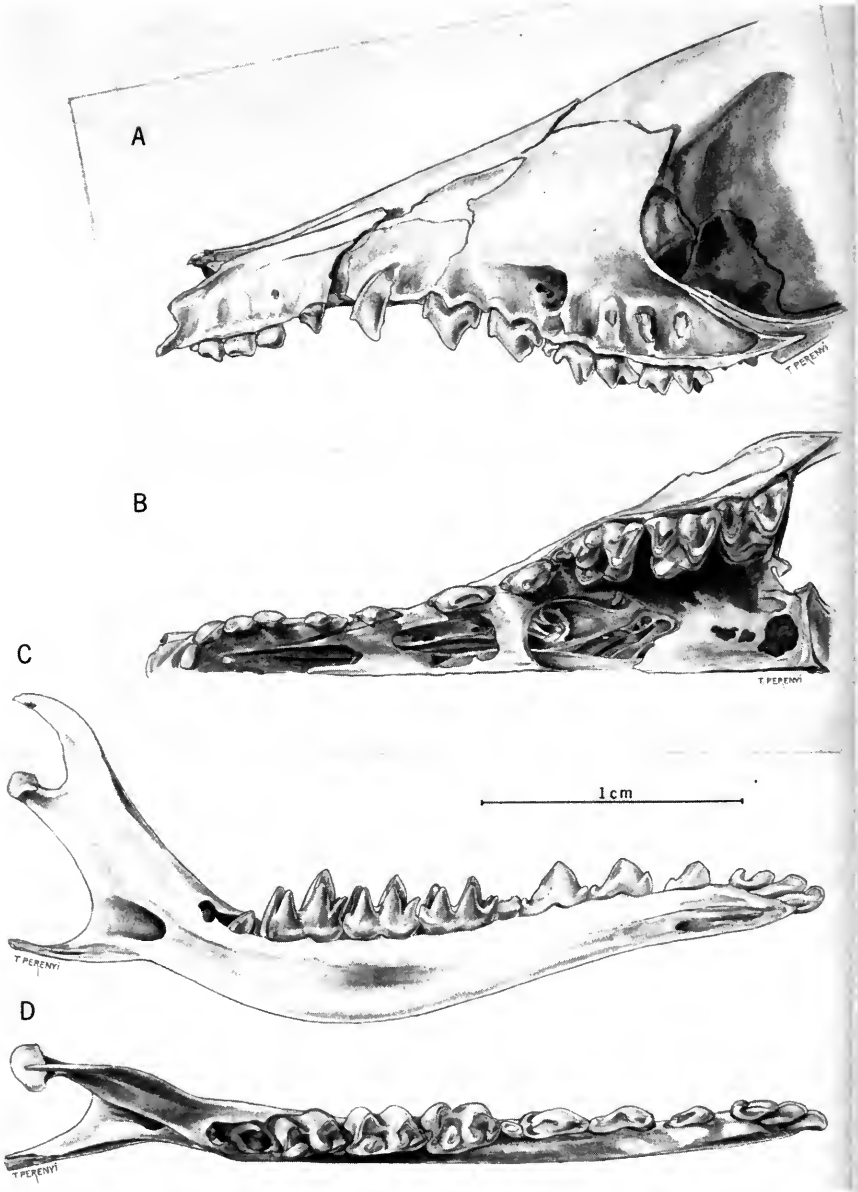

FIG. 3. *Perameles myosura notina* Thomas = *P. bougainvillei*. Specimen 9.2.182, a juvenile, Odontological Museum, Royal College of Surgeons, London. **A & B,** Left lateral and ventral views of the facial portion of the skull with its dentition. **C & D,** Lingual and crown views of the left ramus and its dentition.

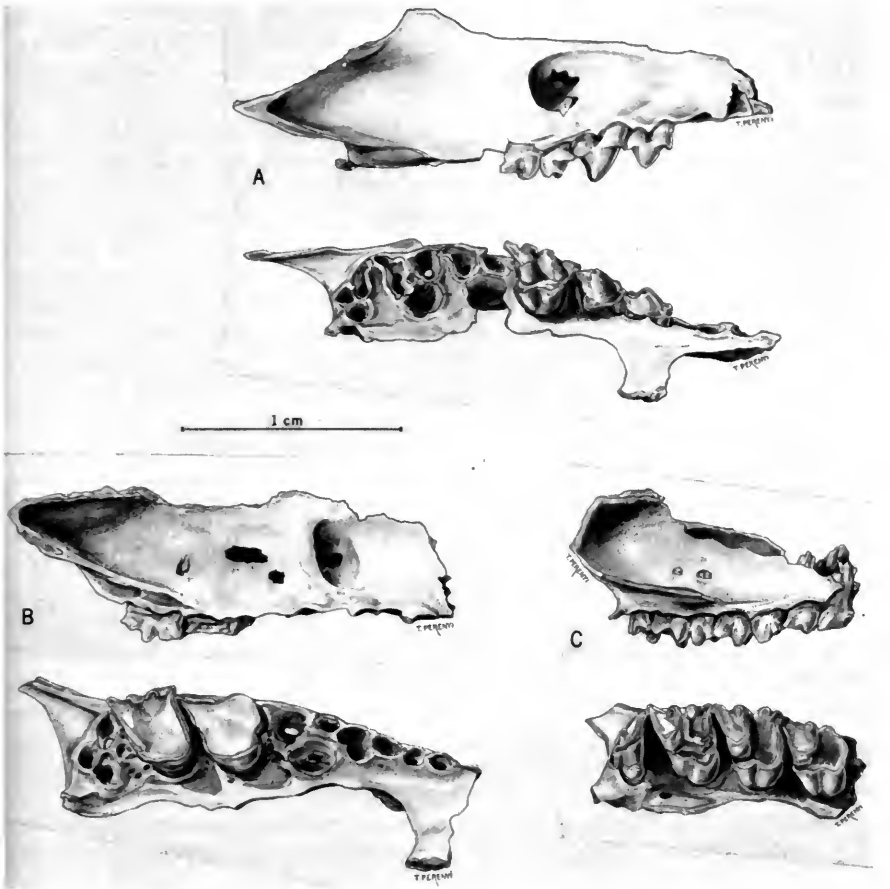

FIG. 4. *Perameles bougainvillei* from Madura Cave. **A**, TMM 41106-363, a right maxillary with P^3-M^1 shown in lateral and crown views. Specimen is from Trench 3, Unit 2, Level 1. **B**, PM 13340, a right maxillary with M^{2-3} heavily worn, shown in lateral and crown views. Specimen is from Trench 3, Unit 2, Level 1. **C**, TMM 41106-512, a right maxillary fragment with all molars, shown in the same standard views. Specimen is from Trench 4, Unit 1, Level 1.

inent stylar shelf with cusps that connect to the paracone (except M^1) and metacone (except M^4) by crests so that a characteristically pinched, double V-shaped ectoloph results. They are all three-rooted teeth. Many of these crown features may be eroded by wear, and it is a common occurrence to find specimens in which all crown features are gone (fig. 4B).

The M^1 is approximately square in occlusal outline, with the parastyle and metastyle projecting anteriorly and posteriorly, respectively, along the labial edge. The metacone is the most prominent cusp, but it is not nearly as massive as the less prominent protocone. It is joined to the metastyle and to stylar cusp l (ectostyle, see Hershkovitz, 1971) to form a prominent triangle. The paracone is usually joined only to cusp k and consequently it does not usually form the apex of a triangle. Rarely does M^1 have a weak crest to the parastyle. The protocone

and the hypocone are crescentic, and the protocone is the much larger of the two. The posterior crest of the hypocone extends around onto the posterior face of the metacone and rises towards the roots. A deep ectoflexus notch separates stylar cusps k and l.

The M^2 and M^3 are similar and will be described together. They both take the form of a truncated triangle in occlusal outline (fig. 4C), with the lingual side slightly shorter than the labial, although M^3 tends to be somewhat more triangular, with its lingually bulging protocone and more reduced hypocone. The metacone is the most prominent cusp, and its relationship to the stylar cusps is the same as with M^1. The paracone joins stylar cusp k and the parastyle by its crests. Protocone and hypocone are crescentic, the latter being much reduced in M^3. Other differences between M^2 and M^3 are related to the positioning of the stylar cusps; the parastyle and metastyle being located farther labially with respect to cusps k and l in M^3 than in M^2 where all stylar cusps are in a straight line.

The M^4 is reduced, especially posteriorly (fig. 4C). It is a triangular tooth, the longest edge being the transversely oriented anterior one. The paracone, which is the largest cusp, is located near the lingual edge of the tooth and is connected to the parastyle by a long paracrista (I′). A short postparacrista—premetacrista (I‴ a & b) or centrocrista (I‴)—extends posteriorly from the paracone and turns abruptly linguad at the posterior end of the tooth. The labial edge of the stylar area is almost straight from the parastyle to the posterior end of the tooth where it too turns abruptly linguad and makes a hooklike projection. This posterior cusp at the junction of the back of the stylar shelf and the centrocrista (I‴) could be a fused metacone-metastyle, but its homology is quite uncertain. Several small tubercles are present on the stylar shelf. The protocone is small and crescentic; its crests encircle the lingual part of the base of the paraconid.

Mandible.—The horizontal ramus of the mandible is slender (figs. 5-7). The ventral margin is convex beneath the molars and the P_4 and concave from there to the anterior end.[1] The dorsal edge of the horizontal ramus is twisted to the outside anteriorly. The symphysis is long, extending from the region of P_1-P_3 to the anterior end of the ramus. The symphysial area is concave, rugose, and has one prominent foramen. The lingual surface has a broad, shallow groove in the region underlying the molars. The major mental foramen is located under the P_2. Other small foramina are variably located both anterior and posterior to the large one.

The ascending ramus rises at a low angle to the tooth row (less than 45°). Its anterior margin has a complex outline. Only the relatively short coronoid process rises steeply (at about 80°), and its tip is hooked posteriorly. The lower half of the ascending ramus is convex, and its upper half is concave. The masseteric fossa is narrow and has essentially the same width throughout its length. The posteroventral margin of the masseteric fossa is marked by a distinct ridge that parallels the anterodorsal margin. The ventral margin is broadened laterally to form a short shelf with a tubercle above the base of the angular process. The angular process tapers rapidly and evenly to a point. Its inner surface is concave.

The mandibular foramen lies in a broad depression above the anterior part of

[1]In one specimen, TMM 41106-177 (fig. 6A, B), there is a prominent, pointed projection beneath P_3, which is an abnormality that probably resulted from an injury.

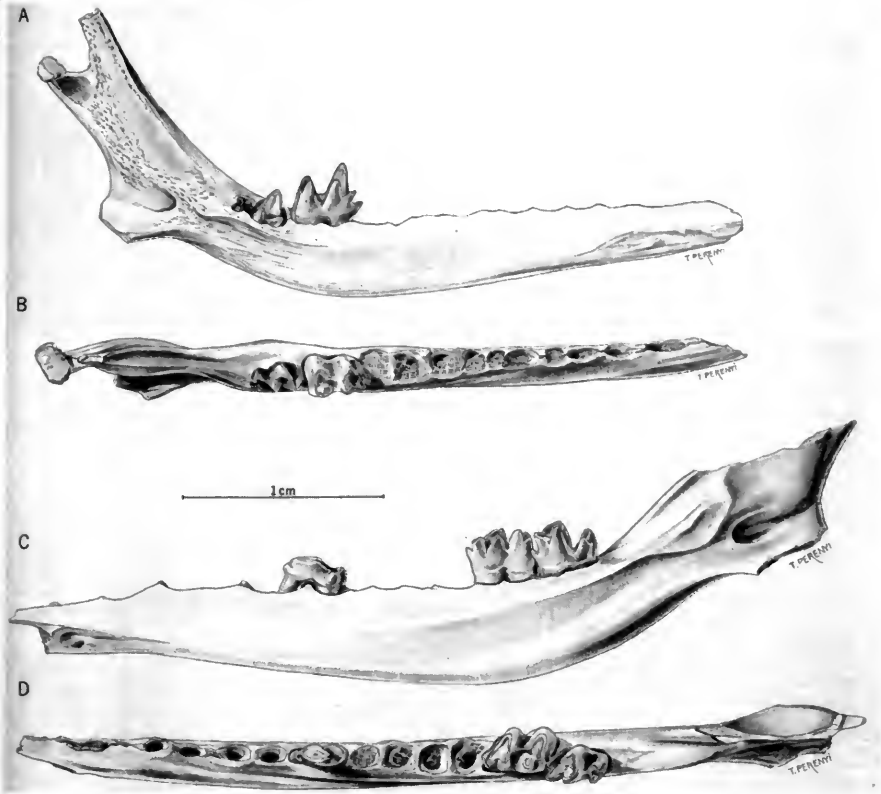

FIG. 5. *Perameles bougainvillei* from Madura Cave. **A & B,** TMM 41106-2771, a left mandible with M_{3-4}, alveoli of the rest of the dentition shown in lingual and crown views. Trench 4, Unit 2, Level 4. **C & D,** PM 27238, a right mandible with P_4, M_{3-4}, and alveoli of the other teeth, shown in lingual and crown views. Trench 4, Unit 2, Level 1.

the base of the angular process. The medial surface of the ascending ramus is smooth and slightly convex.

The condyle is high with respect to the tooth row and is close to the coronoid process. Its articular surface is oval in outline but is slightly concave transversely and convex anteroposteriorly.

There are diastemata between I_3 and C, between C and P_1, and a very short one between P_1 and P_3. That between I_3 and C is usually ridged (sometimes double ridged) and sharp, and the ridge is turned labially. That between the C and P_1 is usually double ridged, but occasionally is only single ridged. The double ridges tie to the labial and lingual borders of the alveolus for the canine.

Lower dentitions.—No Madura Cave specimen has an incisor in place. There are a great many isolated incisor teeth, but we cannot be certain about their taxonomic assignments. A number of I_3s that in the relatively unworn state are strikingly mitten-shaped most probably belong to this taxon because they compare closely with a sub-Recent specimen from Murraelellevan Cave (see figs. 1C, D; 2C, D; 3C, D). The alveolar pattern within the constricted anterior end of the

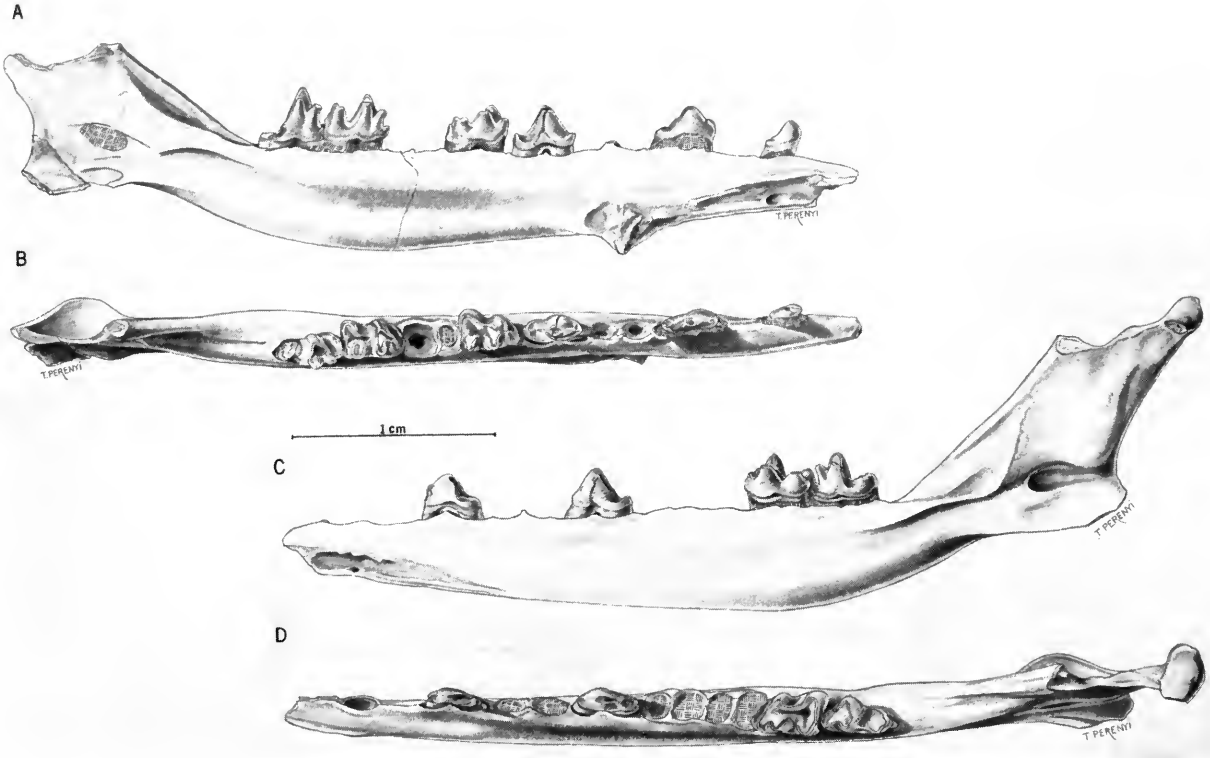

FIG. 6. *Perameles bougainvillei* from Madura Cave. **A & B,** TMM 41106-177, a left mandible with C, P_1 (or P_2), P_4, M_1, M_{3-4}, and alveoli of the other teeth, shown in the same standard views. Trench 3, Unit 2, Level 1. **C & D,** PM 27242, a right mandible with P_1 (or P_2), P_4, and M_{3-4}, alveoli of rest of the teeth, shown in the standard views. Trench 4, Unit 2, Level 1.

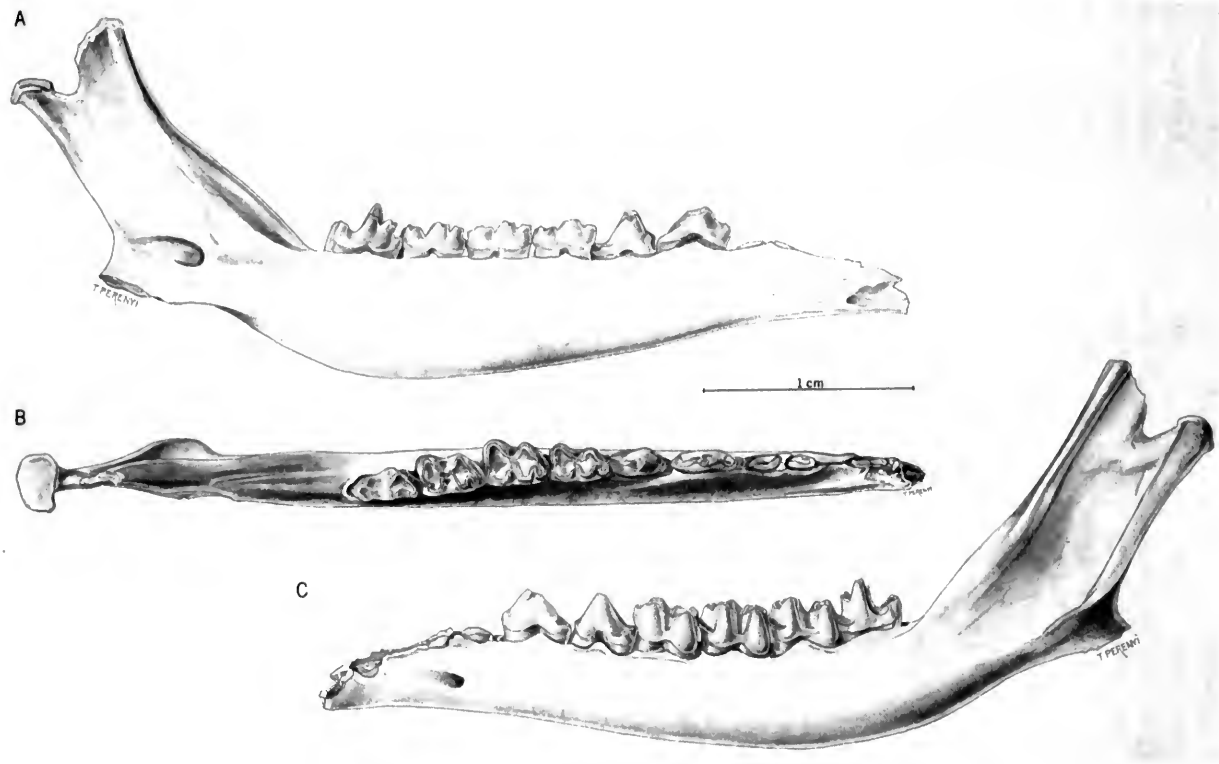

FIG. 7. *Perameles bougainvillei* from Madura Cave, TMM 41106-2753, a left mandible with P_3-M_4 and alveoli or roots of the other teeth, shown in lingual **(A)**, crown **(B)**, and labial **(C)** views. Trench 3, Unit 2, Level 1.

horizontal ramus shows a pinched condition of the roots whereby I_2 is consistently squeezed up into a higher position than I_1, which is always tight against the symphysis, and I_3, which is low and farthest laterally for most of the length of its root.

The lower canine is relatively short anteroposteriorly, low, and very compressed laterally. The anterior edge is rounded, and there is no anterior cingular cuspule. The posterior edge is narrow but not sharp in the unworn state and terminates ventrally in a posterior cingular tubercle. Wear occurs at the top and dorso-posterolingual side of the tooth and results in shifting the posterior ridge labially. No sexual dimorphism is apparent, either in the few specimens with canine teeth in place or in the many jaws with empty canine alveoli. Measurements of maximum anterior-posterior length at crown-root junction (normal to ramus) for the only specimens with canines in place and for the associated alveoli are:

Specimens	Crown length (mm)	Alveolar length (mm)
WAM 75.1.19	2.43	3.65
TMM 41106-172	2.60	3.65
TMM 41106-177	2.43	3.50

The two anterior lower premolars, here designated P_1 and P_3, are much alike. Each is double rooted, compressed laterally, and has its principal cusp located in the anterior half of the tooth and turned slightly lingually at its apex. They have anterior and posterior cingular cuspules. The anterior edge of the principal cusp of each is rounded, but the posterior edge has a thin sharp ridge in the unworn state. The posterior ridge that joins the posterior cuspule is rapidly modified by wear, most heavily on the lingual side of the posterior edge of the principal cusp. Both teeth have a faint posterior cingulum. The P_3 is the longest premolar.

The P_4 is approximately the same length as the P_3 but is less compressed laterally. Its principal cusp, which is located anterior to the mid-length, is relatively higher and wider than that of P_1 or P_3. Its lingual surface is flat, but the labial surface is strongly convex. Like the P_1 and P_3, the anterior edge of the principal cusp of P_4 is rounded, and the posterior edge is ridged. There are anterior and posterior cingular cuspules. The posterior one is joined by the ridge on the posterior edge of the principal cusp. A strong posterior cingulum extends over the posterior root on both sides. Wear rapidly removes the ridge on the posterior edge of the principal cusp, and in late wear stages the cusp is reduced to the level of those of P_1 and P_3.

All of the lower molars have a slightly modified tribosphenic pattern, and with the exception of the M_1 are rather rectangular in crown view. All have tooth base hypsodonty (White, 1959) but to a lesser extent than in the other peramelids in the Madura Cave assemblage (*Isoodon*, *Chaeropus*, and *Macrotis*). It is strongest under the labial cusps. The paracristid and epicristid in all molars lack a carnassial notch.

The trigonid of the M_1 is distinctly narrower than the talonid, with a protoconid that has a more rounded, less protruding lingual outline. The other trigonid cusps are smaller and more tightly spaced than in the more posterior molars. The protoconid and metaconid of M_1 are the same size, but the pro-

toconid is slightly higher in an unworn tooth. The paraconid is smaller and lower than the others and shows no tendency to be laterally compressed as is the case in many dasyurids. The hypoconid and entoconid are the main cusps of the talonid. They are approximately the same height but are differently shaped. The entoconid is circular in cross section when unworn and is not connected to any other cusp. It has an upstanding, high conical shape initially, and wear on its labial surface alters the cross section to an oval shape. The hypoconid is crescentic and is connected to the posterolingual part of the base of the protoconid and to the hypoconulid. The hypoconulid is low and projects backward. There is no posterior cingulum and usually only a trace of an anterior one. Sometimes the anterior cingulum is distinct but small, sometimes absent. A small cingulum occupies the notch between protoconoid and hypoconid near the base of the former.

The M_2 and M_3 are similar in size and morphology. Both have a trigonid that is wider than long, as a result of the far lingual placement of the protoconid and the closely spaced paraconid and metaconid. The protoconid and metaconid are equal in size and height; the paraconid is smaller. The talonid of both M_2 and M_3 is like that of M_1 in size and arrangement of the hypoconid and entoconid. The hypoconulid of M_2 is smaller than that of the M_1, and that of M_3 is virtually gone. In M_2, the posterior crest of the hypoconid joins the hypoconulid as in the M_1. In the M_3, this crest either joins the vestige of the hypoconulid or it disappears at the posterior side of the entoconid. Both teeth lack a posterior cingulum, and each has the small labial one between protoconid and hypoconid. The M_2 and M_3 differ from one another and from M_1 and M_4 in the size of the anterior cingulum. It is weakest on M_1 and becomes progressively larger toward M_4. The trigonid of the M_2 is narrower than that of the M_3. This character, which is easily observed in specimens with the teeth in jaws, is of little use in distinguishing isolated M_2s and M_3s because the variations in absolute size and extent of wear are great enough to cause broad overlap of measurements.

The M_4 resembles the M_2 and M_3 in the arrangement of its cusps, but it is narrower, and the relative sizes are different. The protoconid is the largest cusp, and the paraconid and metaconid are equal in size. The talonid is reduced in comparison with the other molars. A distinct basin is bordered by a tall conical entoconid and a crescentic hypoconid, the crests of which go to the anterior and posterior sides of the base of the entoconid. No hypoconulid is present. As a result of the failure of the cristid obliqua to join the epicristid, the talonid basin is joined to the trigonid only by the hypoflexid at the lingual edge of the tooth. The area labial to the hypoflexid slopes downward labially into another basin that is bordered labially by the cingulum that joins the protoconid and hypoconid.

Fossil bandicoots lose their teeth more readily than most other mammals. Hence, a high proportion of isolated teeth is encountered. The more distinctive first and last molars cause no problems of identity, but M^2s and M^3s are so similar to one another (as are M_2s and M_3s) that their separation is far less certain when they are recovered as isolates. The M^2s can be distinguished from M^3s most of the time by the more nearly equal-sized protocone and hypocone; also the M^3 has a smaller hypocone than the M^2. The stylar cusps of the M^2s tend to be arranged in a straight line, whereas in the M^3s the parastyle and metastyle tend to be located labial to stylar cusps k and l. Standard measurements fail to separate the M^2s and M^3s (fig. 8).

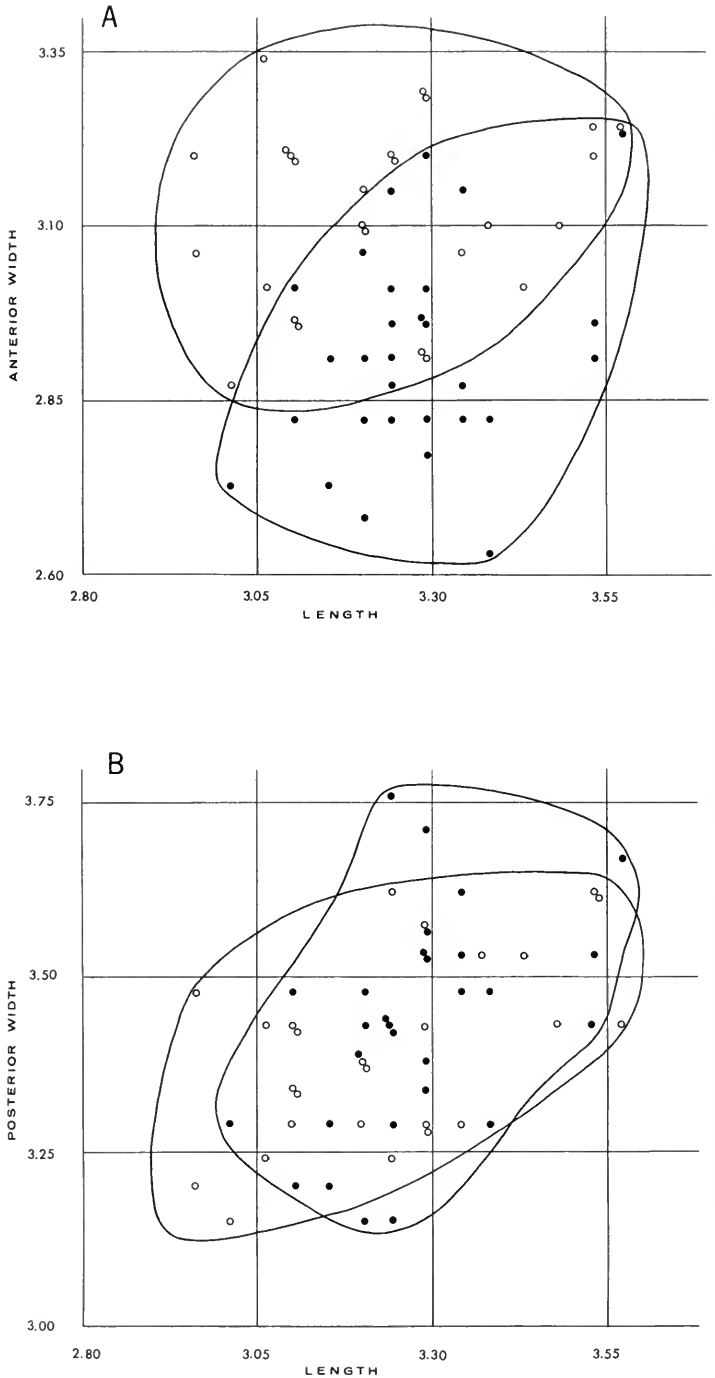

FIG. 8. Bivariate graphs of the cheek teeth of *Perameles bougainvillei*. **A & B,** Plots of length vs. anterior width and length vs. posterior width, showing extensive overlap of M^2s and M^3s. Initial determination based on visual criteria. All are from Trench 4, Units 4-5. Dots indicate M^2s, circles M^3s. Measurements are in millimeters.

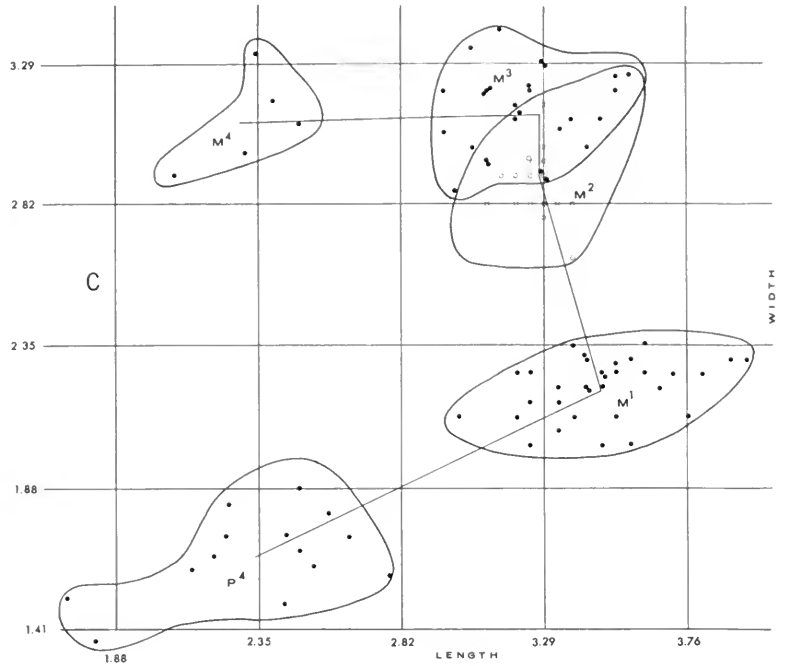

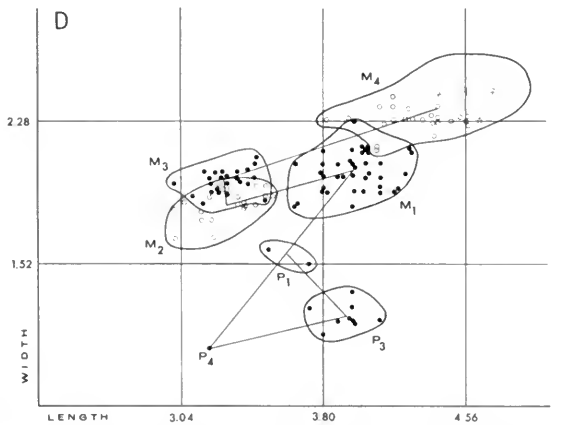

FIG. 8. **C & D,** Length vs. width plots of tooth measures for identified cheek teeth from Madura Cave. Means for each adjacent tooth are connected to form a pattern. In **C,** the upper cheek teeth are shown, in **D,** the lowers. For the premolars, the ordinate measure is the greatest width perpendicular to tooth length; for the molars, it is anterior width.

In crown view, the M2s differ from the M3s in having talonids that are relatively wider than the trigonids. Scatter diagrams of length versus anterior width and length versus posterior width show no separation (fig. 9B, C), but scatter diagrams of anterior width versus posterior width and length versus AW/PW confirm the visual observation, although the clouds of points almost touch (fig. 9A, D).

Discussion

Perameles bougainvillei (following Tate, 1948, and Wakefield, 1966, including *P. myosura*, *P. fasciata*, *P. notina*, and *P. eremiana*) is widely distributed through the drier parts of southern and western Australia (Shortridge, 1909; Jones, 1924; Troughton, 1962; Marlow, 1962; Freedman, 1967; Ride, 1970; Brooker, 1977). Abundant remains of *P. bougainvillei* that are found in surface deposits of caves

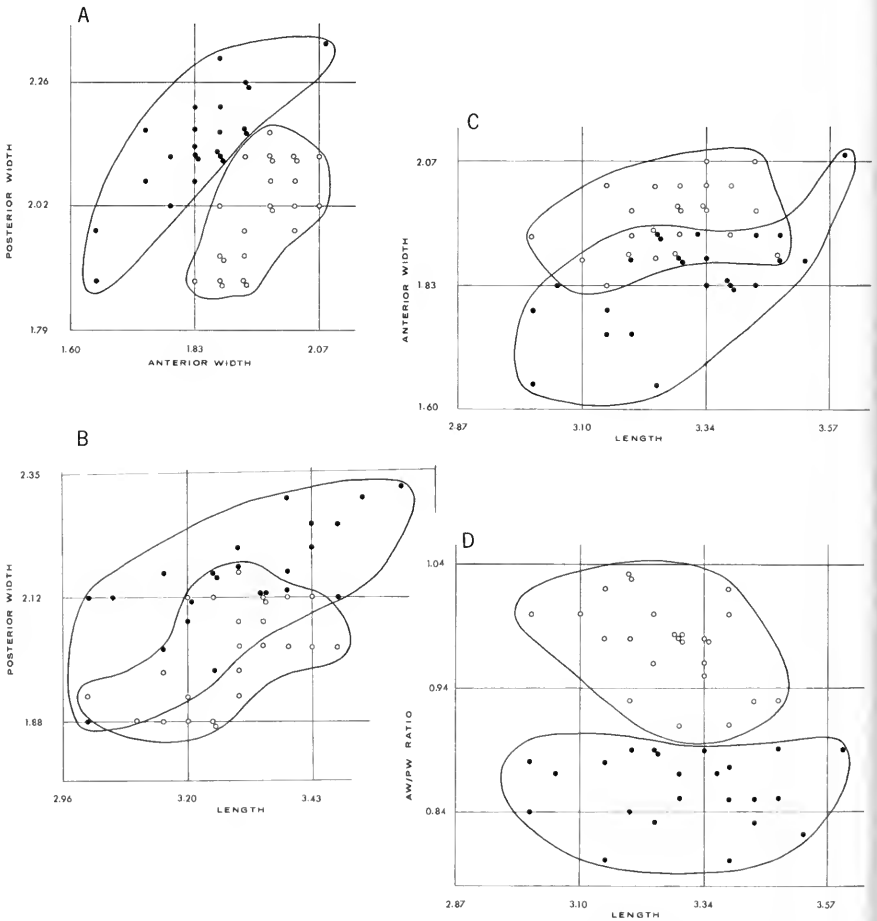

Fig. 9. Bivariate graphs of isolated M2s and M3s of *Perameles bougainvillei*. Initial determination based on visual (proportion) criteria. M2s shown by dots, M3s by circles. In **A** and **D**, complete separation is shown; in **B** and **C**, overlap.

on the Nullarbor Plain attest to its Pleistocene and Recent occupancy of this region. On the basis of means of dental measures, the Madura Cave populations are closer to the Recent South Australian *P. b. notina* sample analyzed by Freedman and Joffe (1967) than to the Recent *P. b. bougainvillei* sample from Bernier and Dorre Islands.

Parameles bougainvillei is found in abundance throughout the stratigraphic sequence at Madura Cave. A comparison of qualitative characters of samples from units 1 and 4-5 shows no apparent differences. It might be expected that the Pleistocene representatives of the species would be larger than those of Holocene age, as is the case with many mammals (Marshall, 1974; Marshall & Corruccini, 1978). A comparison of means for pairs of measures (tables 1, 2) shows that in most instances those of the samples from unit 4-5 are indeed larger than those from unit 1. One-sided "t" tests on nine sets of dental measures show significant differences in three cases (table 3). However, a sign test (Siegel, 1956, p. 68) for directionality of the differences of the means gives an insignificant result ($P = .090$ for a one-sided test). Clearly this is a borderline situation in which the differences between the materials from these two units are slight.

Smith (1972, p. 128, table 5) shows that a Pleistocene sample of *P. bougainvillei* from Victoria Cave in South Australia tends to have larger means than those of a Holocene sample from Fromm's Landing (also in South Australia; Wakefield, 1964). In this parallel case, four out of 13 one-sided "t" tests are significant (table 4). Here a sign test gives a significant result ($P = .046$ for a one-tailed test).

TABLE 1. Numerical data on some dental measurements of *Perameles bougainvillei* from units 1 and 2 of Madura Cave.

Variate	Sample size	Observed range	Mean ± standard error	Standard deviation	Coefficient of variation (%)
Unit 1					
M^1 L	10	3.24-3.76	3.48±.054	0.172	4.92
AW	9	2.05-2.66	2.35±.070	0.210	8.94
PW	9	2.82-3.47	3.16±.066	0.198	6.25
M^2 L	9	3.07-3.38	3.21±.038	0.117	3.58
AW	9	2.67-3.06	2.89±.054	0.161	5.56
PW	9	3.20-3.62	3.37±.041	0.123	3.60
M^3 L	4	2.91-3.20	3.07	0.129	
AW	5	2.98-3.20	3.11	0.102	
PW	4	3.29-3.38	3.34	0.038	
M^4 L	2	2.44-2.82	2.63		
AW	2	2.92-3.24	3.08		
PW	2	1.55-1.83	1.69		
Unit 2					
M_1 L	2	2.82-2.85	2.84		
AW	2	1.44-1.64	1.54		
PW	2	1.94-2.07	2.01		
M_2 L	3	2.94-3.29	3.14	0.169	
AW	3	1.82-1.93	1.88	0.047	
PW	3	2.18-2.28	2.23	0.047	
M_3 L	3	2.89-3.29	3.09	0.200	
AW	3	1.82-2.03	1.91	0.108	
PW	3	2.03-2.18	2.10	0.076	

TABLE 2. Numerical data on some dental measurements of *Perameles bougainvillei* from units 4-5 of Madura Cave.

Variate	Sample size	Observed range	Mean ± standard error	Standard deviation	Coefficient of variation (%)
M^1 L	32	3.01-3.95	3.48±.037	0.211	6.05
AW	32	2.02-2.35	2.21±.017	0.096	4.34
PW	32	2.30-2.68	2.53±.019	0.109	4.32
M^2 L	29	2.78-3.57	3.19±.034	0.181	5.67
AW	29	2.65-3.24	2.91±.028	0.151	5.17
PW	29	3.15-3.76	3.43±.030	0.159	4.63
M^3 L	26	2.95-3.57	3.23±.035	0.177	5.48
AW	26	2.91-3.34	3.12±.025	0.128	4.11
PW	26	3.15-3.62	3.39±.026	0.133	3.90
M_2 L	23	3.01-3.62	3.30±.034	0.163	4.93
AW	23	1.64-2.07	1.84±.020	0.094	5.10
PW	23	1.86-2.35	2.15±.022	0.107	4.99
M_3 L	24	3.01-3.48	3.28±.023	0.111	3.40
AW	24	1.86-2.07	1.96±.013	0.065	3.31
PW	24	1.86-2.16	2.01±.019	0.094	4.69

TABLE 3. Results of "t" tests of some dental measurements of *Perameles bougainvillei* from units 1 and 4-5 of Madura Cave.

Measurement	"t"	Degrees of freedom	Probability (one-sided test)
M^1 L	...**	...	...
AW	2.900	39	$P < .005$*
PW	12.628	39	$P < .001$*
M^2 L	.310	36	$.35 < P < .40$
AW	.342	36	$.35 < P < .40$
PW	1.036	36	$P > .15$
M^3 L	1.726	28	$P < .05$*
AW	.164	29	$.40 < P < .45$
PW	.737	28	$.20 < P < .25$

*Significant at .05 level.
**Means identical.

TABLE 4. Results of "t" tests on means of some mandibular and dental measurements of *Perameles bougainvillei* from Victoria Cave, South Australia, and Fromm's Landing, South Australia (based on data from Smith, 1972, table 5).

Measurement	"t"	Degrees of freedom	Probability (one-sided test)
Length M^{1-4}	2.497	6	$P < .025$*
Length ascending ramus	1.883	32	$.05 > P > .025$*
Mandible breadth at M_2	1.263	41	$.15 > P > .10$
Mandible height at M_2	0.741	38	$.25 > P > .20$
P_4 L	0.768	11	$.25 > P > .20$
M_1 L	0.067	5	$P > .9$
PW	2.473	6	$.05 > P > .025$*
M_2 L	3.875	11	$.005 > P > .0005$*
PW	1.420	10	$.1 > P > .05$

TABLE 4. *Continued*

Measurement	"t"	Degrees of freedom	Probability (one-sided test)
M_3 L	0.559	14	.30 > P > .25
PW	0.737	14	.25 > P > .20
M_4 L	1.364	15	.1 > P > .05
PW	0.131	15	.45 > P > ,40

*Significant at .05 level.

Both of these situations indicate a post-Pleistocene reduction in size in *Perameles bougainvillei*, although the magnitude of the change was less than that reported for larger animals (Marshall & Corruccini, 1978).

Isoodon Desmarest, 1817

Isoodon obesulus (Shaw and Nodder, 1797)

MATERIAL

Trench 2, 2½ ft

PM 25224, left ramus with M_3 and alveoli of P_4-M_2 and M_4 (fig. 11G)

Trench 4, Unit 1, top 1 ft

TMM 41106-568, fragment of upper molar
TMM 41106-669, right M^3
TMM 41106-672, left M^2 (fig. 11B)
TMM 41106-673, left M^3 (fig. 11D)
TMM 41106-675, left M_2
TMM 41106-677, right $M_{2 \text{ or } 3}$
WAM 75.1.124, left maxillary fragment with M^3
PM 26331, left ramus fragment with M_4, juvenile
PM 26362, very worn lower molar, probably M_1

Trench 4, Unit 2, Level 1

TMM 41106-708, right $M^{3 \text{ or } 2}$

Trench 4, Unit 2, Level 2

TMM 41106-705, left M^1 (fig. 11A)
TMM 41106-706, left $M_{2 \text{ or } 3}$
TMM 41106-710, left M^2
TMM-41106-711, right M^3
TMM-41106-712, left $M^{2 \text{ or } 3}$
PM 26307, left M_1 (fig. 11F)
PM 26334, left ramus with M_4 and condyle (fig. 11H)

Trench 4, Units 4-5

TMM 41106-709, right M^2
TMM 41106-714, right $M_{2 \text{ or } 3}$
TMM 41106-715-6, two right M^1s
TMM 41106-717, 19-20, three right M^3s
TMM 41106-721, right M^3 (fig. 11C)
TMM 41106-722, left M^3
TMM 41106-723, left M^2

Trench 4, Units 4-5 (continued)
TMM 41106-724, left $M^{2 \text{ or } 3}$
TMM 41106-725, left M^2
TMM 41106-726, left $M^{2 \text{ or } 3}$
TMM 41106-727, left M^2
WAM 75.1.125, left $M_{2 \text{ or } 3}$
PM 26308, left $M_{2 \text{ or } 3}$
PM 26309, talonid of a left lower molar
PM 26310, right $M_{2 \text{ or } 3}$
PM 26311, left $M_{2 \text{ or } 3}$
PM 26312, right M_4
PM 26313, left M_4 (fig. 11I)
PM 26314, left M^2
PM 26315, fragment of left $M^{2 \text{ or } 3}$
PM 26316, right M^1
PM 26317, left $M^{2 \text{ or } 3}$
PM 26320-3, four right M_1s
PM 26324, left $M^{2 \text{ or } 3}$
PM 26325, left M_3
PM 26326, right M^2
PM 26327, left M_4
PM 26328, left lower molar
PM 26329, left M_2
PM 26962, left M^4 (fig. 11E)
PM 27740, left $M_{2 \text{ or } 3}$
PM 30552, edentulous right ramus
PM 33660-2, three left M^1s

Trench 5, Unit 5
WAM 75.1.126-7, two broken right lower molars

Descriptions

Upper molars.—The upper molars have all the characters seen in extant specimens of *Isoodon obesulus* (fig. 10A-C). The first through the third molars are nearly square in occlusal view with moderate tooth base hypsodonty (White, 1959), especially in that part of the tooth that supports the protocone and hypocone. As with most peramelids, the labial part of the tooth is offset from the lingual part so that it extends farther ventrally (or where seen in palatal view appears to be raised above the lingual side).

The M^1 (fig. 11A, TMM 41106-705) is slightly rectangular in occlusal view. The anterior end is somewhat narrower than the posterior end. The wear facets indicate that the protocone is slightly taller than the hypocone in an unworn tooth, although wear rapidly brings them to the same level. They are joined at a higher level than the central basin. The protocone merges with an anterior lingual cingulum that extends across the anterior face of the tooth and nearly joins a smaller cingulum from the parastyle. A similar but larger postcingular ridge extends from the hypocone across the posterior face of the tooth nearly to the posterolabial corner.

The paracone is joined to the weak stylocone by a curved ridge that extends on to cusp k. The ridge joining the paracone and parastyle is sometimes faintly visible on the anterior face of the paracone (TMM 41106-705, -716, and PM 26316). The parastyle is much smaller than in the posterior molars. The metacone is joined to the anterolingual base of the mesostyle and to the metastyle to form a triangle as in M^2 and M^3. A smaller stylar cusp is present anterior to the metastyle in TMM 41106-705, -715, but is absent in -716 and PM 26316 (probably as a result of wear in the latter). The metastyle is located farther posterolabially than in most specimens of M^2 and M^3. In all of these features, the Madura Cave specimens conform to the comparative specimens available to us [TMM M-851, FMNH 98899 (fig. 10A, B), both Recent specimens; and PM 25506, -7, and -9, all Pleistocene to post-Pleistocene specimens from caves in the Margaret River area of Western Australia].

The M^2 and M^3 of *I. obesulus* are so alike that separation of isolated teeth is uncertain. They either lack a stylocone or have only a weakly developed one. They are square in contrast to those of *Perameles*, in which the labial edge is longer than the lingual edge (fig. 11B, C; TMM 41106-672, an M^2; and -721, an M^3).

The protocone and hypocone are crescentic when unworn and are joined above the level of the central basin. The protocone is slightly higher than the hypocone. In some specimens (TMM 41106-673, -709, -710, and -721), a low, indistinct ridge extends from the junction of the protocone and hypocone into the central basin where it disappears. This area of the tooth is flat in the other Madura fossils and in our comparative specimens. A ridge extends anteriorly from the protocone for a variable distance around the paracone. It disappears on the anterior face of the tooth near the base of the parastyle in TMM 41106-669 and -672. In TMM 41106-673 (fig. 11D) and -719, it joins the parastyle. A similar ridge usually extends posteriorly from the hypocone around the metacone almost to the posterolabial corner of the tooth. In TMM 41106-669, -712, and -720, this ridge disappears about halfway across the posterior face of the tooth.

The labial two-thirds of the occlusal surface is occupied by two triangles whose apices are the paracone and metacone. The paracone is not as tall as the metacone and is joined to the apex of the parastyle and the base of cusp k by the eocrista (I'y and I'''a, respectively). Cusp k has a crest that extends toward crest I'y in TMM 41106-673. It meets and joins a very weak crest from I'y in the intervening valley. The metacone is joined to the base of the mesostyle (the cusp lettered l) by the crista (I'''b) and to the apex of the metastyle by a crista (I''). A small stylar cusp (m) is present anterior to the metastyle.

Cusp k and the mesostyle (l) are approximately the same size, are larger than the parastyle and metastyle, and are weakly connected at their base. Cusp k is oval in cross section, and the mesostyle (l) is circular.

In an attempt to find a way of distinguishing M^2s from M^3s, and M_2s from M_3s, a number of bivariate graphs were drawn, based upon the usual dental measures, none of which gave plots without some degree of overlap of the clouds of points. Figure 12 shows two of these in which length vs. anterior width are plotted for four small samples of Recent and fossil specimens of *I. obesulus*. The most successful plot is shown in (A) wherein M^2s and M^3s can be separated about three-fourths of the time. The sort of plot shown in (B) for the same measures for the lower teeth is more typical, however, and illustrates the

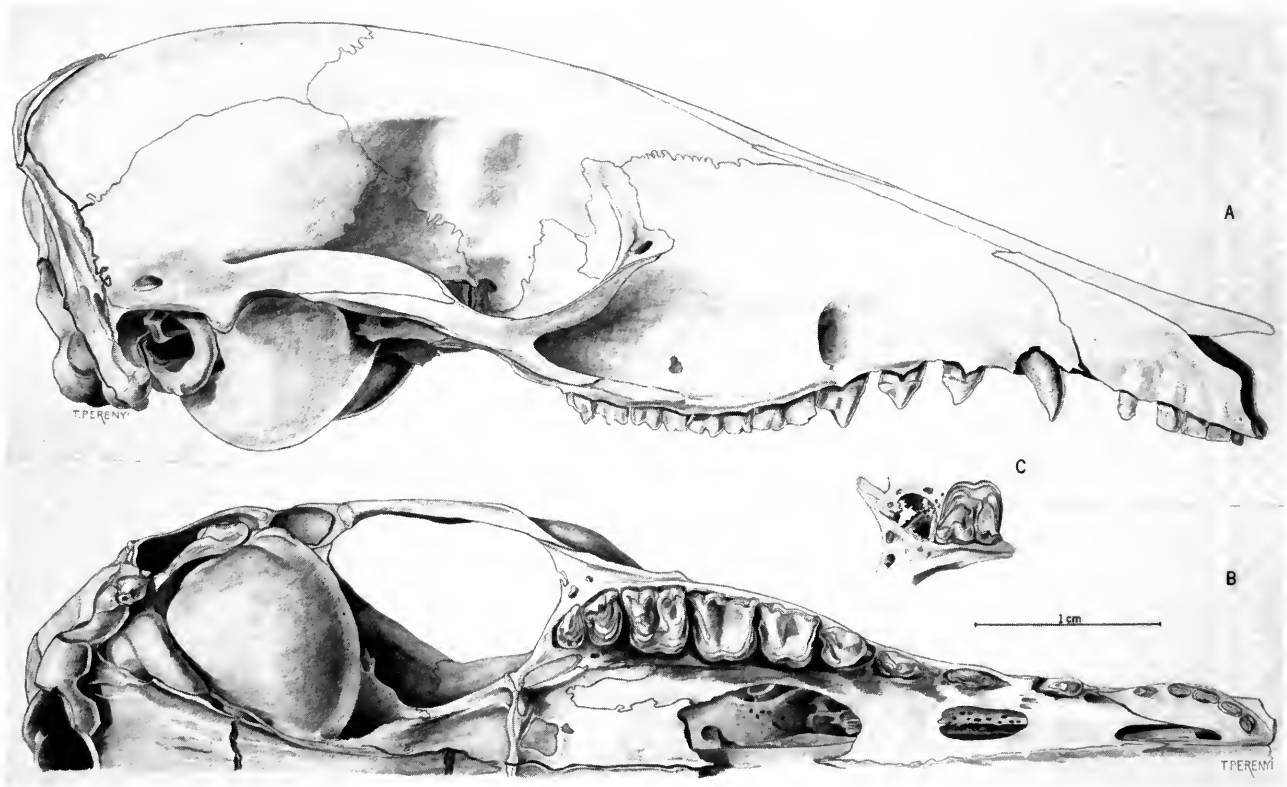

FIG. 10. *Isoodon obesulus affinis* (Waterhouse), FMNH 98899, from Wynyard, Tasmania. **A & B,** Right lateral and ventral views of the skull and its dentition. Note the aberrant condition shown by this individual; on the right side there are five molars, whereas on the left the usual four were present, **C** shows M^3 in place, and the alveoli of M^4 indicate the normal molar count for the left side.

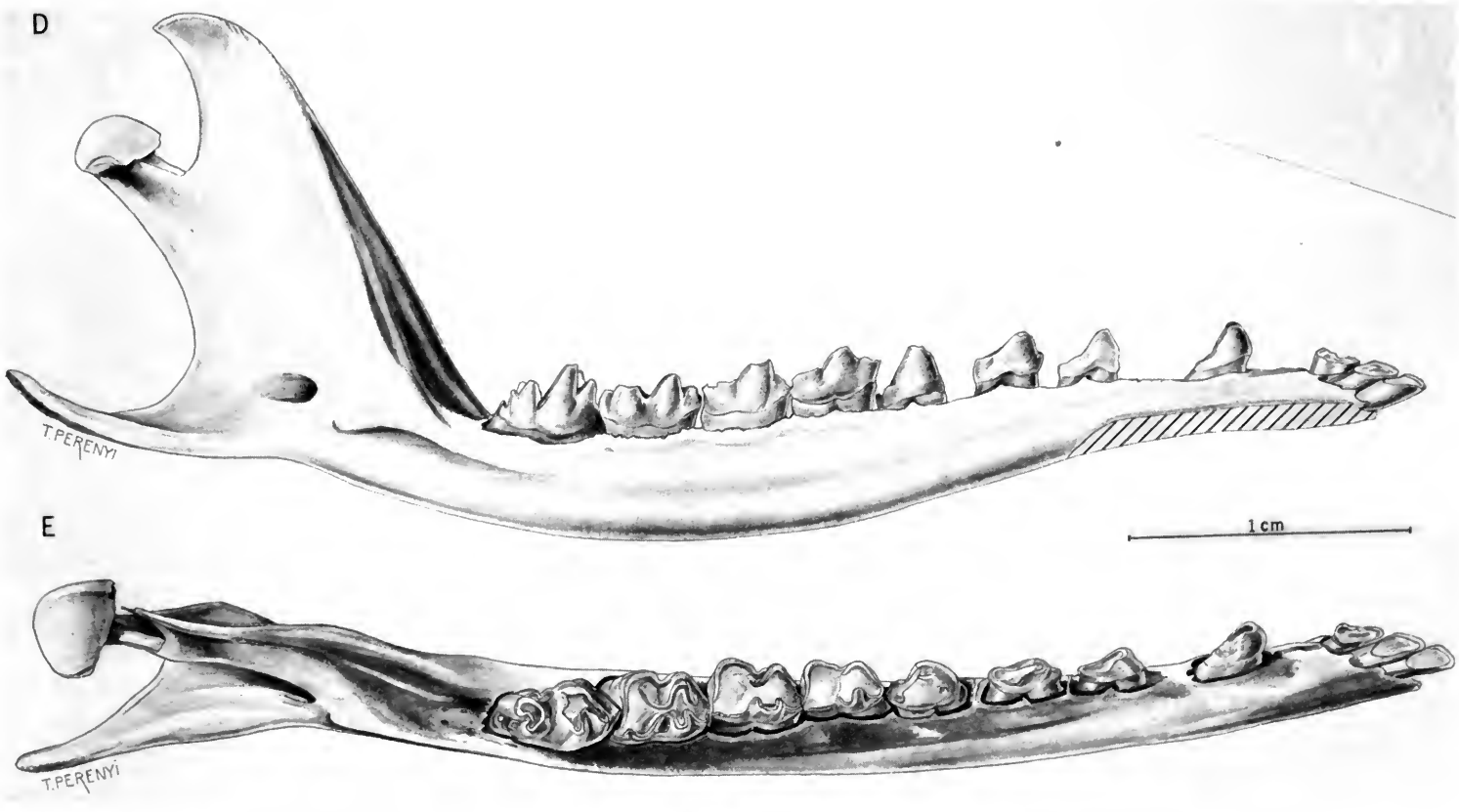

FIG 10. **D & E,** Lingual and occlusal views of the left mandible and its dentition. On both sides, the lower tooth count is normal.

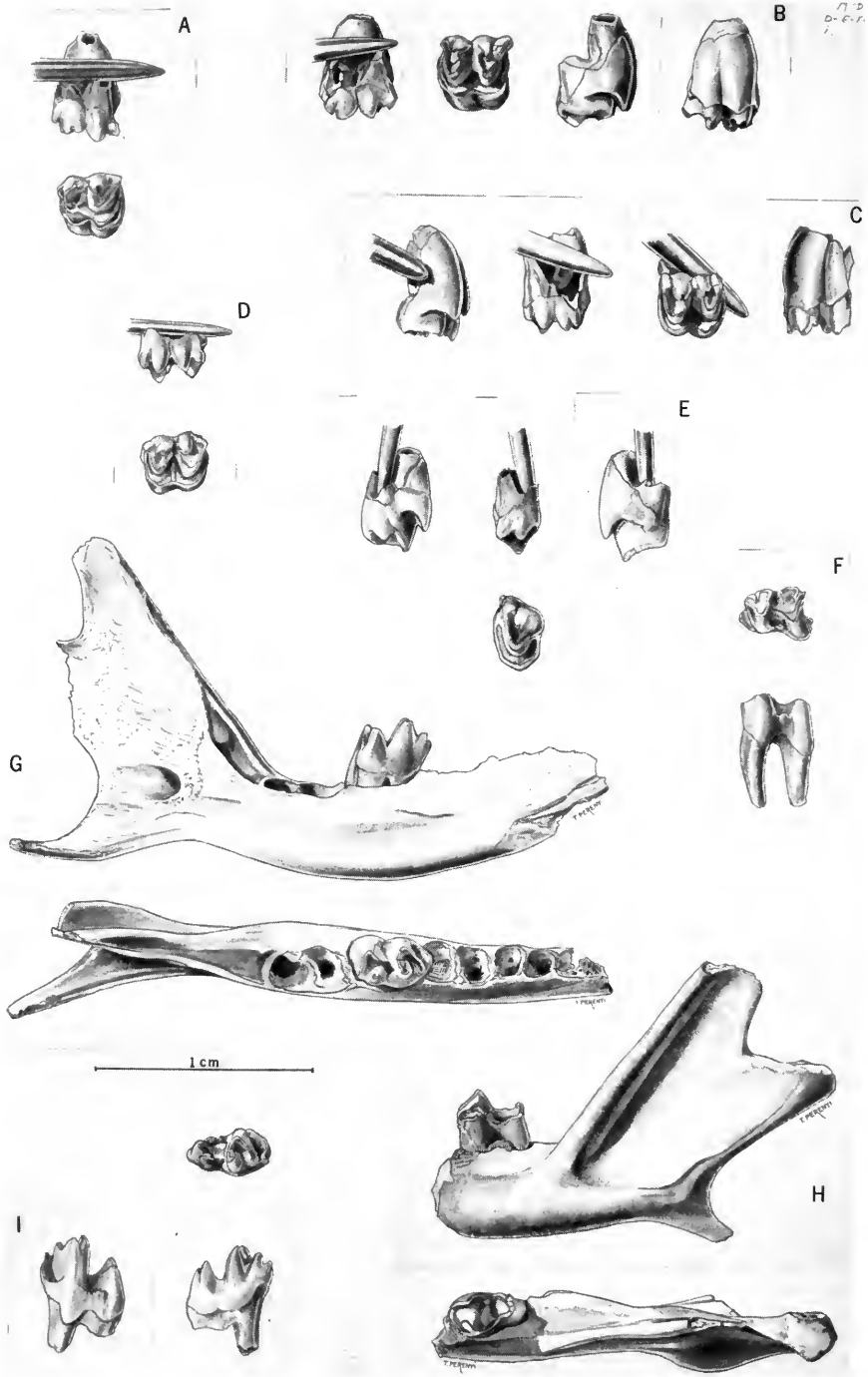
A
B
C
D
E
F
G
H
I
1 cm

need to find some discrete features or other kinds of dental measures than these standard ones if positive separations are to be achieved. Similar results were obtained with the Madura Cave teeth (fig. 13).

The M^4 differs from the other upper molars in the extreme reduction of the posterior cusps (fig. 11E; PM 26962). It is ovoid in occlusal view. There are three principal cusps—protocone, paracone, and cusp k. The paracone and protocone are crescentic cusps with prominent anterior and posterior ridges. Those of the paracone both reach the labial edge of the tooth. The anterior one joins a small, indistinct stylocone-parastyle at the labial edge of the tooth. The posterior ridge of the protocone reaches the labial edge of the tooth, but the anterior one does not. Cusp k is a conical cusp that is situated on the labial edge of the tooth between the ends of the ridges of the paracone. There is no trace of a posterior cusp, unlike the situation in most of the Recent specimens we have examined, which have a small posterolabial cusp.

Mandible.—Three partial mandibles of *Isoodon* are present in the Madura Cave collection. All represent the posterior part of the mandible. The horizontal ramus is slender and relatively shallower than that of dasyurids of comparable size. It is deeper and wider than that of *Perameles*. The angular process is directed inward and posteriorly, is broad basally, and tapers rapidly to a slender termination. The mandibular foramen is located above the anterior part of the base of the angular process.

The ascending ramus is broad. Its anterior border rises steeply, forming an angle of more than 45° with the line of the tooth row (fig. 11G, PM 25224). In this character, *Isoodon* resembles the dasyurines, *Chaeropus* and *Macrotis*, and differs from *Perameles* in which this angle is less than 45°, and the masseteric fossa is narrow. The ventral margin of the masseteric fossa is marked by a prominent shelf that is expanded laterally over the base of the angular process.

The condyle is located closer to the coronoid process than to the angular process. The articular surface of the condyle is broadly oval in outline (fig. 11H; PM 26334). It has no curvature transversely but is gently convex anteroposteriorly.

Lower molars.—All lower molars have well-developed trigonids but lack carnassial notches on the major crests. They have tooth base hypsodonty especially beneath the hypoconid. The trigonid is higher than the talonid on all molars.

The M_1 is an elongate tooth that tapers anteriorly (fig. 11F; PM 26307). The trigonid is distinct but relatively smaller than in M_2-$M_{2\text{-}4}$. The protoconid and metaconid are subequal, and the paraconid is distinctly smaller and lower. There is no anterior cingulum, but there is a slight concavity (on the anterolateral side of the tooth) between the protoconid and paraconid.

Opposite:

FIG. 11. *Isoodon obesulus* from Madura Cave. **A**, Crown and labial views of TMM 41106-705, a left M^1. **B**, Labial, crown, distal (posterior), and lingual views of TMM 41106-672, a left M^2. **C**, Proximal (anterior), labial, crown, and lingual (inverted) views of TMM 41106-721, a right M^3. **D**, Crown and labial views of TMM 41106-673, a right M^3. **E**, Distal, lingual, proximal, and crown views of PM 26962, a left M^4. **F**, Crown and labial views of PM 26307, a left M_1. **G**, Lingual and dorsal views of PM 25224, a left ramus with M_3, and alveoli of P_4-M_2 and M_4. **H**, Labial and dorsal views of PM 26334, a left ramus fragment with M_4. **I**, Crown, labial, and lingual views of PM 26313, a left M_4.

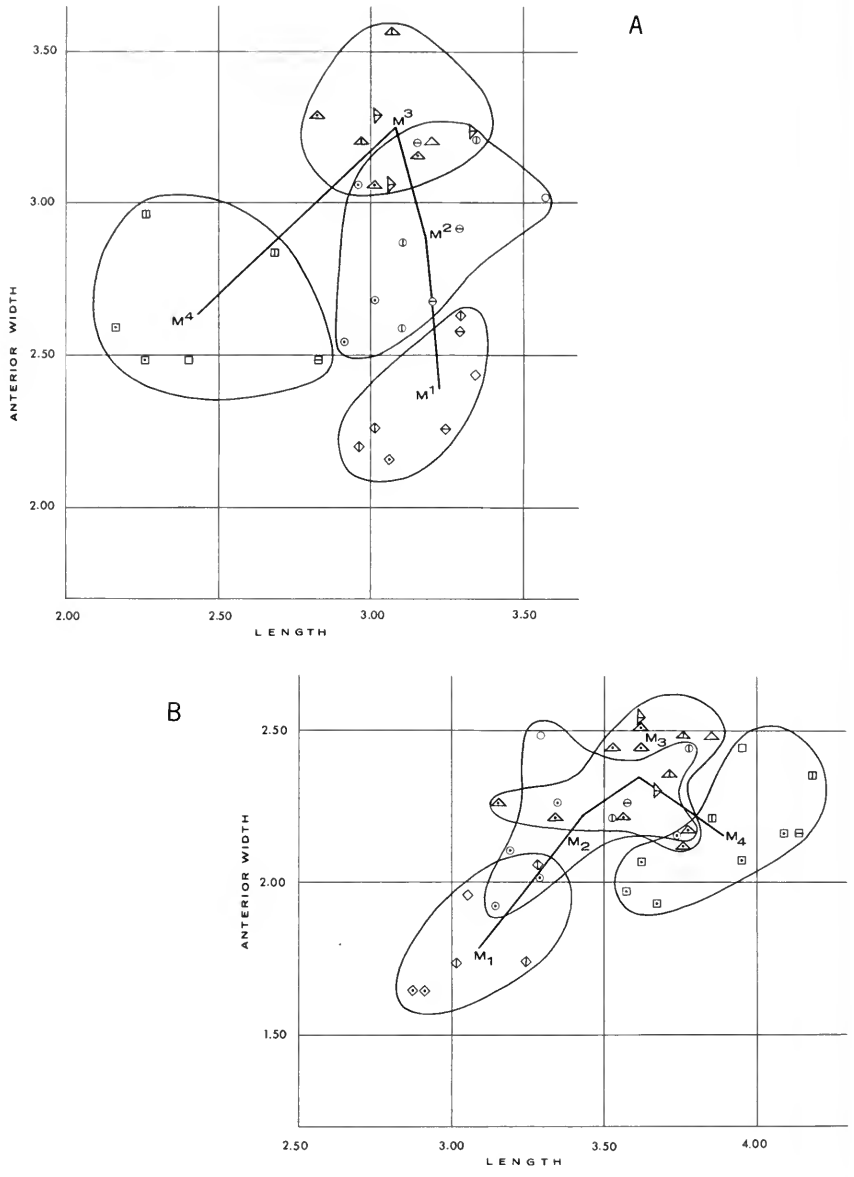

FIG. 12. Bivariate graphs of length vs. anterior width measurements of upper and lower molars of Recent and fossil specimens of *Isoodon obesulus*. In **A**, the bivariate plots for the upper molars show a clear separation for M^1s and M^4s, but only a partial separation between M^2s and M^3s. In **B**, similar plots for the lower molars show extensive overlap between adjacent teeth. Straight lines connect the midpoints of the plots for adjacent teeth. Measurements are in millimeters.

The talonid is broader than the trigonid. The entoconid is the highest cusp. It is subconical in shape and occupies almost all of the lingual edge of the talonid. The hypoconid is slightly lower than the entoconid but is more massive because of the underlying tooth base hypsodonty. The hypoconulid is the smallest of all the cusps and the most subject to erasure by wear. In an unworn or little-worn tooth, it projects posteriorly behind the entoconid in line with all the other lingual cusps.

The hypoconid is tapered toward its apex so that in an unworn or little-worn tooth its crests make a tight V. With wear, this V becomes more open. The cristid obliqua (I'''b) connects the hypoconid to the midpoint of the base of the epicristid (II) of the trigonid. The postmetacristid (I'') connects the hypoconid to the hypoconulid. In an unworn tooth, this ridge has a slight posterior curvature but becomes straight with wear.

There is a small cingulum in the reentrant between the protoconid and hypoconid. It may bear a small cuspule. In an unworn specimen, this cingulum is located halfway between the top of the cristid obliqua and the enamel line between the roots.

The M_2 and M_3 are so similar in both size and morphology (fig. 11G) that they cannot be reliably separated and are therefore treated together. Both are similar to the M_1 in general morphology. They can be distinguished from the M_1 by the presence of a prominent bulging anterolabial cingulum, a more massive trigonid, and larger size. The most consistent difference between M_2 and M_3 seems to be the degree of development of the hypoconulid: larger on M_2 than M_3. Since this feature is reduced by wear, it is best seen in unworn specimens (PM 26325, 26329). Recent specimens with all teeth in place show a gradual decrease in development of the hypoconulid from M_1 through M_3. The lingual cusps of the M_2 and the M_3 do not fall on a straight line as they do in *Perameles*, but form a curved line, with the paraconid and hypoconulid located labial to the metaconid and entoconid.

The M_4 differs from the M_{2-3} primarily on the structure of the talonid and its slightly greater length. The trigonid of the M_4 has the same construction as that of the M_{2-3} but is slightly more massive (fig. 11H, I; PM 26334 and PM 26313). The talonid is elongate but is otherwise reduced. The hypoconid and entoconid are the two principal cusps. The entoconid is higher, but the hypoconid is more massive and crescentic. The connection to the trigonid is variable, ranging from no ridge through a broad, rounded ridge, to a weakly developed, but sharp, ridge. The hypoconulid may be present or absent. Where present, it is small and below the notch between the hypoconid and entoconid. The cingulum between the protoconid and hypoconid is larger than on the other molars. It has a variable number of cuspules and isolates a small basin.

Comparisons.—A comparison of the Madura Cave specimens with Recent and fossil specimens from southwestern Australia shows them to be similar in morphology but different in size (table 5). The means of the measures of the Recent southwestern specimens are larger than those of the Madura Cave specimens, but there is overlap in many measures. A comparison of the Madura Cave material with specimens from Hasting's Cave, Western Australia (TMM 40236-3, -7, -8; PM 7272-81, PM 25510-15) shows that the remains from these two localities are alike both in size and morphology.

The smaller size of *Isoodon* from the drier areas of Australia has been noted in other studies. Wakefield (1964, pp. 494-498) reported that *Isoodon* from

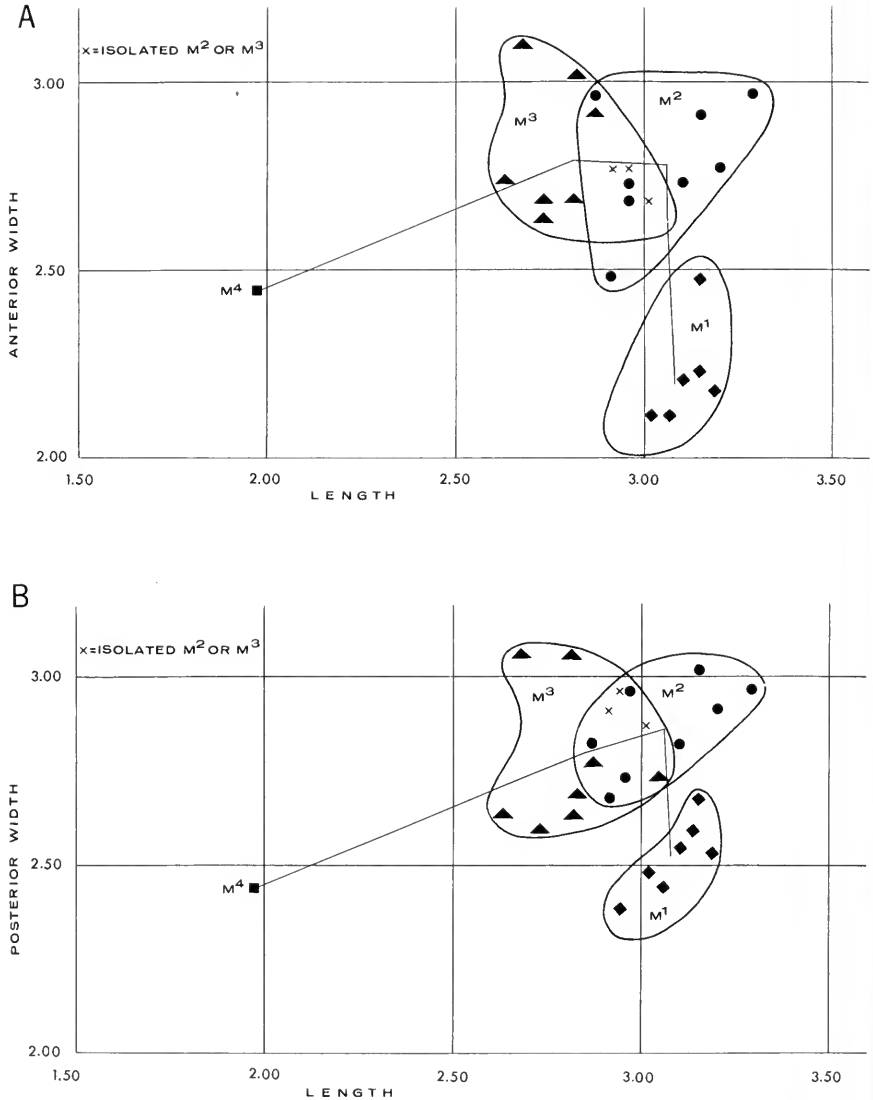

FIG. 13. *Isoodon obesulus* from Madura Cave. In **A & B**, bivariate plots of molar tooth measures of length vs. anterior width and length vs. posterior width are shown. The solid symbols designate teeth whose positions are known with certainty; the x symbols indicate isolated M^2s and M^3s, which we cannot distinguish from one another with certainty.

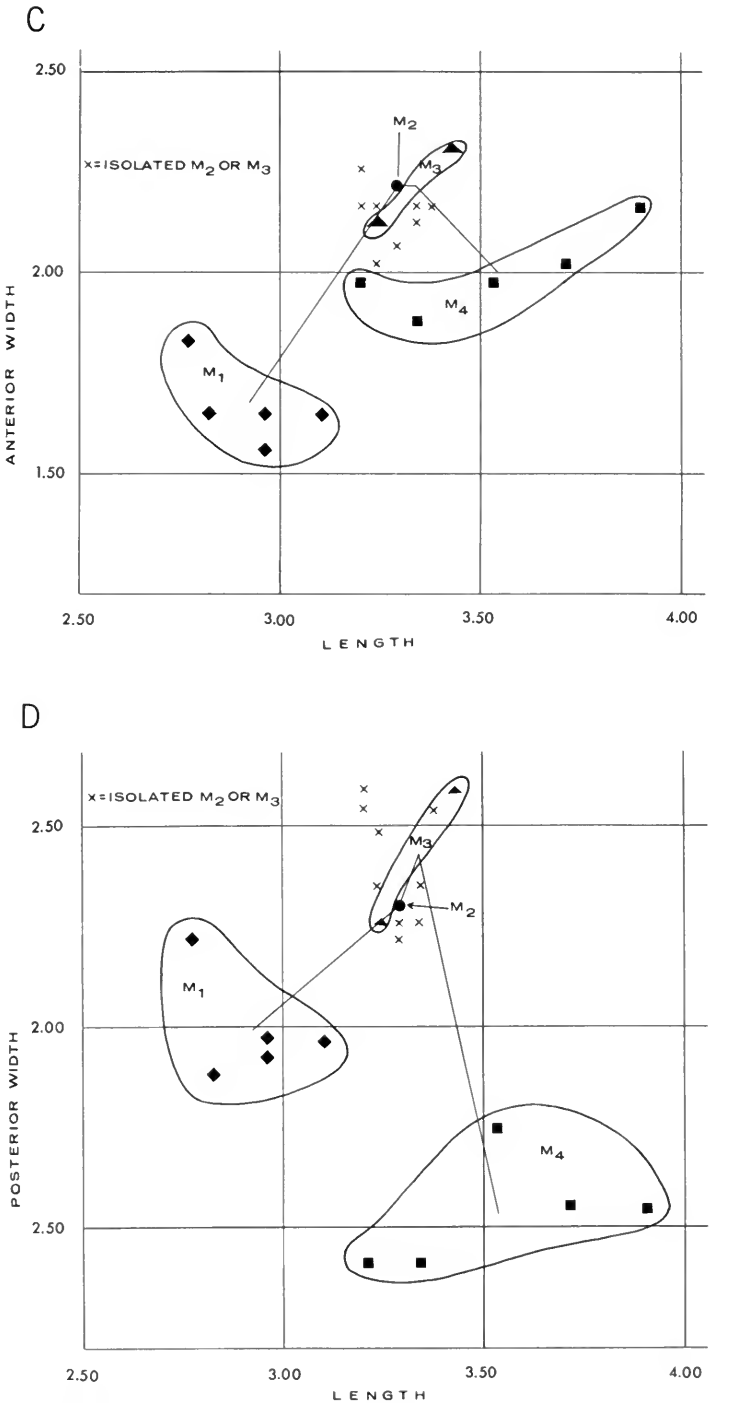

FIG. 13. In **C & D,** similar plots for the lower molars show extensive overlap of M_2s and M_3s. Isolated teeth indicated by *x*. Straight lines connect the midpoints of the plots for adjacent teeth.

TABLE 5. Numerical data on dentitions of various fossil and Recent samples of *Isoodon obesulus*.

	Madura Cave			Recent, southern Western Australia			Fossil, southern Western Australia			Hasting's Cave, Western Australia			
Variate	N	Observed range	Mean	N	Observed range	Mean	N	Observed range	Mean	N	Observed range	Mean	FM 98899 Tasmania
M^1 L	4	3.01-3.15	3.08	3	2.96-3.29	3.09	2	3.24-3.29	3.27	1	—	3.06	3.34
AW	4	2.12-2.49	2.24	3	2.21-2.63	2.37	2	2.26-2.59	2.43	1	—	2.16	2.44
PW	4	2.44-2.68	2.54	3	2.49-2.87	2.63	2	2.54-2.77	2.66	1	—	2.59	2.77
M^2 L	8	2.87-3.29	3.06	3	3.10-3.34	3.18	3	3.15-3.29	3.21	3	2.91-3.01	2.96	3.57
AW	8	2.49-2.96	2.78	3	2.59-3.20	2.89	3	2.68-3.20	2.93	3	2.54-3.06	2.76	3.01
PW	8	2.68-3.01	2.86	3	2.63-3.29	2.98	3	2.82-3.20	3.01	3	2.82-3.20	2.98	3.15
M^3 L	9	2.63-3.06	2.81	2	2.96-3.06	3.01	3	3.01-3.34	3.14	3	2.82-3.15	2.99	3.20
AW	9	2.63-3.10	2.79	2	3.20-3.57	3.39	3	3.06-3.29	3.20	3	3.06-3.29	3.17	3.20
PW	9	2.59-3.06	2.79	2	3.20-3.43	3.32	3	2.96-3.29	3.12	3	2.87-3.29	3.12	3.15
M^4 L	1	—	1.97	2	2.26-2.68	2.47	1	—	2.82	2	2.16-2.26	2.21	2.40
W	1	—	2.44	2	2.73-2.96	2.85	1	—	2.49	2	2.49-2.59	2.54	2.49
M_1 L	5	2.77-3.01	2.92	2	3.01-3.29	3.15	1	—	3.24	2	2.87-2.91	2.89	3.06
AW	5	1.55-1.83	1.67	2	1.74-2.07	1.91	1	—	1.74	2	1.65	1.65	1.97
PW	5	1.88-2.21	1.99	2	2.16-2.63	2.40	1	—	2.21	2	1.93-1.97	1.95	2.21
M_2 L	1	—	3.29	2	3.53-3.78	3.66	1	—	3.57	5	3.15-3.78	3.35	3.29
AW	1	—	2.21	2	2.21-2.44	2.33	1	—	2.26	5	1.93-2.26	2.10	2.49
PW	1	—	2.30	2	2.59-3.10	2.85	1	—	2.68	5	2.35-2.68	2.45	2.63
$M_{2 \text{ or } 3}$ L	9	3.20-3.38	3.28	—	—	—	—	—	—	—	—	—	—
AW	9	2.02-2.26	2.13	—	—	—	—	—	—	—	—	—	—
PW	9	2.21-2.59	2.40	—	—	—	—	—	—	—	—	—	—
M_3 L	2	3.24-3.43	3.34	2	3.71-3.76	3.74	2	3.62-3.67	3.65	7	3.15-3.78	3.54	3.85
AW	2	2.12-2.30	2.21	2	2.35-2.49	2.42	2	2.30-2.54	2.42	7	2.12-2.44	2.26	2.49
PW	2	2.26-2.59	2.43	2	2.68-2.91	2.80	2	2.73-2.82	2.78	7	2.12-2.82	2.44	2.63
M_4 L	5	3.20-3.90	3.54	2	3.85-4.18	4.02	1	—	4.14	5	3.57-4.09	3.78	3.95
AW	5	1.88-2.16	2.00	2	2.21-2.35	2.28	1	—	2.16	5	1.93-2.16	2.04	2.44
PW	5	1.41-1.74	1.53	2	1.97-2.12	2.05	1	—	1.79	5	1.50-1.65	1.56	1.97

Holocene deposits in the Fromm's Landing shelters are smaller than the modern ones from Western Victoria, but he gave no measurements. Small *Isoodon* from the arid zone of Australia were referred to *I. auratus* by Finlayson (1961). Marshall (1973) found no overlap in size in 13 dental measures of two samples of these small-sized *Isoodon* from central and Western Australia and a sample of *I. obesulus* from Victoria. His single specimen from a Holocene deposit at Lake Victoria falls within the range of the central Australian sample and accordingly was assigned to *I. auratus*.

The samples from Madura Cave and Hastings Cave are intermediate in size between those of *I. auratus* and *I. obesulus*, but are closer to the *I. obesulus* samples from southwestern Australia and Victoria (table 5). The significance of these size differences is not clear. Tate (1948) considered *I. auratus* to be a subspecies of *I. obesulus*. Marshall (1973) followed Finlayson (1961) and considered *I. auratus* to be a separate species. A revision of the genus is needed and is rendered more difficult in the face of the new evidence of the Madura and Hastings Caves samples. The Madura Cave material is referred to *I. obesulus* on the basis of the closer resemblance to modern samples of that taxon.

Discussion

Isoodon obesulus is found today in southwestern and southeastern Australia, Nuyts Archipelago, Tasmania, and Cape York Peninsula. *Isoodon macrourus* is found along the east coast of Australia, Arnhem Land, and north Kimberley. *Isoodon auratus* is found in northwestern Australia, central Australia, and Barrow Island (Ride, 1970). The record of *I. obesulus* in the deposits of Madura Cave is close to halfway between its westernmost record in South Australia (Kangaroo Island) and its easternmost record in Western Australia. Its presence in units 1, 2, and 4-5 demonstrates that it was an element of the faunas of terminal Pleistocene and early Holocene times on the Nullarbor Plain and that its disappearance from the area is relatively recent. Its absence from unit 7 may be an accident of sampling because the total amount of material recovered from that unit is small. We have been unable to find a definite record of its occurrence on the Nullarbor Plain within historic times. It is found today in situations that are considerably more mesic than exist now on the Nullarbor Plain, but it is also found in ones with xeric conditions similar to those of the Nullarbor (and with similarly erratic rainfall).

Merrilees (1967) has pointed out that the broad distribution of *Isoodon* with respect to rainfall in Western Australia throws doubt on its use as an indicator of climatic change. Heinsohn (1966) in a study of *Perameles* and *Isoodon* in Tasmania found that *Isoodon* kept to brushy areas even when feeding, whereas *Perameles* fed in more open situations. This suggests that the disappearance of *Isoodon* from the Nullarbor Plain in the last 7,000 years was caused by the disappearance of the appropriate vegetation, not by increasing aridity as such, although the change in plant cover is almost certainly a result of increasing aridity.

Palynological studies at Madura Cave indicate a decrease in the mallee cover from about 5,000 to 6,000 years B.P. to present (Martin, 1973). This change is attributed to a combination of increased aboriginal fire pressure and a decrease in rainfall. The climatic interpretations based on the disappearance of *Isoodon* are consistent with the pollen record.

Chaeropus Ogilby, 1838

Chaeropus ecaudatus Ogilby, 1838

Material

Trench 3, Unit 2
TMM 41106-695, right M^2 (fig. 16A)

Trench 3, Unit 3
TMM 41106-2763, edentulous right ramus fragment with alveoli of premolars (fig. 16D)

Trench 4, Unit 1, Level 1
TMM 41106-674, right $M_{2 \text{ or } 3}$
PM 27218, right $M^{2 \text{ or } 3}$ (fig. 16B)
PM 36828, right $M_{2 \text{ or } 3}$ (fig. 16F)

Trench 4, Unit 2, Level 1
TMM 41106-670, right $M_{2 \text{ or } 3}$
TMM 41106-671, right $M_{2 \text{ or } 3}$

Trench 4, Units 4-5
TMM 41106-683, right $M_{2 \text{ or } 3}$ (fig. 16E)
WAM 75.1.140, left M^2 (fig. 16C)

Trench 4, Unit 7, Level 2
WAM 75.1.141, right $M_{2 \text{ or } 3}$
TMM 41106-731, left M^2
TMM 41106-732, left M^2
PM 26333, left $M_{2 \text{ or } 3}$

Descriptions

This is the rarest bandicoot in the Madura Cave fauna, with only 13 specimens recognized as representing the taxon. The molar teeth are quite unmistakable because of their disproportionate labial and lingual hypsodonty. This condition gives the molars a characteristic diagonally sloping crown surface and renders them easily recognizable.

We have no Recent comparative material, hence comparisons are made with more complete sub-Recent fossils from other Nullarbor Caves, including: a right maxillary with M^1 from Weebubbie Cave (fig. 14A, PM 36806); a right maxillary fragment with $M^{1\text{-}3}$ (fig. 14C, TMM 41209-572) and a left maxillary fragment with $M^{1\text{-}4}$ (fig. 14B, TMM 41209-885), both from Webb's Cave; a right mandible with P_1, P_4, and $M_{3\text{-}4}$ from a cave between Kestrel #1 and #2 (fig. 15A-C, PM 36807); and a right mandible with P_1 and $M_{2\text{-}4}$ from Webb's Cave (fig. 15D-F, TMM 41209-573).

A characteristic of *Chaeropus* upper molar teeth is their shallow root condition. This makes them especially prone to dropping out after death. The alveoli of these teeth are distinctive too: the labial pair are deepest, but are very compressed anteroposteriorly, whereas the lingual two are fused into one, which is much expanded to accommodate the nearly completely fused roots supporting the paracone and hypocone (fig. 14A). A faint ridge marks the line of fusion and gives a slight constriction to the oval alveolar outline.

In the mandible, the alveoli of the molars are deeper to accommodate the

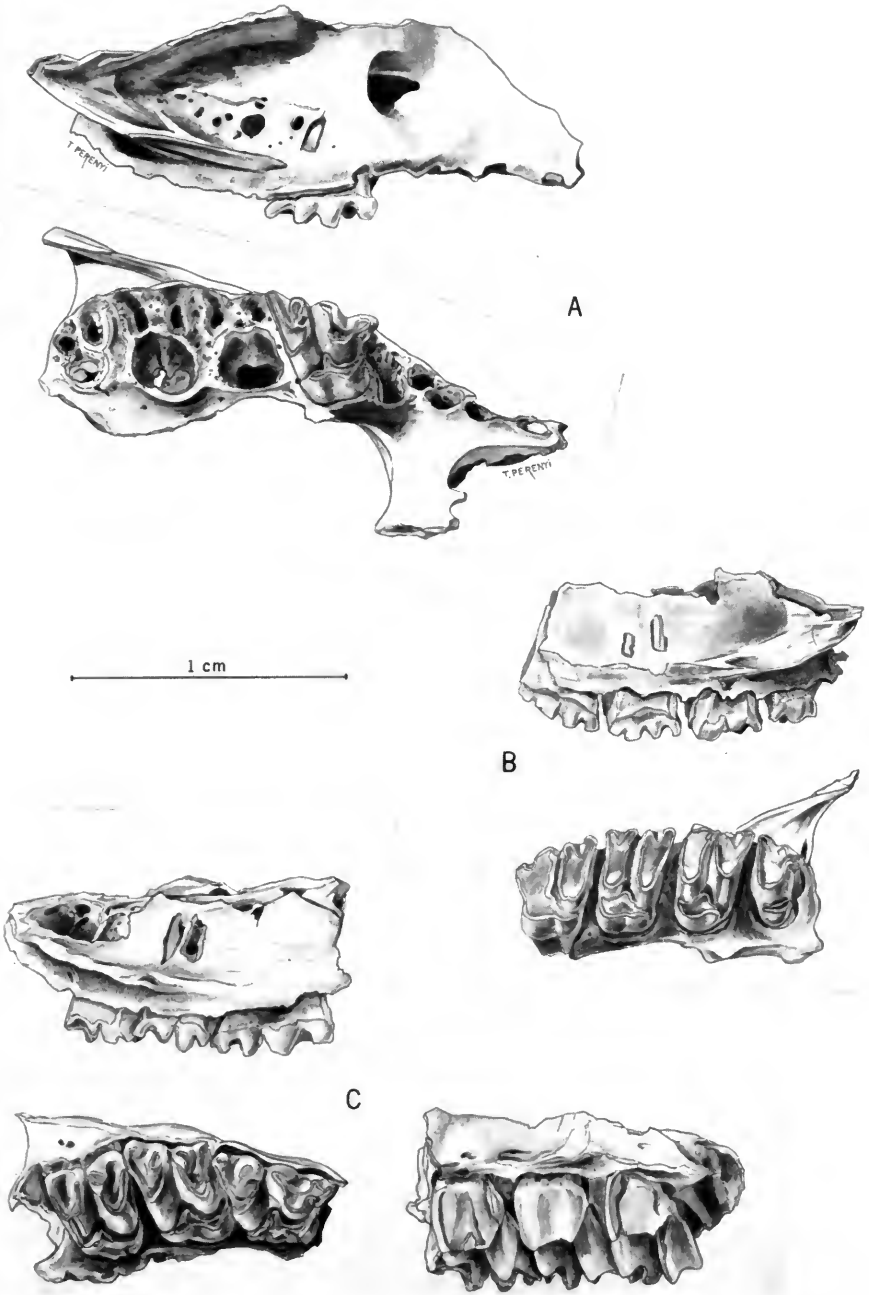

FIG. 14. *Chaeropus ecaudatus*, sub-Recent fossil specimens from several other Nullarbor Caves. A, PM 36806, a specimen from Weebubbie Cave (north of Eucla, Western Australia) that consists of a right maxillary with M^1 and that preserves the alveoli of the other molars, the premolars, and the canine. It is shown in labial and palatal views. B, TMM 41209-885, a left maxillary fragment with M^{1-4} from Webb's Cave, shown in labial and crown views. C, TMM 41209-572, a right maxillary fragment with M^{1-3} from Webb's Cave, shown in labial and crown views.

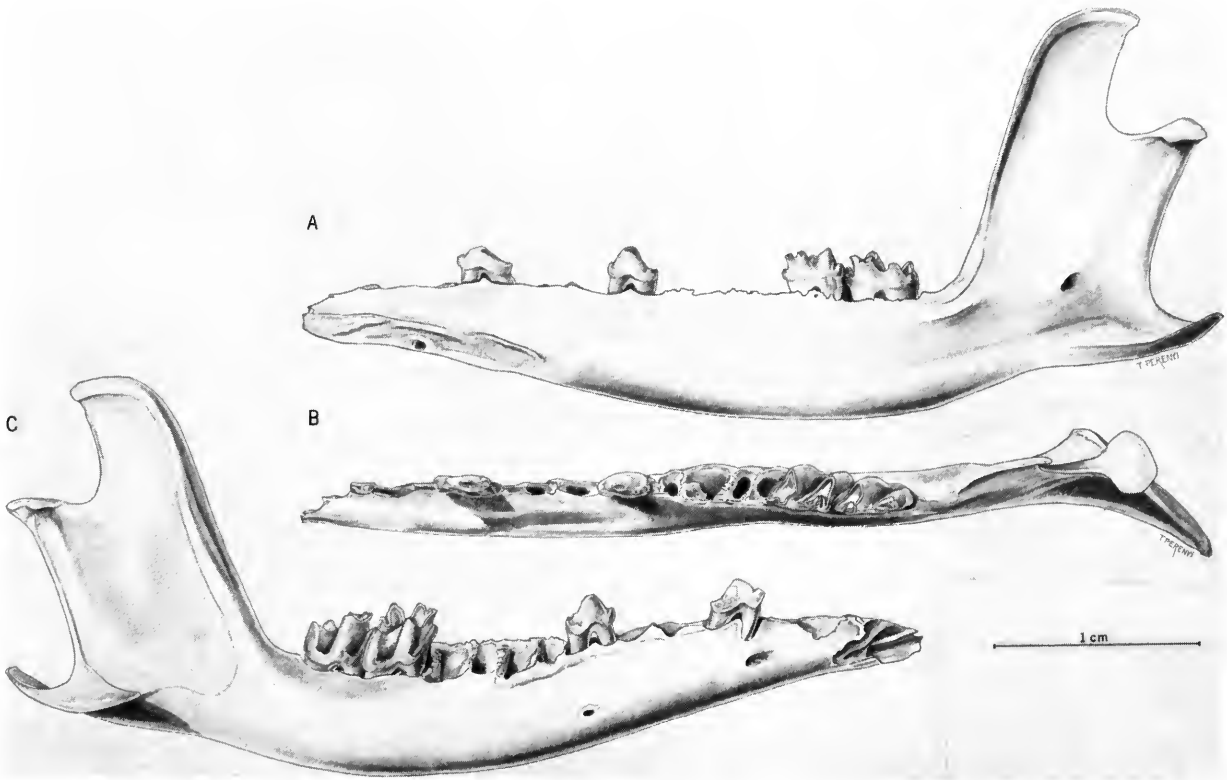

FIG. 15. *Chaeropus ecaudatus*, sub-Recent fossil specimens from several other Nullarbor Caves. **A-C**, PM 36807, a right mandible with P_1, P_4, M_{3-4}, and the alveoli of the rest of the teeth, from a cave between Kestrel #1 and #2, shown in lingual, occlusal, and labial views.

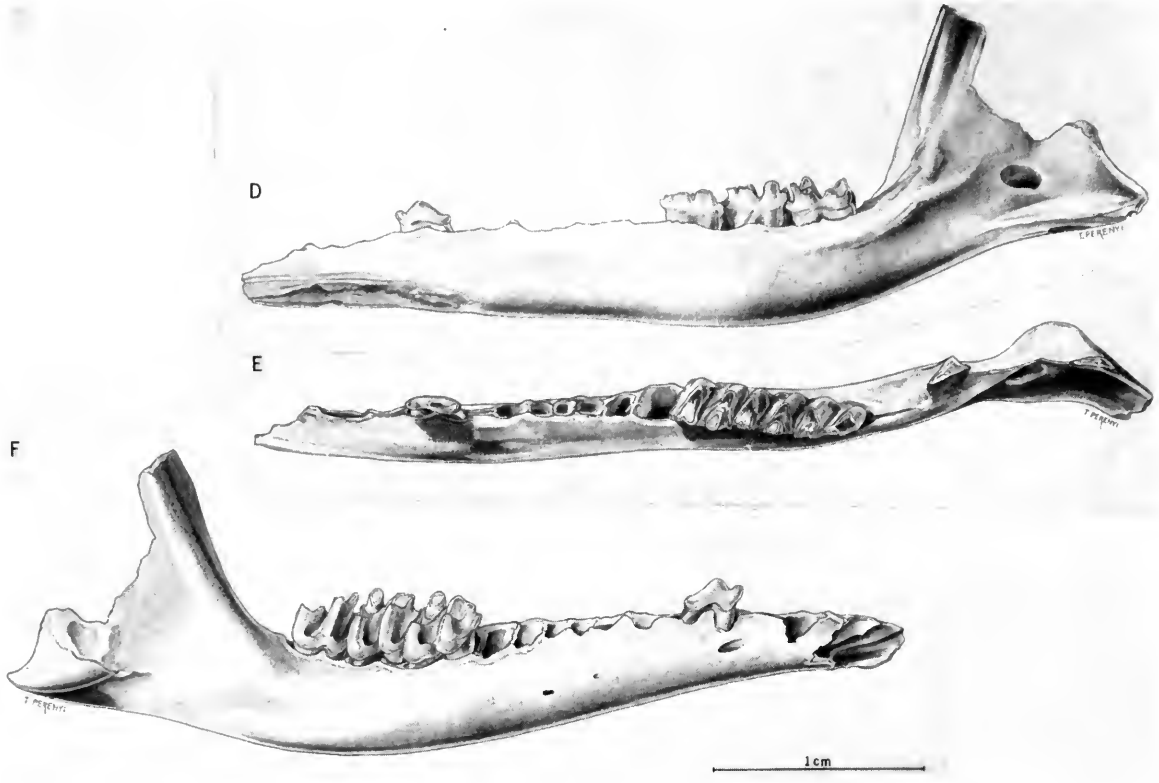

FIG. 15. D-F, TMM 41209-573, a right mandible with P_1, M_{2-4}, and alveoli of the other teeth, from Webb's Cave, shown in lingual, occlusal, and labial views.

long, tapered roots of the molar teeth. The labial side of the alveolar margin is markedly lower than the lingual side (fig. 15C, F), and the ramus is deeper than in *Perameles*. The ascending ramus is wide from front to back, very different from its narrow condition in *Perameles*, and is much more like that in *Isoodon*.

Upper molars.—The upper molars are square in crown view and have a peculiar sort of tooth base hypsodonty, especially that part of the tooth underlying the protocone, hypocone, paracone, and metacone. The stylar area of the tooth is significantly less hypsodont. No M^1s or M^4s are present in our Madura Cave sample.

The M^2 and M^3 are very similar (table 6; fig. 17A) but usually can be distinguished by features of the stylar shelf. Two specimens from Webb's Cave (TMM 41209-572, -885; fig. 14B, C), which have $M^{1\text{-}3}$ and $M^{1\text{-}4}$, respectively, show that M^2 has the metastyle more labially located than does M^3. This results in reversed asymmetries in the shape of the ectoloph, especially in little-worn teeth. In M^3, the metastyle protrudes farther labially than the other cusps; in M^2, the parastyle is the more labial cusp. These specimens also show that the M^2 is further characterized by a rounded ridgelike extension of stylar cusp 1 into the V formed by the ridges of the metacone. If these specimens are typical, it seems unlikely that any M^3s are present in the Madura Cave collection. TMM 41106-695 (fig. 16A) is used to illustrate the upper molars.

The protocone is crescentic when unworn. It is higher and more extensive than the hypocone. Anteriorly, the protocone extends rootward onto the anterior face of the tooth. Posteriorly, it extends around the base of the paracone and into the central basin between the paracone and the metacone. The hypocone is a flattened column that expands toward its base. It is fused to the posterior limb of the protocone nearly to its apex. When worn, the posterior part of the protocone that projects labially into the curved valley appears to be a spur from the joined protocone and hypocone. Posteriorly, the hypocone extends rootward to the posterolingual corner of the tooth. There is a broad but prominent vertical groove on the lingual face of the tooth that separates the protocone and hypocone. This groove is better developed in *Chaeropus* than in *Isoodon*.

The paracone and metacone are very high, prominent cusps that, as in *Isoodon*, are the apices of V's that open on the labial border of the tooth. The metacone stands higher than the paracone. The paracone is joined to the parastyle (a) via the stylocone (j) by a straight eocrista (preparacrista or I'x). A straight postparacrista (I'''a) joins the paracone with the posterior side of the base of cusp k.

The metacone is joined to the metastyle by a postmetacrista (I'') and to the anterior side of the base of the mesostyle (cusp l) by a premetacrista (eocrista or I'''b). A distinct, small stylar cusp m is present on TMM 41106-695 and PM 27218 (fig. 16A, B). It would be rapidly removed by wear and therefore is not distinguishable on worn teeth.

As in *Isoodon*, the cusp k and the mesostyle (cusp l) are about the same size and are larger than the parastyle and metastyle. Both cusps, k and l, are oval in cross section with their long axes oriented nearly transversely. Cusp k gives rise to a ridge that extends lingually from its apex for a short distance between the arms of the paracone crests, turns posteriorly, and joins the postparacrista. The mesostyle gives rise to a ridge that extends deeply into the V between the crests

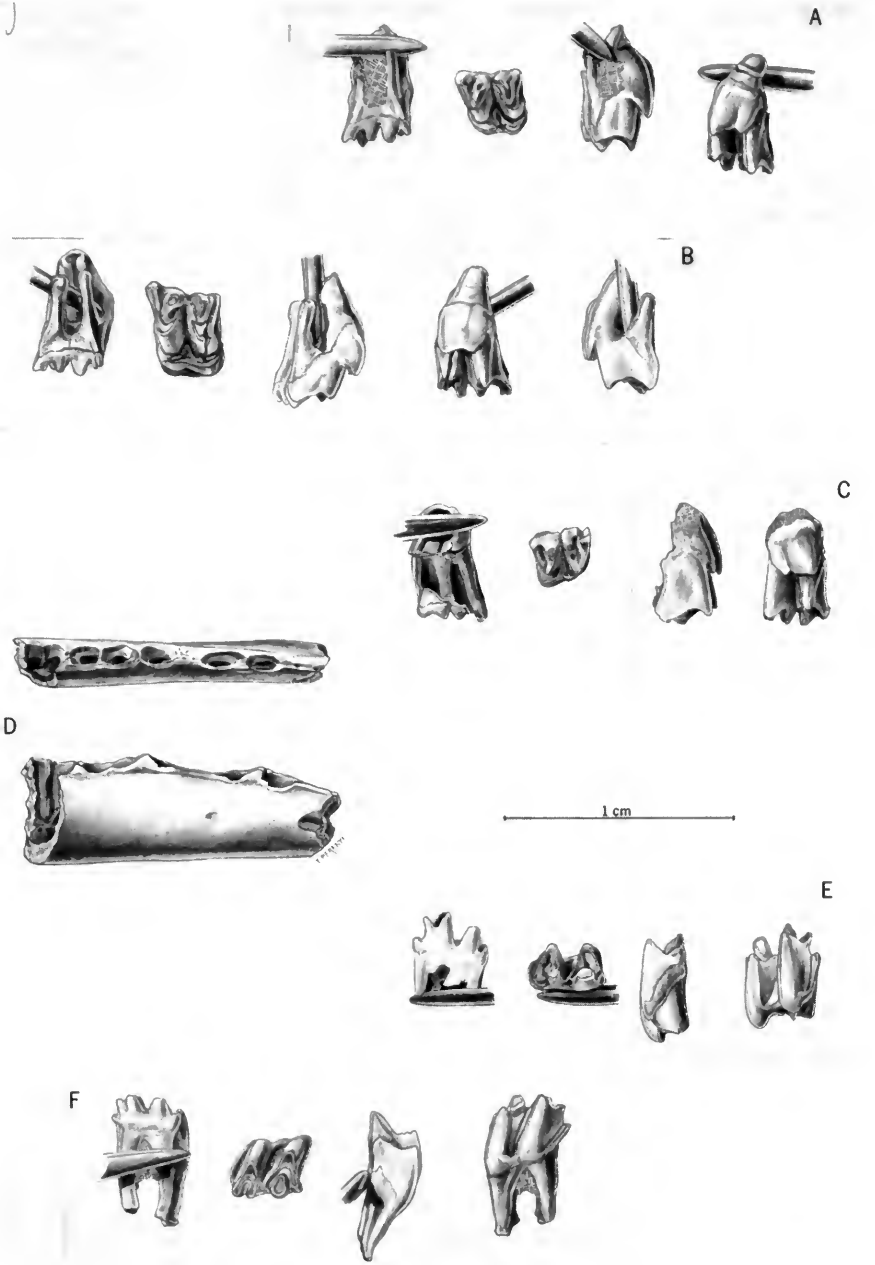

FIG. 16. *Chaeropus ecaudatus* from Madura Cave. **A,** TMM 41106-695, a right M^2 shown in labial, crown, anterior (mesial), and lingual views. **B,** PM 27218, a right M^2 or M^3 shown in labial, crown, anterior (mesial), lingual, and posterior (distal) views. **C,** TMM 41106-684, a left M^2 shown in labial, crown, anterior (mesial), and lingual views. **D,** TMM 41106-2763, an edentulous right ramus fragment with the alveoli of the three premolars shown in dorsal and lateral (labial) views. **E, F,** TMM 41106-683 and -694, two right M_2s or M_3s shown in lingual, crown, anterior (mesial), and labial views.

TABLE 6. Numerical data on dentitions of two samples of *Chaeropus ecaudatus*.

	Madura Cave			Other Nullarbor Caves (fossil)		
Variate	N	Observed range	Mean	N	Observed range	Mean
M^1 L	—	—	—	3	3.48-4.09	3.78
AW	—	—	—	3	2.49-2.68	2.59
PW	—	—	—	3	2.77-3.20	2.96
M^2 L	4	2.96-3.01	2.97	2	2.68-2.87	2.78
AW	4	2.82-3.15	2.94	2	3.15-3.24	3.20
PW	4	2.77-3.01	2.89	2	3.06-3.24	3.15
M^3 L	—	—	—	2	2.68-2.87	2.78
AW	—	—	—	2	3.20-3.34	3.27
PW	—	—	—	2	2.91-3.06	2.99
M^4 L	—	—	—	1	—	1.88
W	—	—	—	1	—	2.54
M_1 L	—	—	—	1	—	3.24
AW	—	—	—	1	—	1.41
PW	—	—	—	1	—	2.44
M_2 L	—	—	—	2	3.15-3.20	3.18
AW	—	—	—	2	2.21-2.44	2.33
PW	—	—	—	2	2.30-2.59	2.45
$M_{2 \text{ or } 3}$ L	6	3.24-3.52	3.35	—	—	—
AW	7	2.12-2.30	2.19	—	—	—
PW	7	2.16-2.35	2.27	—	—	—
M_3 L	—	—	—	4	3.06-3.24	3.15
AW	—	—	—	4	2.12-2.30	2.24
PW	—	—	—	4	2.07-2.26	2.18
M_4 L	—	—	—	5	3.38-3.57	3.44
AW	—	—	—	5	1.74-1.93	1.82
PW	—	—	—	5	1.27-1.41	1.37

of the metacone where it climbs partway up the labial face of the metacone. In some teeth (TMM 41106-732; WAM 75.1.140, fig. 16C), a short ridge extends from the lingual end of the mesostyle to the premetacrista. The labial ends of the V's are higher than the central areas, resulting in the formation of basins.

Mandible and lower molars.—The one mandibular fragment (TMM 41106-2763; fig. 16D) is slender and deep and has the alveoli of all the premolars. It is referred to *Chaeropus* on the basis of the distinctive form of the ramus and upon the presence of a prominent diastema in front of and behind the first premolar (compare fig. 16D with figs. 6D and 10E). Other peramelids have much less space between the first two premolars, P_1 and P_3, than does *Chaeropus* and the ramus is shallower.

No M_1s or M_4s were recovered, and M_2 and M_3 are so similar in size (table 6; fig. 17B) and form that we cannot be certain about a means of distinguishing them when they are found as isolated teeth. The lower molars of *Chaeropus* have the basic structure seen in most peramelids (figs. 15B, E; 16E, F). There is a high degree of the same sort of asymmetrical crown hypsodonty as in the upper teeth, particularly in the area underlying the protoconid and hypoconid. The trigonid is well defined in an unworn tooth, but its three cusps are close together, and the trigonid basin is small. The protoconid lies at the apex of an equilateral triangle formed by the anterior half of the eocristid and is joined to

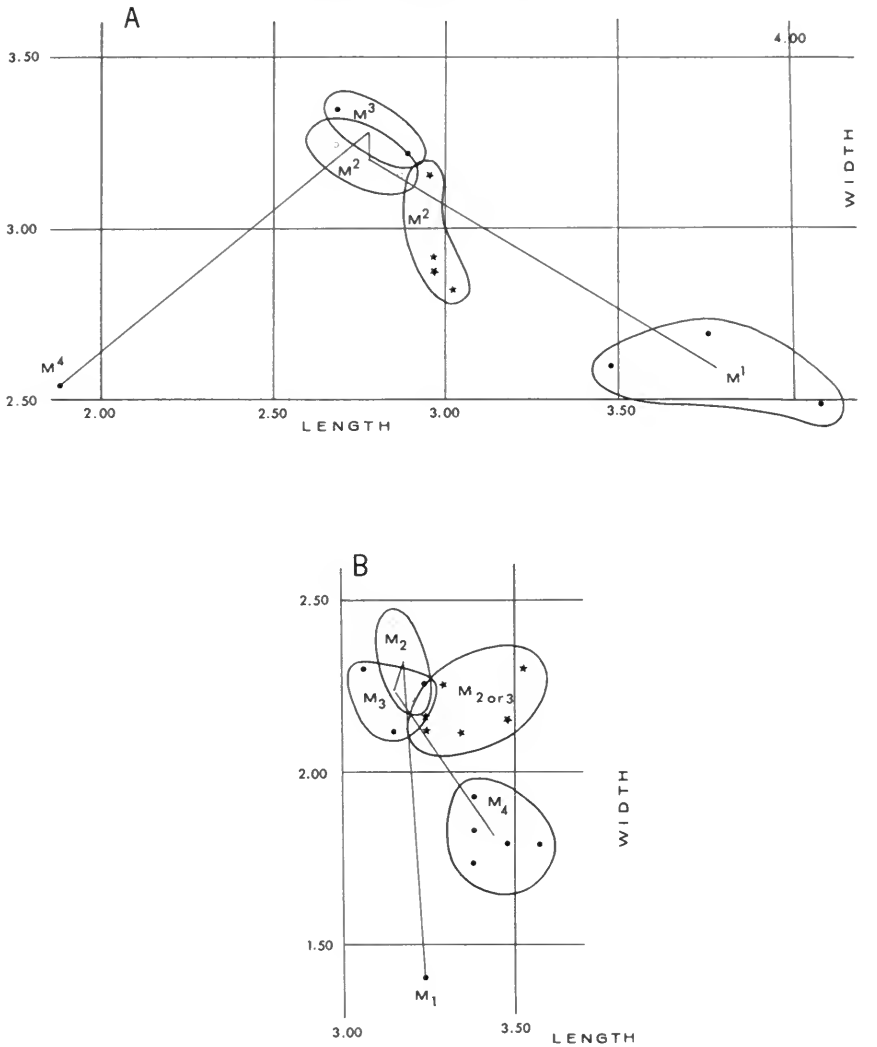

FIG. 17. Bivariate graphs showing plots of length vs. anterior width measures for each of the molar teeth of sub-Recent specimens of *Chaeropus ecaudatus* from several Nullarbor Caves. Stars designate those from the Madura Cave sample. Straight lines connect the midpoints of each tooth cluster of measures to provide the characteristic pattern for the species (compare with figs. 8C, D; 12A, B; 13A, C; 21A, B). Note extensive overlap of M^2s and M^3s and of M_2s and M_3s.

the paraconid and metaconid by the paralophid (paracristid, I') and metalophid (epicristid II', II''), respectively. Each of these ridges has an open V close to its midpoint, but there is no carnassial notch. There is no connection between the paraconid and metaconid, except where their bases abut one another.

The talonid is lower than the trigonid and is also V-shaped. The hypoconid lies at the apex of the V. A cristid obliqua (premetacristid I'''b) joins it to the entocristid (V) at the anterior edge of the entoconid. The postmetacristid (I'')

joins the hypoconid to the small hypoconulid at the posterolingual corner of the tooth. The entoconid is circular in cross section and is located at the lingual edge of the tooth in the V formed by the posterior half of the eocristid. A weak crest (entocristid V) joins the anterior edge of the entoconid to the adjacent cristid obliqua.

Because the cristid obliqua does not join the protolophid, the hypoflexid extends all the way to the entocristid.

A cingulum is present at the base of the tooth between the protoconid and hypoconid. It may or may not bear a small cuspule. A large procingulum extends upward from the base of the protoconid to the base of the paraconid and incorporates a parastylid. It forms a prominent elongate cingular basin.

Discussion

This species has been recorded as a living animal in two disjunct areas. One area includes southwestern New South Wales, much of South Australia, and the southern part of the Northern Territory. The other is a small area near Northam in the inland district of Western Australia. The Madura Cave specimens and notes by Merrilees (1968) and Archer (1972) demonstrate its former presence in an intermediate area. Its Recent occurrence in arid areas in South Australia suggests that it may have been widespread in the arid parts of southern Australia until very recently and that the disjunct nature of its known Recent distribution is the result of either a collecting bias or recent historic restrictions in its distribution. This is supported by the presence of its remains in surficial deposits in other caves of the Nullarbor Plain (Merrilees, 1968; Archer, 1972). Its presence throughout the sequence at Madura Cave indicates that it has had a long residence in this region and that it was one of the species able to tolerate the drying of the climate that took place at the end of the Pleistocene.

Macrotis Reid, 1837

Macrotis lagotis (Reid, 1837)

Material

Trench 3, Unit 1, Level 1

TMM 41106-32, edentulous right ramus fragment, juvenile

Trench 3, Unit 2

TMM 41106-73, left $M_{2 \text{ or } 3}$

TMM 41106-56, right ramus fragment with $M_{2\text{-}3}$ and M_4 removed from crypt (fig. 20A)

TMM 41106-57, edentulous left ramus fragment of juvenile with alveoli of P_4-M_4

TMM 41106-58, edentulous right ramus fragment with alveoli of $M_{2\text{-}4}$

TMM 41106-59, edentulous right ramus fragment with alveoli of $M_{2\text{-}4}$?

PM 26336, left M^1 (fig. 19D)

PM 26337, right $M_{2 \text{ or } 3}$

PM 26338, right $M_{2 \text{ or } 3}$

PM 26339, right $M_{2 \text{ or } 3}$

PM 26340, left M_1 (fig. 20B)

PM 26341, left $M_{2 \text{ or } 3}$

PM 26342, edentulous left maxillary with alveoli of C-M^1 (fig. 19A)

PM 26343, left P_3 (fig. 20C)

Trench 3, Unit 2 (continued)
PM 26344, right P^1 or P^3 (fig. 19B)
PM 26345, broken left $M^{2 \text{ or } 3}$
PM 26346, right M_1
PM 26347, broken right $M^{2 \text{ or } 3}$
PM 26348, left P_3 (or P_1)

Trench 3, Unit 2, Level 2
TMM 41106-53, left mandibular fragment with alveoli of two molars
TMM 41106-54, right $M^{2 \text{ or } 3}$
PM 26349, right $M^{2 \text{ or } 3}$
PM 26350, right $M^{2 \text{ or } 3}$ (fig. 19E)
PM 26351, left M^1
PM 26352, right $M^{2 \text{ or } 3}$
PM 26353, left $M^{2 \text{ or } 3}$
PM 26354, left M_3 (or M_2)
PM 26355, right $M^{2 \text{ or } 3}$
PM 26356, right M^1
PM 26357, left P^3 (or P^1)

Trench 4, Unit 1, Level 1
TMM 41106-476, right $M^{2 \text{ or } 3}$
TMM 41106-573, right M^1
TMM 41106-575, left M^1 (fig. 19C)
TMM 41106-584, left M_3 (or M_2)
TMM 41106-611, left M^1
TMM 41106-612, right M_3 (or M_2)
TMM 41106-676, left M_1
PM 26358, right M^3 (or M^2) (fig. 19G)
PM 26359, right premolar, probably P_4
PM 26360, anterior half of a left $P^{3 \text{ or } 1}$
PM 26361, right M^3

Trench 4, Unit 2, Level 1
WAM 75.1.128, left P^3?
PM 26363, parastylar area of right $M^{2 \text{ or } 3}$
PM 26364, lingual side upper molar
PM 26365, right M_3 (or M_2)
PM 26366, right $M^{2 \text{ or } 3}$
PM 26367, right $M^{2 \text{ or } 3}$
PM 26368, left $M^{2 \text{ or } 3}$
PM 26369, left M^4 (fig. 19H)
PM 26370, left M_1
PM 26921, right $M^{2 \text{ or } 3}$
PM 26922, right $M^{2 \text{ or } 3}$
PM 26923, left $M^{2 \text{ or } 3}$

Trench 4, Unit 2, Level 2
PM 26924, left M^1
PM 26925, right $M^{2 \text{ or } 3}$
PM 26926, right M_3
PM 26927, left M^1

Trench 4, Unit 2, Level 2 (continued)
PM 26928, right $M_{2 \text{ or } 3}$
PM 26929, left M_1
PM 26930, right M_1

Trench 4, Units 4-5
PM 26931, edentulous right ramus with alveoli of P_4-M_4 (fig. 20D)
PM 26932, left M^1
PM 26933, left M^1
PM 26934, right $M_{2, 3, \text{ or } 4}$
PM 26935, left $M_{2 \text{ or } 3}$

Trench 4, Units 4-5 (continued)
PM 26936, left M_3 (or M_2)
PM 26937, right M^1
PM 26938, left $M^{2 \text{ or } 3}$
PM 26939, right M^1
PM 26940, left M_3 (or M_2)
PM 26941, right M_4
PM 26942, edentulous left ramus with alveoli of P_1-M_4 (fig. 20E)
PM 26943, edentulous left ramus with alveoli of $M_{1\text{-}4}$
PM 26944, left M_3 (or M_2)
PM 26945, right $M^{2 \text{ or } 3}$ (fig. 19F)
PM 26946, anterior half, left $M_{2 \text{ or } 3}$
PM 26947, right $M^{2 \text{ or } 3}$
PM 26948, left M^1
PM 26949, anterolabial corner of left M^2
PM 26950, trigonid of right $M_{2 \text{ or } 3}$
PM 26951, left upper molar
PM 26952, trigonid of right lower molar
PM 26953, right M_1
PM 26954, trigon of right upper molar
PM 26955, right M^3 (or M^2)
PM 26956, left $M^{2 \text{ or } 3}$
PM 26957, left $M^{2 \text{ or } 3}$
PM 26958, right upper molar fragment, probably $M^{2 \text{ or } 3}$
PM 26959, left P^1 or P^3
PM 26960, left premolar, probably a P_4
PM 26961, right premolar, probably a P_4
PM 30549, right M_1
PM 30550, left M_1

Trench 4, Unit 7
PM 26963, left M^2 (or M^3)

Trench 4, Unit 7, Level 1
PM 26964, left M^2 (or M^3)
PM 26965, left M^3 (or M^2)
PM 26966, right M_1
PM 34417, edentulous ramus fragment

Trench 4, Unit 7, Level 2
WAM 75.1.129, edentulous right maxillary fragment with alveoli of $P^{3\text{-}4}$
PM 26967, right ramus with alveoli of P_4-M_3

Trench 4, Unit 7, Level 2 (continued)
PM 26968, right M^2
PM 26969, right M_3 (or M_2)
PM 26970, left M^2 (or M^3)
PM 26971, left M_3 (or M_2)
PM 26972, right M^1
PM 26973, right M^1
PM 26974, left M_1
PM 26975, right $M_{2 \text{ or } 3}$
PM 26976, right M_2

Trench 5, Unit 5
PM 26335, right ramus fragment with alveoli of P_1-M_2 (fig. 20F)
PM 26977, left M_2 (or M_3)
PM 26978, left M_2 (or M_3)
PM 26979, left M_3 (or M_2)
PM 26980, right M^3 (or M^2)
PM 26981, left M^1 fragment
PM 26982, left M^1 fragment
PM 26983, right $M^{2 \text{ or } 3}$
PM 26984, left $M^{2 \text{ or } 3}$
PM 26985, partial right $M^{2 \text{ or } 3}$

Trench 5, Unit 5 or 6?
PM 26986, left M_1
PM 26987, left P_3 (or P_1) } possibly from the same individual
PM 26988, right P_3 (or P_1) }
PM 26989, left P_3

Descriptions

Skull.—Very little cranial material of this species is represented in the Madura collection. Most of the specimens represent immature individuals, probably indicating that owls were the predators responsible for bringing the material to the cave. An adult *Macrotis* is probably too large to be regularly taken by owls.

One edentulous left maxilla of a juvenile (PM 26342, fig. 19A) is the only specimen that represents the skull. It has alveoli for the canine, the first two upper premolars, and dP^4, and the M^1. The developing alveolus for the unerupted P^4 is located lingual to that of the dP^4. The infraorbital foramen is located above the anterior edge of the alveolus of M^1. It is elliptical in cross section and opens into a broad rounded groove on the lateral face of the maxilla.

A comparison of the Madura Cave specimen with the skull of a Recent specimen (FM 35331; fig. 18) reveals no differences that are not the result of the difference in ontogenetic age. The Madura Cave specimen is slightly younger, and the anterior part of the maxillary that carries the premolars is relatively shorter than in the Recent specimen.

Upper premolars.—Several upper premolars have been recognized. In one of them (PM 26344), a worn right P^1 or P^3, the form agrees well with the modern comparative specimen. The tooth is double rooted, and the anterior root has a distinctive, markedly curved appearance. There is a single, large, central cusp with rounded crests. The anterior crest is very weak, and there is no anterior

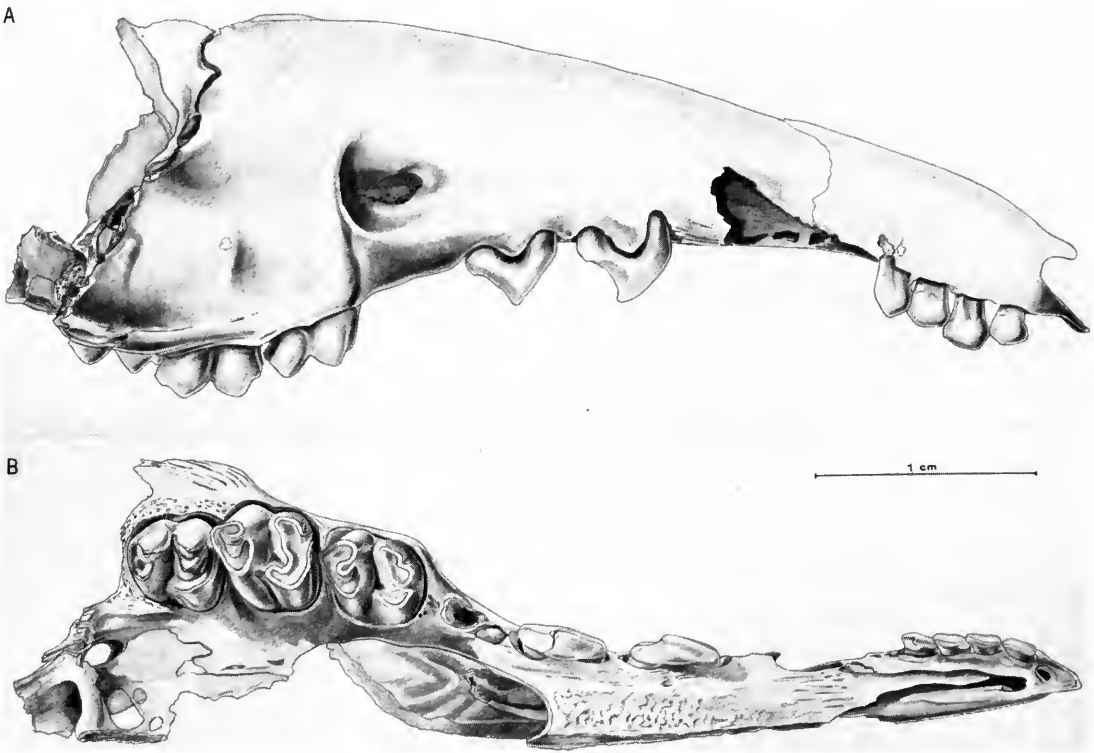

FIG. 18. *Macrotis lagotis* (Reid), FMNH 35331, a Recent juvenile specimen from Woyaline Wells, Pingelly, Western Australia. **A & B,** Right lateral and occlusal views of the facial-palatal portion of the skull. The I^1 and canine have been lost from their sockets, and the dP^4 had either been shed shortly before the animal was taken or it too has been lost from its socket. P^4 and M^3 are still within their crypts, the latter beginning to erupt.

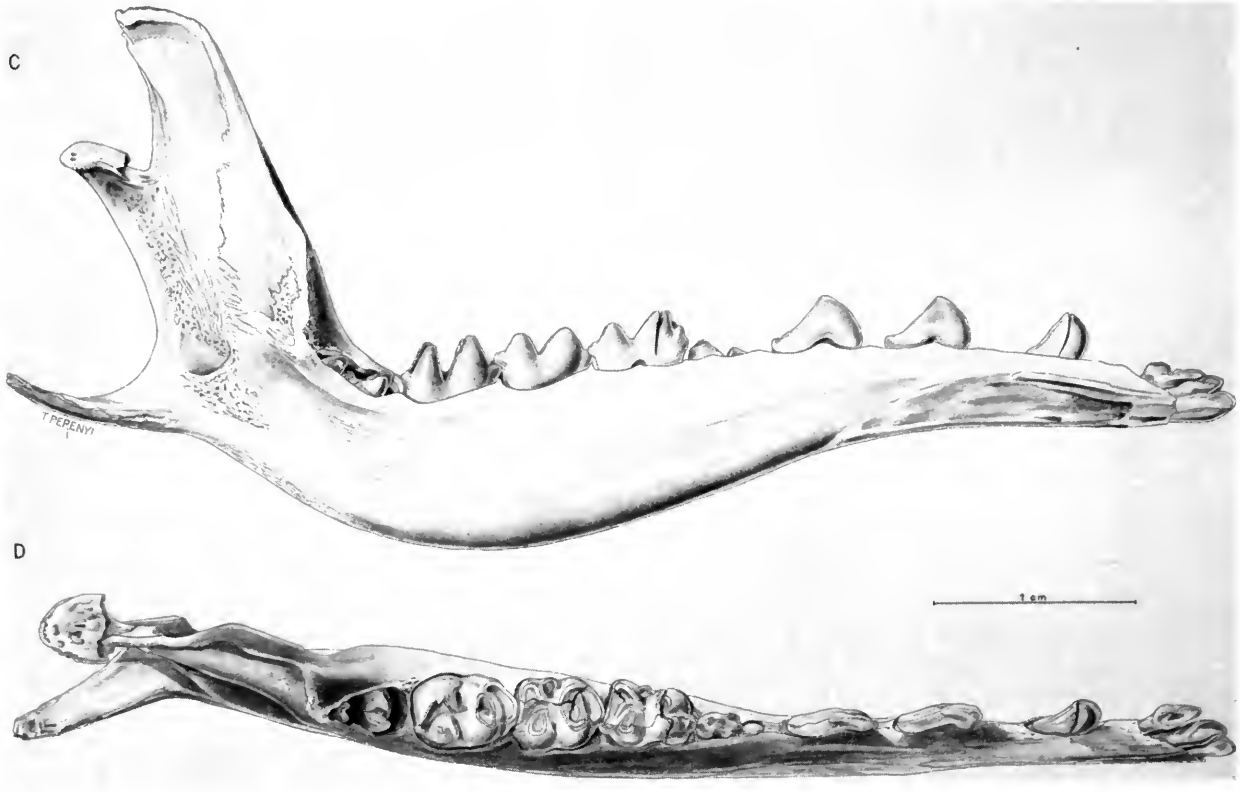

FIG. 18. **C & D,** Left mandible shown in medial and occlusal views. The dP_4 is in place but is reversed front to back (probably an artifact of preparation), and the P_4 can be seen beneath (and in front of) it within its own crypt. The I_1 has been lost and has been drawn in by reversing that of the right side.

cingular cuspule. The posterior crest runs to a posterior cingular cuspule that shows wear lingually. The crown is slightly narrower than that of the modern specimen when viewed occlusally. Another specimen (WAM 75.1.128), a left P^3 (or P^1), is also worn. It is wider in the area of the posterior root than is PM 26344 and the recent specimen, and the anterior crest of the central cusp is more distinct as in the recent specimen. In PM 26959, a left P^1 or P^3, there is a minute but distinct anterior cingular cuspule. None of the other teeth shows this feature, nor does the modern specimen. In PM 26357, a left P^3 or P^1, the profile is unusual in that instead of being convexly curved from crown tip to root tip, here there is a slight concavity between the tip of the cusp and the base of the crown.

Upper molars.—The upper molars, with the exception of M^4, are roughly rectangular in occlusal view when unworn. When worn, they become more square. The M^{1-3} have achieved this shape by an enlargement and lingual movement of the metacone rather than by the addition of a hypocone as in *Isoodon* and *Chaeropus*. The M^4 has the shape of a rounded triangle. All have massive rounded cusps and tooth base hypsodonty that is more developed on the lingual half of the tooth.

The M^1 is characterized by the presence of a well-developed parastyle with a medially directed crest that joins the paracone so as to delimit a tiny basin and the crowding together of the subequal-sized paracone and stylocone. The metacone is the largest cusp. It has the shape of an asymmetrical crescent in occlusal view, with the short anterior horn extending to the base of stylar cusp l. The longer posterior horn joins the metastyle. The protocone is the lowest major cusp on the tooth. It is elongated anteroposteriorly and reaches from the anterolingual corner of the tooth to the metacone. There is no connection with the parastyle.

Stylar cusp l is the tallest cusp on the tooth. It is rounded anteriorly where it is separated from the stylocone by a sharp valley. It is compressed posteriorly into a ridge that approaches but does not join the metastyle in the unworn state. With wear they become joined. A slight bulge on this ridge might represent stylar cusp m (PM 26336, PM 26351). Specimens TMM 41106-573 and 41106-575 (fig. 19C), although little worn, do not show this feature. Wear results in a joining of the metacone and stylar cusp l around the posterior part of the tooth and at a later stage in the joining of the paracone and stylocone, which in still later stages are joined to the protocone.

The M^2 and M^3 are so similar that they will be treated together. The stylocone and stylar cusp l are nearly equal in size and height and are the two highest cusps on the tooth. In the M^2, the anterior face of stylar cusp l usually has a ridge (PM 26350 lacks this ridge: fig 19E), which is absent on the M^3. The labial face of the stylocone of the M^2 bulges more than in M^3, and the base of the enamel swings sharply toward the parastyle. In the M^3, the labial surfaces of these two cusps bulge more nearly equally, and the labial enamel line does not turn toward the parastyle. The posterior face of the stylocone is ridged, usually better developed in the M^2.

The metacone is the largest cusp. It is like that of the M^1, with a long posterior part that extends around the posterior part of the tooth and joins the metastyle. The anterior arm swings labially to the base of stylar cusp l. In the M^3, the crescents of metacone and paracone are not as disproportionate in size as in the M^2, mostly because the crescent of the metacone is tighter in M^3 than it is in the M^2.

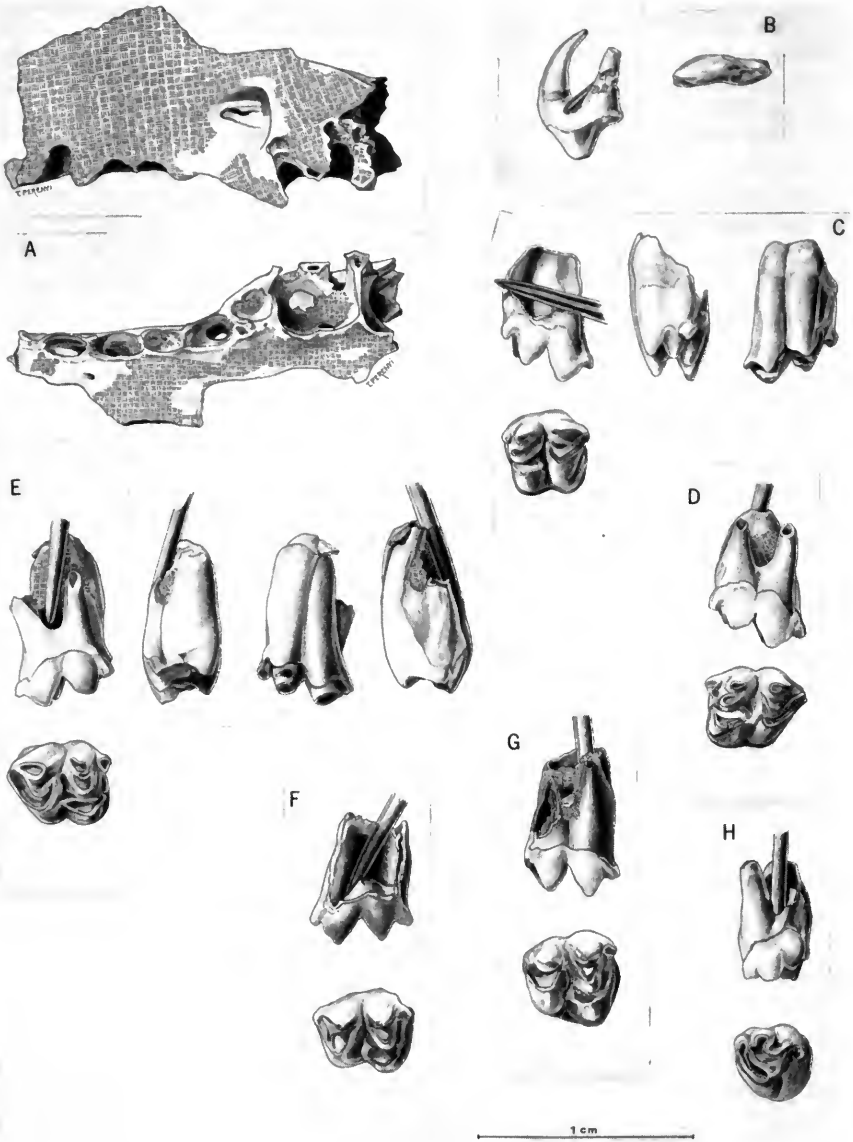

FIG. 19. *Macrotis lagotis* specimens from Madura Cave. **A,** PM 26342, an edentulous left maxillary fragment with the alveoli of C, P_1, P_3, dP_4, M_{1-2}, shown in labial and palatal views. Note the characteristic, large molar alveolus for the root of the protocone (and hypocone) which can be seen in the palatal view. Note too that the dP_4 had its two roots fused. **B,** PM 26344, a right P^1 or P^3 shown in lingual and crown views. **C,** TMM 41106-575, a left M^1 shown in labial, mesial, lingual, and crown views. **D,** PM 26336, a left M^1 shown in labial and crown views. **E,** PM 26350, a right M^2 or M^3 shown in labial, mesial, lingual, distal, and crown views. **F,** PM 26945, a right M^2 or M^3 shown in labial and crown views. **G,** PM 26358, a right M^3 or M^2 shown in labial and crown views. **H,** PM 26369, a left M^4 shown in labial and crown views.

The protocone is the lowest major cusp. It extends from the base of the metacone around the anterolingual corner of the tooth and joins an anterior cingulum that continues to the parastyle. The paracone is V-shaped, with the anterior arm joining the base of the stylocone at the notch between the stylocone and parastyle.

In unworn or little-worn teeth, M^2 can be distinguished from M^3 by its narrower anterior absolute (but not relative) width (fig. 18B). This is demonstrated by the Recent specimens that have both teeth present in the maxillary. In the plot of the Madura Cave sample, we interpret the group with the narrower anterior width measure to be the M^2s; that with the wider anterior width to be the M^3s (fig. 21). At advanced wear stages in which all cusp, crest, and valley features of the crown have been worn away, the anterior width measures of M^2 and M^3 have become reversed. This reflects the nature of the crown hypsodonty in which the taper causes the anterior width vs. transverse proportions to shift at the different heights (wear stages).

The M^4 is a three-rooted tooth with the shape of a rounded triangle in cross section (fig. 19H). The posterior part of the tooth is reduced. The paracone is the largest cusp on the tooth. It is crescentic, with the anterior arm joining the base of a reduced stylocone. The posterior arm ends against a small cuspule on the labial edge of the tooth. A well-developed anterior cingulum extends from the parastyle to the base of the paracone or a fused paracone-protocone. The latter alternative is suggested by the shape of the worn crescent. The posterior edge of the tooth is marked by a small cuspule. Wear removes these features early in the life of the tooth. The result is an enamel ring surrounding the dentine core of the tooth.

Mandible.—Three specimens (fig. 20A, F, D), TMM 41106-156, PM 26335, and PM 26931, provide the basis for the description of the mandible of *M. lagotis* from Madura Cave. The horizontal ramus is characterized by its rapid increase in width at M_1 to accommodate the wide molars. The entire ramus is twisted so as to turn the anterior alveoli outward. A mental foramen is located under the P_1. The posterior end of the symphysis is located between P_1 and P_2.

The anterior edge of the ascending ramus makes a high angle (more than 45°) with the tooth row. The masseteric fossa is broad and bordered by ridges that become better defined with age. The ventral ridge of the masseteric fossa is enlarged above the angular process and forms a tubercle. A flattened rugose ridge extends from this tubercle onto the lateral edge of the angular process. The mandibular foramen, which is located in a broad, posteriorly open groove, opens near the anterior edge of the base of the angular process. The condyle is located closer to the top of the coronoid process than to the angular process. Its articular surface is almost circular. It is slightly concave transversely and convex anteroposteriorly.

Lower premolars.—Eight lower premolars have been recognized. Five of them (PM 26343, 26348, and PM 26987-9) are very much alike and are comparable to P_1 and P_3 of the modern form. They consistently differ from the modern form in having a wider posterior half of the crown base. They all show traces of two subsidiary cusps associated with the crests of the primary cusp, one on each crest. In the modern specimen, only one of the four teeth bears one of these features. On some of the fossils, there is a slight bulge where the anterior cingular cusp might be expected, but none has a cuspule.

The P_4s (PM 26359 and PM 26960-1) are shorter anteroposteriorly than the other premolars, and the crown base is proportionately wider. The crown has a central cusp as its main feature, and this is laterally compressed and has anterior and posterior crests. The cingulae show variation. There is a weak anterior cingulum enveloping the anterior quarter of the crown base. On two (PM 26960-1), there is a small cusp present, and on one (PM 26359), this cusp is missing, and instead on the anterolingual side there are two minute cuspules tight against the base of the central cusp just where the cingulum rises slightly before it merges into the base of the central cusp. All have a distinct posterior cingular cusp at the rear end of the posterior crest, usually somewhat lingually situated. In PM 26960 and 26961, short cingulae extend forward from this cusp, one on each side along the crown base margin for up to a fourth of the length of the tooth. In PM 26359, from the rear side of this posterior cingular cusp or heel, a weak cingulum runs down and labially across the midaxis of the tooth and then rises and runs forward for about one fourth the length of the tooth to merge with the base of the main cusp. It bears two minute, freestanding cuspules. There is no lingual cingulum going off from this posterior cusp as in the other teeth.

Lower molars.—The M_1 of *M. lagotis* is elongate and tapers toward the anterior end. There is considerable tooth base hypsodonty beneath the protoconid as compared with the lingual side of the tooth where there is little or none and a much greater development of tooth base hypsodonty beneath the hypoconid similar to that of the labial side of the rest of the molars. The trigonid is narrow and small and variable in its development. It is slightly raised above the talonid, which is much wider. The protoconid and metaconid are subequal in size and height and are connected by a weakly developed epicristid (II′ and II″) that runs across the valley between the cusps to connect to their back edges. The protoconid part of the epicristid lies just ahead of a better developed postparacristid (I‴a).

The paraconid is the smallest and lowest trigonid cusp, but it is better developed than on the Recent comparative specimen (FMNH 35331; fig. 18D). It lies ahead of the metaconid, appressed against its base. There usually is a connection to the protoconid by a paracristid (I′). In PM 26930, PM 26953, and PM 26966, this is a weak connection, but in PM 26370, PM 26974, and PM 30549, it is a stronger one, and in PM 26340 (fig. 20B), the ridges from each cusp are strong yet they fail to meet in the valley. In PM 26346, PM 26929, and PM 26986, there are not even any ridges suggestive of a connecting crest.

There is always a parastylid that is low and lies anterior to the paraconid, near the crown base at the anterolingual corner of the tooth. It too varies in size and in the extent to which it tends to be extended labially into a short cingular ridge. In most, it is nearly a small cone, whereas in PM 26346, PM 26370, PM 26974, and PM 30549, there is an expressed tendency for the cingular crest to form.

In the talonid, the entoconid and hypoconid stand about equally high in an unworn tooth, but the latter, with its extreme crown base hypsodonty, is far larger. The entoconid is rounded posteriorly and ridged from its crest both anteriorly and anterolabially. The anterior crest runs toward the transverse central valley and bends labially without entering the bottom of the valley. The anterolabially directed crest also fails to reach the base of the cusp.

The hypoconid has a crescentic form with an anterior crest, the premetacristid

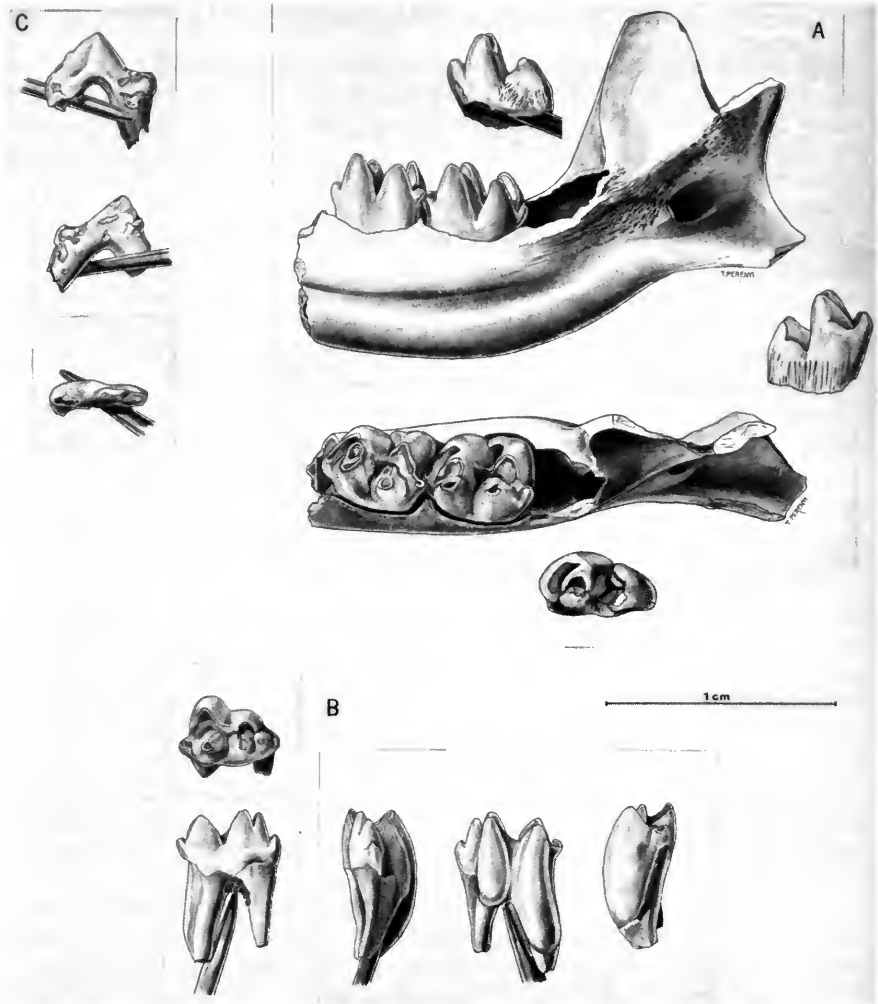

FIG. 20. *Macrotis lagotis* from Madura Cave. **A,** TMM 41106-156, a right mandibular fragment with half of the horizontal ramus, most of the coronoid and angular processes, but lacking the condyle. M_2 and M_3 are in place, and the unerupted M_4 has been removed from its crypt. The jaw is shown in medial and dorsal views, the M_4 in lingual, labial, and crown views. **B,** PM 26340, a left M_1 shown in crown, lingual, mesial, labial, and distal views. **C,** PM 26343, a left P_3 shown in labial, lingual, and crown views.

Opposite:

FIG. 20. **D,** PM 26931, an edentulous partial right mandible of a juvenile individual shown in lingual and dorsal views. Preserved is the ascending ramus and the posterior portion of the horizontal ramus, with part of the alveolus of dP_4, part of the crypt of P_4, the alveoli of M_{1-3}, and the crypt for P_4. **E,** PM 26942, an edentulous left ramus with the alveoli of P_1 and P_3, dP_4, and P_4 at an early developmental stage within its crypt (the tip of the main cusp is broken off), the alveoli of M_{1-3}, and the crypt for M_4. **F,** PM 26335, an edentulous right ramus fragment of a juvenile individual with alveoli of P_1- M_2 including that for dP_4 and the crypt of P_4, shown in labial and crown views.

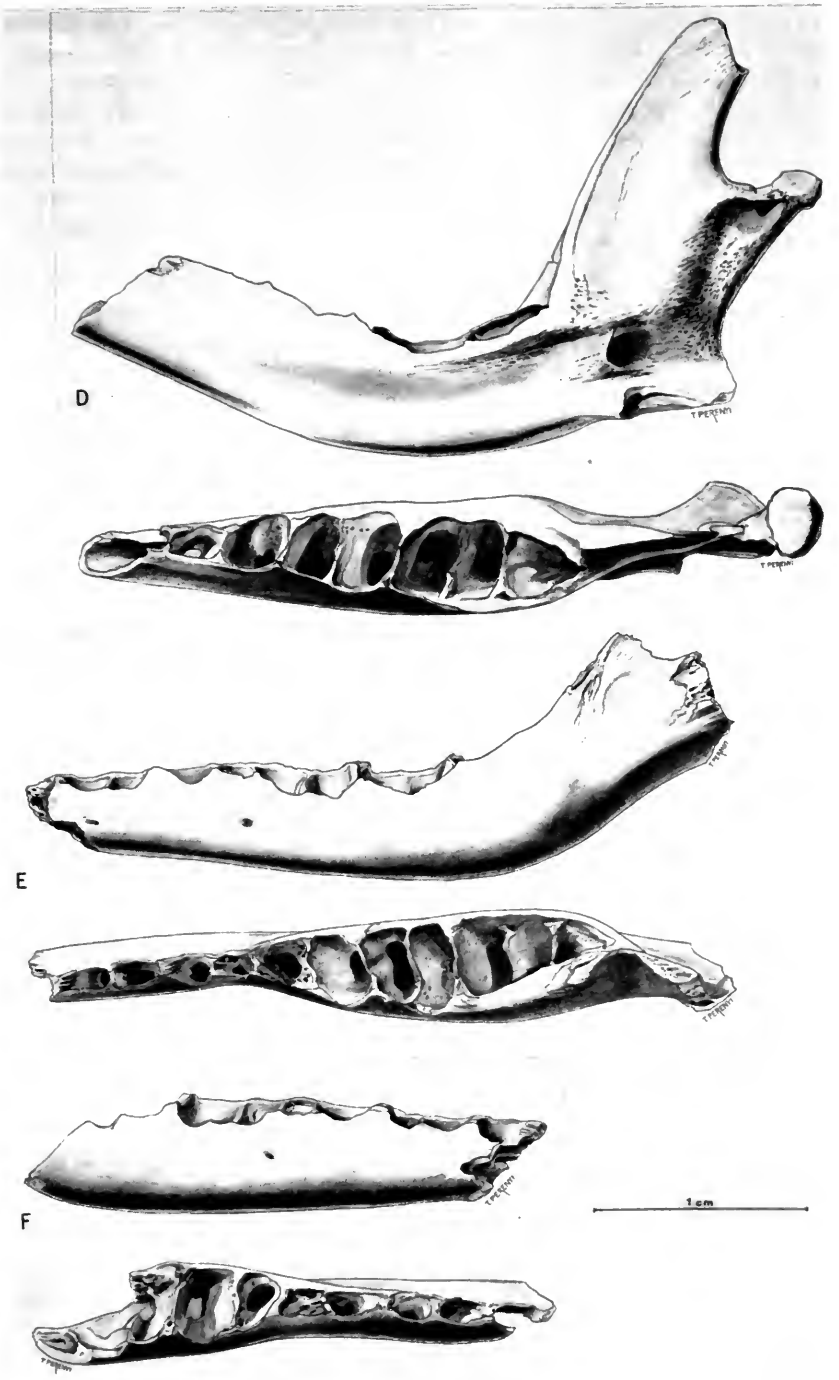
D
E
F
1 cm

or cristid obliqua (I'''b), which runs anterolingually to join the postparacristid behind the protoconid above the transverse valley floor. The posterior crest of the hypoconid, the postmetacristid (I''), runs labially to join the hypoconulid at the posterolingual corner of the tooth. The hypoconulid is a rounded projection with a weakly developed crest connecting it to the base of the entoconid. In four specimens there is a spur from the postmetacristid to the base of the entoconid (PM 26340, PM 26370, PM 26986, and PM 30550). Occasionally there may be a small cingular cuspule between the protoconid and hypoconid (PM 26370 and PM 26986), but usually there is no trace of this element.

Comparisons with the M_1 of two subfossil specimens (PM 4979 and PM 4980) from Murraelellevan Cave on the Nullarbor are very close. They have the crested parastylid, but it is even more expanded and complex than in the Madura Cave specimens. Also, each has a spur from its postmetacristid to the base of the entoconid, and one (PM 4979) has the paracristid developed, the other does not, and neither has the small cingular cusplet between the protoconid and hypoconid as do a few of the Madura Cave specimens.

The major difference between the fossils and the Recent specimen is the much more reduced paraconid in the latter as well as a strong cingular cusp between protoconid and hypoconid.

The M_2 and M_3 are roundly rectangular teeth in crown view, and they are so similar that one description fits them both almost completely. The metaconid and entoconid are the highest cusps, and the former reaches slightly higher than the latter. The protoconid and hypoconid are smaller and lower, and in the unworn state the protoconid is slightly higher, but the hypoconid is a larger cusp with more open crescentic form than the protoconid—especially in M_2. There is no paraconid on M_2: the paracristid simply runs from the protoconid to the anterolabial base of the metaconid. In M_3 there is a small bulge at the union of crest and cusp that may be the homologue of the paraconid, and in one specimen, PM 26337, there is a weak crest from this "paracristid" to the parastylid. The epicristid connects the back sides of protoconid and metaconid. The trigonid of M_2 is distinctly narrower than the talonid, whereas in M_3 both are about equal in width or the trigonid may be slightly wider. There is a heavy procumbent anterior cingulum that commences in a cuspule one-half to two-thirds of the way up the anterolingual side of the protoconid. The cingulum runs forward and swings labially to form the stout parastylid labial to the mid-axis of the tooth. It thereby cuts off a deep, curved depression between its crest and the anterolabial wall of the protoconid. There is a weak postparacristid that joins the cristid obliqua above the floor of the transverse valley. Usually the hypoconid in its hypsodonty suddenly flares forward, occluding the labial side of the transverse valley so that it abuts the back of the protoconid for the ventral one-half to two-thirds of the height of the crown beneath these cusps. An exception to this is seen on PM 26337 where the flare is gentle and the protoconid also flares backward a bit. In another specimen (PM 26365), neither cusp flares, they just gradually expand. The posterior arm of the hypoconid crescent, leading to the hypoconulid, sends off a spur to the base of the entoconid. The hypoconulid of M_2 is slightly larger than that of M_3, and either tooth may have minute cingular cuspules associated with it. In one specimen (PM 26337), an M_3, there is no hypoconulid, and the postmetacristid just fades away without reaching the posterolingual corner of the tooth.

The M_2s and M_3s are similar in size and morphology but can be separated on

bivariate scatter diagrams of tooth length vs. anterior and posterior widths. In each case, M_2s are shorter than M_3s (fig. 21B). The scatter diagram of L vs. AW shows the M_2s to be narrower, too, so that there is a clear separation into two discrete groups. In M_3, the two width measures do not show a significant difference, and although there is a complete separation along the length scale, there is no gap between the clouds of points. Larger samples might be expected to show some overlap.

The M_4 has a well-developed trigonid and a reduced and posteriorly tapered talonid (fig. 20A). The protoconid and metaconid lie close to one another, about as in the M_1, and they are nearly equal in size. Both are somewhat crescentic. The posterior arm of each crescent descends, and they meet in the center along the back edge of the trigonid. The anterior arm of the metaconid is enveloped by that of the protoconid. This results from the more open crescentic form of the protoconid. The anterior cingulum is pronounced and is similar to those of M_2 and M_3. The two basins in the trigonid region, a central trigonid basin and an anterior cingular basin, are joined. The central basin that lies between the facing crescents of protoconid and metaconid is small and has an anterolingually directed valley leading from it. The anterior cingular basin lies transverse to the tooth axis, and at its lingual end it joins the lingual end of the valley of the central basin. There may or may not be a common exit to the lingual side of the tooth. A parastylid cusp is incorporated into the lingual terminus of the cingulum. The trigonid is raised above the talonid. The entoconid is the largest talonid cusp, and it is weakly crescentic. The hypoconid is very low and not well defined, and there is only the faintest trace of a hypoconulid. The talonid basin is triangular and deeply clefted labially.

Comparisons.—The M^1s from Madura Cave and those of young individuals from Murraelellevan Cave (PM 4872) have a well-developed parastyle. The more complete specimens in the Murraelellevan sample show that this feature is soon reduced, then eliminated by wear. One Recent specimen from Woyaline Wells (FMNH 35331; fig. 18A, B) has no parastyle on its M^1. Its absence cannot be attributed to wear because this specimen is a juvenile with M^3 still incompletely erupted, with P^4 and M^4 within their respective crypts.

On M^1, the Madura Cave specimens have no anterior cingulum connecting protocone to parastyle as is seen in unworn specimens from Murraelellevan Cave. Such a cingulum is present on all the other molars of the Madura Cave materials and in unworn or little worn M^2-M^4 of all of our comparative specimens.

On M^2 of the Murraelellevan Cave specimen, the anterior ridge of the paracone also goes to the parastyle; in the Madura Cave specimens of M^2 and in M^2 of the comparative materials and in all M^3s, this ridge goes toward the notch between the parastyle and stylar cusp 1.

Last molars are rare in spite of a relatively large number of specimens of *Macrotis* in the Madura Cave fauna. This correlates with the young age stages of most of the other teeth. The M^4s and M_4s had not fully formed at the time of death. The other lower molars compare well in their main features to the available Recent and fossil materials.

Discussion

Macrotis lagotis is known as a living animal from widely scattered areas in the dryer parts of Australia, including two localities, Ooldea and Rawlinna, on the

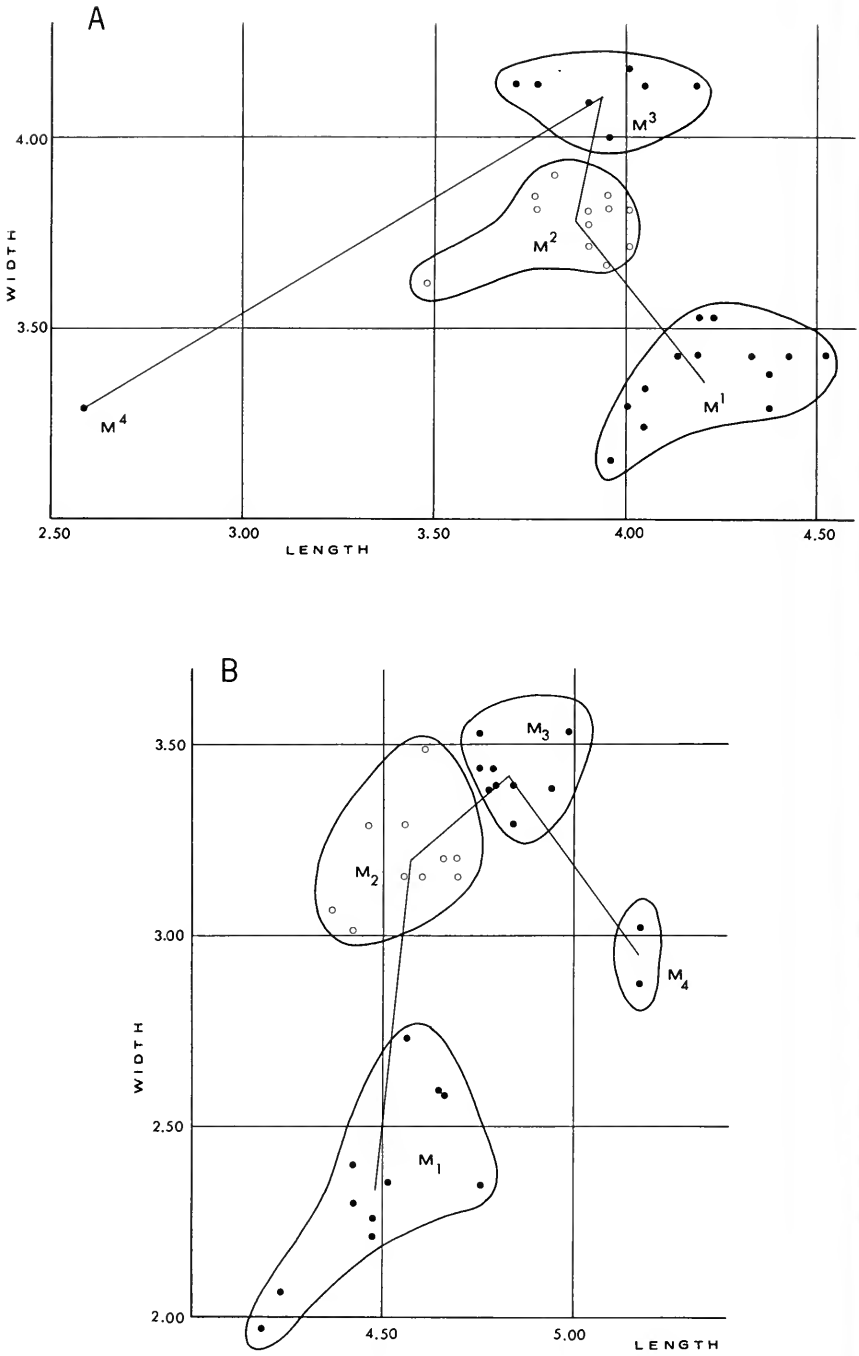

FIG. 21. Bivariate graphs of length vs. anterior width for the upper (**A**) and lower (**B**) molars of *Macrotis lagotis* from Madura Cave, showing complete separation of all molars. The means for adjacent teeth are connected by straight lines to form the patterns for the species. Measurements are in millimeters.

TABLE 7. Numerical data on upper dentitions of fossil and Recent samples of *Macrotis lagotis*.

	Madura Cave					Other Nullabor Caves			Recent		
Variate	Sample size	Observed range	Mean ± standard error	Standard deviation	Coefficient of variation (%)	Sample size	Observed range	Mean ± standard error	Sample size	Observed range	Mean
P^1 L									6	3.76-4.42	4.15
W									5	1.03-1.55	1.32
P^3 L									6	3.90-4.32	4.11
W									5	1.32-1.65	1.45
P^4 L									4	3.15-3.90	3.47
W									4	1.55-1.97	1.83
M^1 L	15	3.95-4.51	4.20±.046	0.177	4.21				6	3.62-4.18	3.88
AW	14	3.15-3.53	3.36±.033	0.123	3.64				6	2.96-4.56	3.56
PW	14	3.10-3.67	3.38±.040	0.151	4.47				6	3.10-4.70	3.89
M^2 L	12	3.48-4.00	3.86±.042	0.146	3.78	3	3.95-4.14	4.04	6	3.48-4.23	3.88
AW	12	3.62-3.90	3.78±.024	0.083	2.19	3	3.95-4.23	4.06	6	3.90-4.56	4.15
PW	12	3.20-3.90	3.55±.054	0.188	5.30	3	3.62-4.00	3.78	6	3.53-4.56	4.17
M^3 L	7	3.71-4.18	3.93	—	—	4	3.62-4.09	3.82	6	3.53-4.14	3.94
AW	7	4.00-4.14	4.10	—	—	1	—	4.62	6	4.04-4.61	4.28
PW	7	3.53-4.00	3.64	—	—	1	—	4.00	6	3.38-4.42	3.82
M^4 L	1	—	2.59	—	—				4	2.59-3.67	3.27
W	1	—	3.29	—	—				4	2.91-4.23	3.75

TABLE 8. Numerical data on lower dentitions of fossil and Recent samples of *Macrotis lagotis*.

	Madura Cave					Other Nullarbor Caves					Recent		
Variate	Sample size	Observed range	Mean ± standard error	Standard deviation	Coefficient of variation (%)	Sample size	Observed range	Mean ± standard error	Standard deviation	Coefficient of variation (%)	Sample size	Observed range	Mean
P_1 L											5	3.95-4.56	4.23
W											5	0.94-1.18	1.06
P_3 L											6	4.32-4.98	4.58
W											5	1.08-1.41	1.21
dP_4 L	—	—	—	—	—	—	—	—	—	—	2	2.12-2.30	2.21
W	—	—	—	—	—	—	—	—	—	—	2	0.94-1.18	1.06
P_4 L											3	3.76-4.14	3.89
W											3	1.55-1.74	1.65
M_1 L	11	4.18-4.75	4.48±.052	0.173	3.84	3	4.75-4.84	4.78			6	3.76-4.84	4.39
AW	11	1.97-2.73	2.35±.068	0.227	9.66	3	2.35-3.40	2.70			6	2.16-3.06	2.59
PW	11	2.73-3.29	3.01±.049	0.161	5.35	3	2.87-3.06	2.96			6	2.96-3.90	3.49
M_2 L	10	4.37-4.70	4.57±.036	0.113	2.48	9	4.28-4.89	4.60±.063	0.190	4.12	6	3.95-5.03	4.42
AW	10	3.01-3.48	3.20±.042	0.132	4.13	9	3.01-3.38	3.17±.043	0.130	4.11	6	3.06-4.09	3.71
PW	10	3.38-3.85	3.62±.048	0.152	4.19	9	3.20-3.85	3.53±.062	0.186	5.28	6	3.34-4.65	4.14
M_3 L	9	4.75-4.98	4.83±.027	0.081	1.67	10	4.32-4.89	4.72±.063	0.199	4.20	6	4.00-4.98	4.44
AW	9	3.29-3.53	3.41±.026	0.077	2.25	10	3.06-3.67	3.37±.062	0.196	5.80	6	3.24-4.51	3.92
PW	9	3.43-4.00	3.69±.071	0.213	5.76	10	3.06-3.67	3.40±.060	0.190	5.58	6	3.57-4.70	4.10
M_4 L	1	—	5.17	—	—	2	4.42-4.47	4.45	—	—	4	4.09-5.47	4.66
AW	2	2.87-3.01	2.94	—	—	1	—	2.73	—	—	4	2.96-4.09	3.51
PW	1	—	2.30	—	—	1	—	1.88	—	—	4	2.16-3.43	2.85

Nullarbor Plain. These are the type localities of two of the six named subspecies of *Macrotis lagotis*, *M. l. nigripes* and *M. l. interjecta*. There is substantial geographic variation in size, but there are few other characters that have been the basis for the erection of a number of subspecies. The existence of extensive size variation between local populations cited by Mack (1961) is supported by a comparison of the range of size of various dental characters of the Madura Cave sample, the other fossil samples, and the Recent samples (tables 7 and 8). The Recent sample, which is geographically heterogeneous, shows the greatest range of size, the younger fossil material from other Nullarbor caves shows less, and the Madura Cave sample, the least. The small range of size of the Madura Cave sample (fig. 21) suggests that there was little change in size in the *M. lagotis* population in the Madura area over approximately 30,000 years (38,000 to 7,500 years B.P.).

It is not possible on the basis of the material available to us to show that the Madura Cave sample is closer to one of the above-mentioned samples than to any of the others. The species now seems to be divided into a number of local populations that show various minor morphological differences. *Macrotis lagotis* is another species that has been resident on the Nullarbor Plain for a long time and that was able to tolerate the changing conditions at the end of the Pleistocene. Brooker (1977) suggested two possible reasons for the absence of this species (as well as many others) since the 1930's and 1940's—the length and severity of the droughts of 1933 and 1935 and the repeated man-set fires, such as the bush fires of 1942.

SUMMARY

The four taxa of peramelids represented in the Madura Cave deposits, *Perameles bougainvillei*, *Isoodon obesulus*, *Chaeropus ecaudatus*, and *Macrotis lagotis* are described. All except *I. obesulus* are elements of the present (or historic) fauna of the Nullarbor Plain. *Isoodon obesulus* today lives in areas that are mostly more mesic than the Nullarbor Plain, but it is known from comparably xeric areas as well. Its presence in the Pleistocene and early Holocene deposits may indicate a change to drier conditions in this region since approximately 7,000 years B.P. Aside from a decrease in size in *Perameles bougainvillei* between units 4-5 (22,200 years B.P.) and unit 1 (7,500 years B.P.), no morphological trends were seen in any of these taxa over the time represented by the deposits sampled.

In the earlier sections, it was shown that units 2-5 of trench 3 and units 2-7 of trench 4 contained remains of a number of extant taxa that are no longer found living on the Nullarbor Plain. They are: *Antechinus flavipes*, *Phascogale calura*, *Parantechinus apicalis*, *Dasyuroides byrnei*, *Sarcophilus harrisii*, and *Thylacinus cynocephalus*. The first three taxa presently live in areas of southwestern and/or southeastern Australia that have more mesic climates than that of the Nullarbor Plain today. *Sarcophilus harrisii* and *Thylacinus cynocephalus* are only recently extinct on the Australian mainland, and their disappearance may have been more the result of the introduction of the dingo than of general environmental change (Archer, 1974; Calaby & White, 1967).

Dasyuroides byrnei is now found in a limited area of desert grassland and desert steppe in northeastern South Australia, southeastern Northern Territory,

and southwestern Queensland (Marlow, 1962). The disappearance of this species that lives today in an arid region seems anomalous. Clearly, the increased aridity had a secondary effect that adversely affected this animal.

The stratigraphic distribution of perameliids in the Madura Cave sequence is consistent with the interpretation of a change toward more arid conditions at the end of the Pleistocene.

ACKNOWLEDGMENTS

In addition to those individuals mentioned in earlier parts of this faunal report, we wish to thank Caroline Grigson of the Odontological Museum of the Royal College of Surgeons, London, and the late Dr. Hobart Van Deusen, The American Museum of Natural History, New York, for the loan of materials.

We are especially appreciative of the fine drawings of the fossils and the Recent comparative specimens made by Dr. Tibor Perenyi, Scientific Illustrator, Field Museum. We thank Victoria Hunter, Jeannette Forster, and Mary Alexander for typing sections of the manuscript and the tables.

Financial support was provided by Grants GB 975, GB 3729, GB 7662 from the National Science Foundation; and by Field Museum of Natural History and the Geology Foundation of the University of Texas at Austin.

Note: Mr. Curtis Bean took the photographs that are montaged together to form Figures 18-23 of the recently published Part III section of The Mammalian Fauna of Madura Cave, Western Australia by Ernest L. Lundelius, Jr. and William D. Turnbull (Fieldiana: Geology, vol. 38). We regret that his name was inadvertently omitted from the list of acknowledgments.

REFERENCES

ARCHER, M. 1972. Nullarbor, 1969, 1970. The Western Caver, **12**(1): 17-24.

————. 1974. New information about the Quaternary distribution of the thylacine (Marsupialia, Thylacinidae) in Australia. J. Roy. Soc. Western Austral., **57**(2): 43-50.

BROOKER, M. G. 1977. Some notes on the mammalian fauna of the western Nullarbor Plain, Western Australia. Western Australian Naturalist, **14**(1): 2-15, figs. 1-7.

CALABY, J. H. AND C. WHITE. 1967. The Tasmanian Devil (*Sarcophilus harrisii*) in northern Australia in Recent times. Austral. J. Sci., **29**(12): 473-475, figs. 1-2.

DESMAREST, A. G. 1817. Nouveau dictionaire d'histoire Naturelle, nouv. ed. **16:** 409-410. Deterville, Paris.

FINLAYSON, H. H. 1961. On central Australian mammals. Part 4. The distribution and status of central Australian species. Rec. S. Austral. Mus., **14:** 141-191.

FREEDMAN, L. 1967. Skull and tooth variation in the genus *Perameles.* Part 1: Anatomical features. Records Australian Museum, **27**(6): 147-166, pls. 16-23, figs. 1-7.

FREEDMAN, L. AND A. D. JOFFE. 1967. Skull and tooth variations in the genus *Perameles.* Part 3: Metrical Features of *P. gunnii* and *P. bougainvillei.* Records Australian Museum, **27**(10): 197-212, pls. 32-34.

GEOFFROY-SAINT-HILAIRE, E. 1803. Bull. Soc. Philom, iii, no. 80, p. 249.

————. 1804. Ann. du Muséum National d'histoire Naturelle IV. Paris, pp. 56-65, pls. 44-45.

GRAY, J. E. 1825. Outline of an attempt at the disposition of the Mammalia into tribes and families, with a list of the genera apparently appertaining to each tribe. Ann. Philos. n.s. **10** (vol. 26 of the whole series), pp. 337-344.

HEINSOHN, G. E. 1966. Ecology and reproduction of the Tasmanian bandicoots *Perameles gunnii* and *Isoodon obesulus*. U. of Calif. Publs. in Zool., **80**: 1-96, illus., maps.

HERSHKOVITZ, PHILIP. 1971. Basic crown patterns and cusp homologies of mammalian teeth, pp. 95-150, figs. 1-17. *In* Dental Morphology and Evolution, A. A. Dahlberg (ed.). Univ. Chicago Press, pp. i-x, 1-350.

JONES, F. W. 1924. The Mammals of South Australia, Part II. The bandicoots and the herbivorous marsupials. Handbooks of the Flora and Fauna of South Australia. Adalaide, pp. 132–270, figs. 89-190.

LUNDELIUS, E. L. 1963. Vertebrate remains from the Nullarbor Caves, Western Australia. J. Roy. Soc. West. Austral., **46**(3): 75-80.

LUNDELIUS, E. L. AND W. D. TURNBULL. 1973. The mammalian fauna of Madura Cave, Western Australia, Part I. Fieldiana: Geol., **31**(1): 1-35, figs. 1-13.

————. 1975. The mammalian fauna of Madura Cave, Part II. Fieldiana: Geol., **31**(2): 37-117, figs. 1-4.

————. 1978. The mammalian fauna of Madura Cave, Part III. Fieldiana: Geol., **38**(1): 1-120, figs. 1-26.

MACK, G. 1961. Mammals from southwestern Queensland. Mem. of the Queensland Museum, **XIII**: 213-229, figs. 1-8.

MARLOW, B. 1962. Marsupials of Australia. Jacaranda Press, Brisbane, pp. 1-141.

MARSHALL, L. G. 1973. Unpublished M.S. Thesis, Monash Univ., Dept. of Zoology. Late Pleistocene-Holocene Fauna from Lake Victoria, N.S.W. Australia. Vol. I, Text pp. i-v, 6 pp. index, 1-433, 22 pp. bibliography. Vol. II, 112 tables, 85 figures, and 80 pp. Appendix I and 4 pp. Appendix II.

————. 1974. Late Pleistocene mammals from the "Keilor Cranium Site," southern Victoria, Australia. Mem. Nat. Mus. Victoria, **35**: 63-86, 11 figs.

MARSHALL, L. G. AND R. S. CORRUCCINI. 1978. Variability, evolutionary rates, and allometry in dwarfing lineages. Paleobiology **4**(2): 101–119.

MARTIN, H. A. 1973. Palynology and historical ecology of some cave excavations in the Australian Nullarbor. Austral. J. Botany, **21**: 283-316.

MERRILEES, D. 1967. Fossil bandicoots (Marsupialia: Paramelidae) from Mammoth Cave, Western Australia, and their climatic implications. J. Roy. Soc. Western Austral., **50**(4) 121-128.

————. 1968. Remains of the pig-footed bandicoot in Nullarbor Caves. Western Austral. Naturalist, **11**(1): 19.

OGILBY, W. 1838. On a new species of marsupial animal found by Major Mitchell on the banks of the River Murray in New South Wales. Part VI, **1838**: 25-27.

QUOY, J. AND P. GAIMARD. 1824. Voyage de l'urainie-Zoologie, **56**, pl. 5, *In* "Voyage Autour du Monde", (ed.) Freycinet, L.D. Paris.

REID, J. 1837. Description of a new species of the genus *Perameles* (*P. lagotis*). Proc. Zool. Soc., Pt. IV, **1836**: 129-131.

RIDE, W. D. L. 1964. A review of Australian fossil marsupials. J. Roy. Soc. Western Austral., **47**(4): 97-131, figs. 1-13.

————. 1970. A Guide to the Native Mammals of Australia. Oxford University Press, Melbourne, pp. i-xiv, 1-249, pls. 1-62.

SHAW, G. AND F. P. NODDER. 1797. Vivarium Naturae or the Naturalist's Miscellany. **VIII**, pl. 298.

SHORTRIDGE, G. C. 1909. An account of the geographical distribution of the marsupials and monotremes of southwest Australia, having special reference to the specimens

collected during the Balston Expedition of 1904-1907. Proc. Zool. Soc., 1909, **LV**, pp. 803-848, figs. 244-277.

SIEGEL, S. 1956. Nonparametric Statistics for the Behavioral Sciences. McGraw-Hill, New York, pp. i-xvii, 1-312.

SMITH, M. J. 1972. Small fossil vertebrates from Victoria Cave, Naracoorte, South Australia. II. Peramelidae, Thylacinidae and Dasyuridae (Marsupialia). Trans. Roy. Soc. South Austral., **96**(3): 125-137, figs. 1-8, tables 1-9.

TATE, G. H. H. 1948. Studies in the Peramelidae (Marsupialia). Results of the Archbold Expeditions No. 60. Bull. Amer. Mus. Nat. Hist., **92**(6): 313-346, 1 fig.

THOMAS, O. 1922. XIII. On bandicoots allied to *Perameles bougainvillei*. Annals and Magazine of Nat. Hist., ser. 9, **10**(55), art. XIII: 143-145.

TROUGHTON, E. 1962. (7th ed.). Furred Animals of Australia. Angus and Robertson, Sydney, i-xxxii, 1-376, pls. 1-25.

TURNBULL, W. D. 1971. The Trinity therians: their bearing on evolution in Marsupials and other therians, pp. 151-179, figs. 1-6. *In* Dental Morphology and Evolution, (ed.) Dahlberg, A. A. Univ. Chicago Press, pp. i-x, 1-350.

WAKEFIELD, N. 1964. Mammal remains, Appendix 1. *In* Mulvaney, D. J., Lawton, G. H. and Twidale, C. R. Archaeological Excavations of Rock Shelter no. 6, Fromm's Landing, South Australia. Proc. Roy. Soc. Vic., **77**: 494-498.

————. 1966. Mammals recorded from the Mallee, Victoria. Proc. Roy. Soc. Vict., **79**(2): 627-636, 1 fig.

WATERHOUSE, G. R. 1838. Catalogue of the Mammalia Preserved in the Museum of the Zoological Society. 2nd ed. Richard & John E. Taylor, London, 68 pp.

————. 1841. Natural history of the Marsupialia or pouched animals. *In* The Naturalist's Library (Jardine). Mammalia **11** (vol. 30 of the whole series). W. H. Lizars, Edinburgh, 330 pp.

WHITE, T. E. 1959. The endocrine glands and evolution, No. 3: os cementum, hypsodonty and diet. Mus. Paleont. Univ. of Mich., Ann Arbor, **13**(9): 211-265.

Field Museum of Natural History
Roosevelt Road at Lake Shore Drive
Chicago, Illinois 60605
Telephone: (312) 922-9410